69-12,926

AL-KHERSAN, Hashim Fadil, 1937-

CARBONATE PETROGRAPHY OF THE RED EAGLE LIMESTONE (LOWER PERMIAN), SOUTHERN KANSAS AND NORTH-CENTRAL OKLAHOMA.

The University of Oklahoma, Ph.D., 1969
Geology

University Microfilms, Inc., Ann Arbor, Michigan

THE UNIVERSITY OF OKLAHOMA

GRADUATE COLLEGE

CARBONATE PETROGRAPHY OF THE RED EAGLE LIMESTONE (LOWER PERMIAN), SOUTHERN KANSAS AND NORTH-CENTRAL OKLAHOMA

A DISSERTATION

SUBMITTED TO THE GRADUATE FACULTY

in partial fulfillment of the requirements for the degree of

DOCTOR OF PHILOSOPHY

BY

FADIL
HASHIM AL-KHERSAN

Norman, Oklahoma

1969

CARBONATE PETROGRAPHY OF THE RED EAGLE LIMESTONE (LOWER PERMIAN), SOUTHERN KANSAS AND NORTH-CENTRAL OKLAHOMA

APPROVED BY

Charles J. Mankin

Arthur J. Myers

G. W. Hanger

Norman Fogel

David B. Ritts

DISSERTATION COMMITTEE

CARBONATE PETROGRAPHY OF THE RED EAGLE LIMESTONE (LOWER PERMIAN), SOUTHERN KANSAS AND NORTH-CENTRAL OKLAHOMA

ABSTRACT

The Red Eagle Limestone in southern Kansas and north-central Oklahoma is considered as a single stratigraphic unit that conformably overlies the Johnson Shale and underlies the Roca Shale. It consists of carbonate rocks interbedded with thin laminae of shale.

Four major facies are recognized in the carbonate rocks. These are: biomicrosparite, intrapelsparite-pelsparite, biosparite, and pelmicrosparite. The biomicrosparite facies is the best developed facies with algae, bryozoans, crinoids, fusulinids, ostracods, and brachiopods comprising the dominant fossil content. Fossil fragmentation is common and probably was done by burrowing organisms.

The microspar was probably formed by abrasion of skeletal fragments and/or directly precipitated from seawater in a slightly agitated environment. The dolomite in the southern part of the area is of a secondary replacement origin.

Terrigenous minerals, such as illite, chlorite and quartz, are the main constituents of the shale and the insoluble residue fraction of the carbonate rocks. These minerals were derived from a sedimentary source area to the south.

Trace element analysis shows a linear relationship between boron and the insoluble residue content. A positive relationship between the amount of insoluble residue and zirconium was also determined. The relationship of strontium and the diagenetic fabric in the carbonate rocks is obscure.

The Red Eagle Limestone was probably deposited in a broad, shallow shelf in an environment fluctuating between carbonate and terrigenous sediment deposition and within the zone of abundant marine animal activity and processes of photosynthesis.

ACKNOWLEDGMENTS

I wish to express my sincere gratitude to Dr. Charles J. Mankin for directing the dissertation. Dr. Mankin has suggested many valuable ideas and has corrected the English; without his help my dissertation would not be in its present form. My thanks are also extended to Dr. Branson for suggesting the project and directing me to most of the studied outcrops. I am also thankful for Drs. C. A. Merritt, A. J. Myers, and C. W. Harper for reading the dissertation and offering helpful suggestions.

I would like to acknowledge the Government of Iraq for giving me a scholarship and an opportunity for higher education. My acknowledgment is also extended to the School of Geology and Geophysics and the Oklahoma Geological Survey for the use of equipment.

My sincere thanks go to Mr. Kenneth Sargent (Graduate Student) for running the trace element analysis.

Finally, the task could not have been completed without the help of my wife (Nateja Alkhersan) and her patience during the whole period of my study, and without the financial support of my parents.

CONTENTS

TABLES

LIST OF ILLUSTRATIONS

INTRODUCTION

Purpose of Investigation

A major activity of geology is the reconstruction of environments of deposition. The purpose of this research project is to reconstruct the environment that was responsible for the deposition of the Red Eagle Limestone in southern Kansas and north-central Oklahoma. The environment of deposition of the Red Eagle Limestone has been interpreted primarily from a detailed petrographic investigation of the carbonate and terrigenous constituents and chemical analyses of several trace elements. The investigation of the various facies in the field and in thin section is necessary for this type of study. The relationship of these facies to each other and their lateral extension represent the distribution and migration of that particular environment which was responsible for the deposition of each facies.

Carbonate sediments are subject to various chemical and mineralogical changes which take place after the deposition. Such diagenetic changes within the Red Eagle Limestone must be investigated and understood before the paleo-environment of the Red Eagle Limestone may be

reconstructed.

The trace elements were selected after scanning several samples, and only those elements present in sufficient amount were chosen. The relative abundance of each trace element and their possible relationship to the diagenetic processes in the carbonate sediments were investigated. Various clay minerals of the insoluble residue and shale beds were mainly identified from the analysis of x-ray diffraction patterns. X-ray techniques were also used for the identification of other terrigenous minerals and were also found useful in the investigation of the various carbonate minerals. Paleoecology of the various fossils found in the Red Eagle Limestone has also been considered in the reconstruction of the environment of deposition.

Methods of Investigation

The field work was completed during late 1967 and early 1968. In the area of investigation good exposures of the Red Eagle Limestone are scarce. More than 18 exposures were examined, but only 9 sections were measured. In this dissertation the Red Eagle Limestone was considered a single stratigraphic unit (see section on stratigraphy). The maximum thickness of the formation is in southern Kansas and northern Oklahoma (30 feet). The Red Eagle Limestone thins abruptly south of the Arkansas River where it is only a few feet thick. The Red Eagle Limestone like

other Council Grove Group units makes a rolling topography along State Highway 18. Most exposures of the Red Eagle Limestone were found along road cuts and in a few scattered quarries in north-central Oklahoma.

The following methods were used in the detailed investigation of the Red Eagle Limestone:

1. More than 120 samples were collected from the field, intervals between two successive samples being one foot. Other samples which showed some interesting features were collected and their stratigraphic position was established. Samples of terrigenous rocks which are interbedded with the limestones were also collected.

2. Each of the collected samples was examined in the field and fully described. The samples were later re-examined under the binocular microscope. The laboratory examination was aided by etching with dilute hydrochloric acid and staining with alizarine red S.

3. A total of 80 thin sections were made for a detailed petrographic examination. The description of most of the examined thin sections is given in Appendix A.

4. X-ray diffraction patterns were run from samples of the carbonate rocks, the shales, and the insoluble residues. These x-ray patterns were necessary for the study of the clay minerals. They were also necessary to obtain a better understanding of the carbonate mineralogy.

5. Thirty grams of each of the 48 selected samples

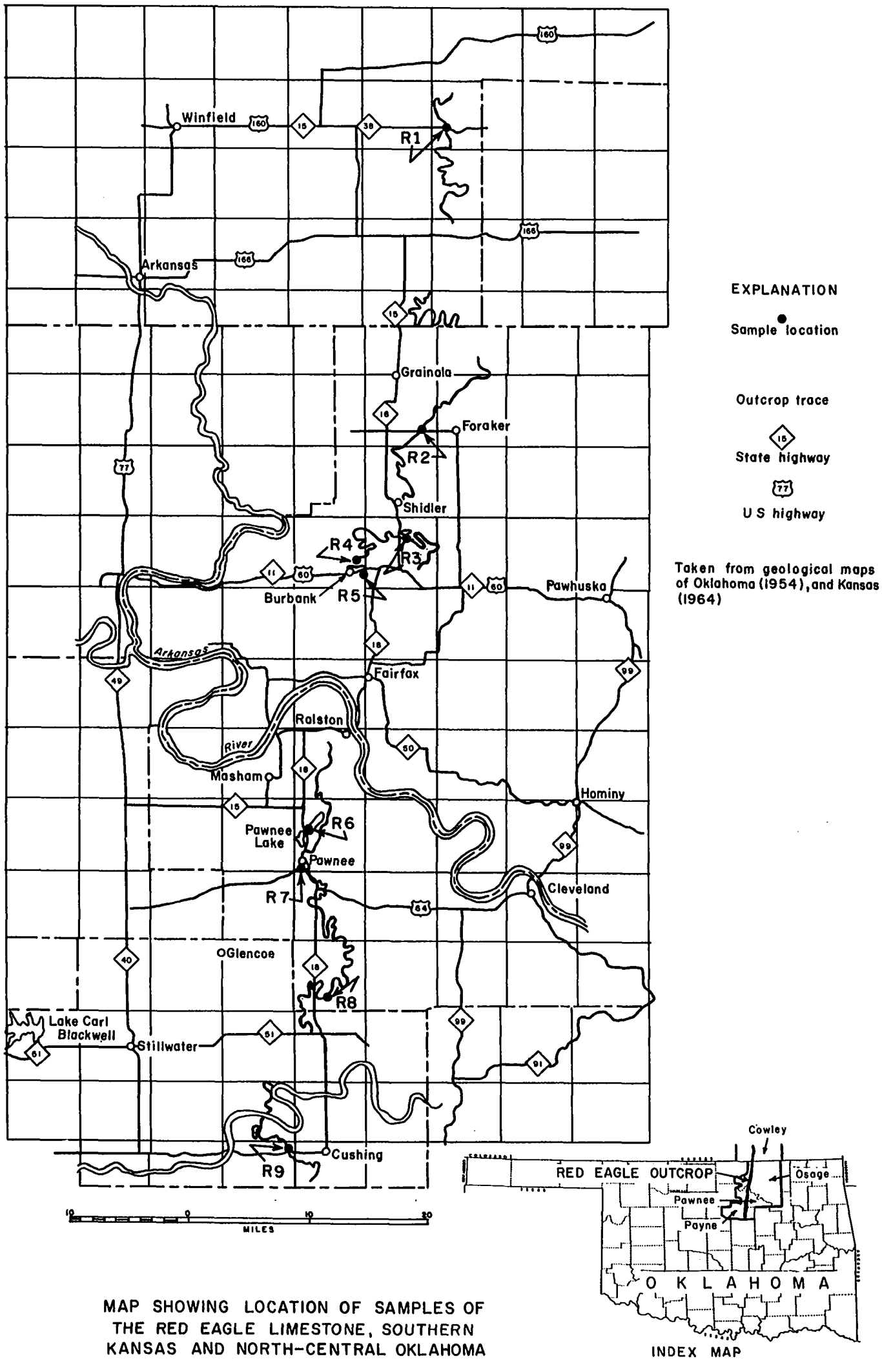

MAP SHOWING LOCATION OF SAMPLES OF THE RED EAGLE LIMESTONE, SOUTHERN KANSAS AND NORTH-CENTRAL OKLAHOMA

Figure 1

H. ALKHERSAN
December, 1968

were treated with cold, 10 percent hydrochloric acid to dissolve the calcite and dolomite. The weight percent of each treated sample was computed, and the insoluble residue was examined for its mineralogical constituents. Examination of the insoluble residue was done with a binocular microscope and by x-ray diffraction.

6. Thirty samples were selected for trace element analysis. The trace elements were selected after scanning through several samples. Only eleven trace elements which are present in sufficient amount were selected after scanning through the samples. The analysis was then done for those eleven trace elements for all the selected samples. The trace element analysis was done on a 1.5 meter Wadsworth Grading Spectrograph, Model 78-000, made by the Jarrel-Ash Company.

Location

The area of investigation is in Cowley County, Kansas and Osage, Pawnee, and Payne Counties, Oklahoma (fig. 1). In many parts of the area, the Red Eagle Limestone is covered. Exposures are found only along road cuts and in several scattered quarries. These quarries range from a few hundreds of square feet to several acres in area. Except for the Burbank quarry, the other quarries are inactive at the present time. The outcrop belt which extends from Kansas State Highway 38 to Oklahoma State Highway 33 in Payne County,

Oklahoma is about 95 miles long. Nine sections were measured in this interval (fig. 1). One stratigraphic section was measured in Kansas in an excellent road cut along Highway 38. Although the uppermost few feet are eroded at this stratigraphic section, it represents the most complete measured section in the area of investigation. Three sections in Oklahoma were measured in quarries and the remaining five were measured in various road cuts. The Foraker measured section, which was considered by Heald (1916) as the type section for the Red Eagle Limestone in Oklahoma, contains only the middle portion of the formation. A better exposure of the Red Eagle Limestone is one mile east of Burbank, Osage County, Oklahoma. This section is about 27 feet thick and represents the upper 7/8 of the Red Eagle Limestone.

Previous Investigations

Several papers are related in various ways to the Red Eagle Limestone. The authors listed below in chronological sequence seem to represent the most useful data related to a study of the Red Eagle Limestone.

1916: K.C. Heald named the Red Eagle Limestone for exposures near the Red Eagle School in the Foraker area, Osage County, Oklahoma.

1934: Moore and Moss redefined the Pennsylvanian-Permian boundary and placed it at the base of

the Admire Group. Thus, the Red Eagle Limestone was transferred from the Upper Pennsylvanian to the Lower Permian Series.

1935: R.E. Condra extended the name to northern Kansas and Nebraska. He also divided the Red Eagle Limestone into three members.

1953: R.C. Taylor mapped the Red Eagle Limestone in the Foraker area. This was part of his thesis entitled "Geology of the Foraker Area, Osage County, Oklahoma."

1954: D.L. Vosburg wrote an M.S. thesis entitled "Geology of the Burbank-Shilder Area, Osage County, Oklahoma." His work was primarily concerned with mapping the rocks of the Wolfcampian Series in the area.

1956: H.C. Fisher, Jr. mapped the rocks of the Wolfcampian and the Virgilian Series. This was the prime purpose of his M.S. thesis entitled "Surface Geology of the Belford Area, Osage County, Oklahoma."

1967: P.B. Greig, Jr., wrote his Ph.D. Dissertation which was concerned with mapping Pawnee County, Oklahoma. This dissertation is entitled "Geology of Pawnee County, Oklahoma."

1963: A.W. McCrone published the "Paleoecology and Biostratigraphy of the Red Eagle Cyclothem

(Lower Permian) in Kansas." The major purpose of this study was the investigation of the sedimentary and ecological setting that resulted in the various lithological and biological facies of the Red Eagle Cyclothem in Kansas. The main emphasis was placed on the biological aspects of the study.

Plate 1

1. Measured section R_4; A view looking north showing the nature of the Red Eagle Limestone beds. The beds in the upper part are partially weathered and brecciated. The lower portion of the Red Eagle Limestone is not exposed at this outcrop. The thickness of the exposed strata is 24 feet.

2. Measured section R_4; A close-up view of the Red Eagle Limestone. Note the many fractures cutting vertically through the beds. Shale laminae are more abundant in the lower part of the picture.

1

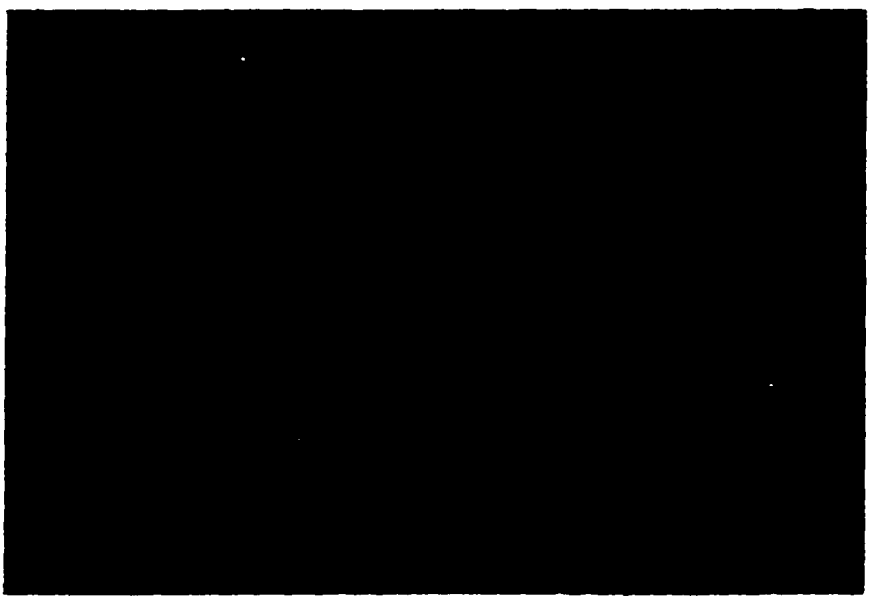

2

PLATE I

Plate 2

1. Measured section R_5; A view looking north in Burbank Quarry south of U.S. Highway 60 showing a fresh exposure of the Red Eagle Limestone. Thick beds in the lower part grade upward into thin, highly fractured beds. The lower portion of the Red Eagle Limestone is not exposed at this outcrop.

2. Measured section R_5; A view looking east showing the Red Eagle Limestone contact with the overlying Roca Shale. The lower portion of the Red Eagle Limestone is not exposed at this outcrop. The thickness of the exposed strata is 20 feet.

1

2

PLATE 2

STRATIGRAPHY OF THE RED EAGLE LIMESTONE

Regional Stratigraphic Setting

The Red Eagle Limestone of the Council Grove Group consists of limestone beds which are, in many places, interbedded with thin laminae of shale. The Red Eagle Limestone conformably overlies the Johnson Shale and underlies the Roca Shale. Both the Johnson and Roca Formations consist of red shale and must have been deposited in a shallow marine environment (McCrone, 1963).

The Red Eagle Limestone consists of three major facies. The microsparite facies comprises the lower and the middle part of the formation. It is well developed in the northern and central parts of the area (fig. 3). This facies grades upward into a sparry calcite facies. The latter is well developed in the northern part of Oklahoma where it is about 8 feet thick. Both the sparry calcite and microsparite facies grade southward into a dolomite which is well developed in the extreme southern part of the studied area.

The Red Eagle Limestone was originally named by Heald (1916) for exposures near the Red Eagle School, southwest of the town of Foraker in section 26, T. 27 N., R. 6 E.,

Osage County, Oklahoma. The Red Eagle School no longer exists.

Red Eagle Limestone Members

Condra (1935, p. 8) divided the Red Eagle Limestone into three members (in ascending order): the Howe Limestone; the Bennett Shale; and the Glenrock Limestone. In northern Kansas and southern Nebraska, the Bennett member is made up entirely of shale beds (max. 10 ft. thick) sandwiched by thin limestone beds of the Howe and Glenrock members which have a maximum thickness of eight and four feet respectively (McCrone, 1963). The contacts between the Red Eagle Limestone members are sharp and can be traced in the field almost across northern Kansas and Nebraska (McCrone, 1963).

Although the divisions of the Red Eagle Limestone by Condra (1935, p. 8) into three members is based entirely upon lithological differences in northern Kansas and Nebraska, these members are extended by McCrone (1963) into southern Kansas and northern Oklahoma on their fossil assemblages. Although fusulinids are common in the Glenrock member, they are also found in the lower part of the Bennett Shale in many places. Besides, the Glenrock member is only a few inches thick and is not exposed in many places in the area. The Bennett member which consists entirely of shale in northern Kansas and Nebraska, grades wouthward into limestone. Thus, in southern Kansas and

north-central Oklahoma the entire Red Eagle Formation is made up of carbonate beds. For these reasons the Red Eagle Limestone is considered in this study as a single carbonate unit. Branson (personal communication) has also suggested that any attempt to extend the above-mentioned divisions of the Red Eagle Limestone into the area would not be successful.

General Lithology

The following description of the Red Eagle Limestone was obtained from field observations and a petrographic study of thin sections. The Red Eagle Limestone crops out in a general north-south direction in southern Kansas and north-central Oklahoma. The Red Eagle Limestone, along with other units of the Council Grove Group, makes a rolling topography in the area of study. Throughout the entire area, the Red Eagle Limestone is homogenous in lithology; it is composed of limestone beds interbedded with thin laminae of shale. The formation has a maximum thickness of less than 30 feet in northern Oklahoma and thins rapidly southward where it is only six feet thick to the south of the Arkansas River. The general color of the weathered outcrops of the Red Eagle Limestone is light brown to gray. The upper portion of the formation, in many places, is stained with iron oxides. The intensity of the iron stain varies from place to place. The iron

STRATIGRAPHIC RELATIONSHIPS OF THE RED EAGLE LIMESTONE IN SOUTHERN KANSAS AND NORTH-CENTRAL OKLAHOMA

SYSTEM	SERIES	GROUP	FORMATION
PERMIAN	GEARYAN	COUNCIL GROVE GROUP	ROCA SHALE
			RED EAGLE LIMESTONE
			JOHNSON SHALE

Figure 2

was probably derived from the overlying Roca Shale. The color of the fresh surface also varies from one outcrop to another. The limestone beds range in thickness from a few inches to 3 feet. The shale laminae are not persistent laterally and normally disappear in a short distance.

The Red Eagle Limestone consists of a microsparite and a sparry calcite facies. These two facies grade southward into a dolomite facies which is persistent in the southern part of the area. The microsparite facies is well developed in southern Kansas and the northern part of Oklahoma. This facies reaches a thickness of 20 feet near Burbank, Oklahoma.

The overlying sparry calcite facies has an irregular thickness and it is weathered in many places. The allochemical constituents of this facies range from very coarse intraclasts of possible algal origin to very fine grains of pellets and algae. A thin biosparite facies is found locally in the Burbank area consisting of crinoids fragments. Dolomitization in the Red Eagle Limestone is of secondary replacement origin. This is well demonstrated by the presence of abundant fusulinids and crinoids in the dolomitized rocks. Silicification in the Red Eagle Limestone is only found on a local scale in southern Pawnee County. The source of the silica is probably from the dissolution of many of the siliceous sponge spicules found associated with the rocks in the area.

Plate 3

1. Fusulinid, packed biomicrosparite. A transverse section of a fusulinid. Note the fusulinid septal pores are filled with recrystallized matrix. Brachiopod fragments and ostracods are also shown. Plain light X25. Red Eagle Limestone (R_1-1)

2. Fusulinid, packed biomicrosparite. Fusulinid chambers filled with microspar. Recrystallization of the matrix is only in the inner part of the fossil. The shell wall has been partially broken on the upper right side of the photograph. Plain light X25. Red Eagle Limestone (R_1-2)

3. Fusulinid, packed biomicrosparite. A longitudinal section of Triticites rockensis. Septal pores are filled with pseudospars. Plain light X25. Red Eagle Limestone (R_1-1)

4. Fusulinid, packed biomicrosparite. A view of the end of the same fusulinid as in No. 3. Plain light X25. Red Eagle Limestone (R_1-1)

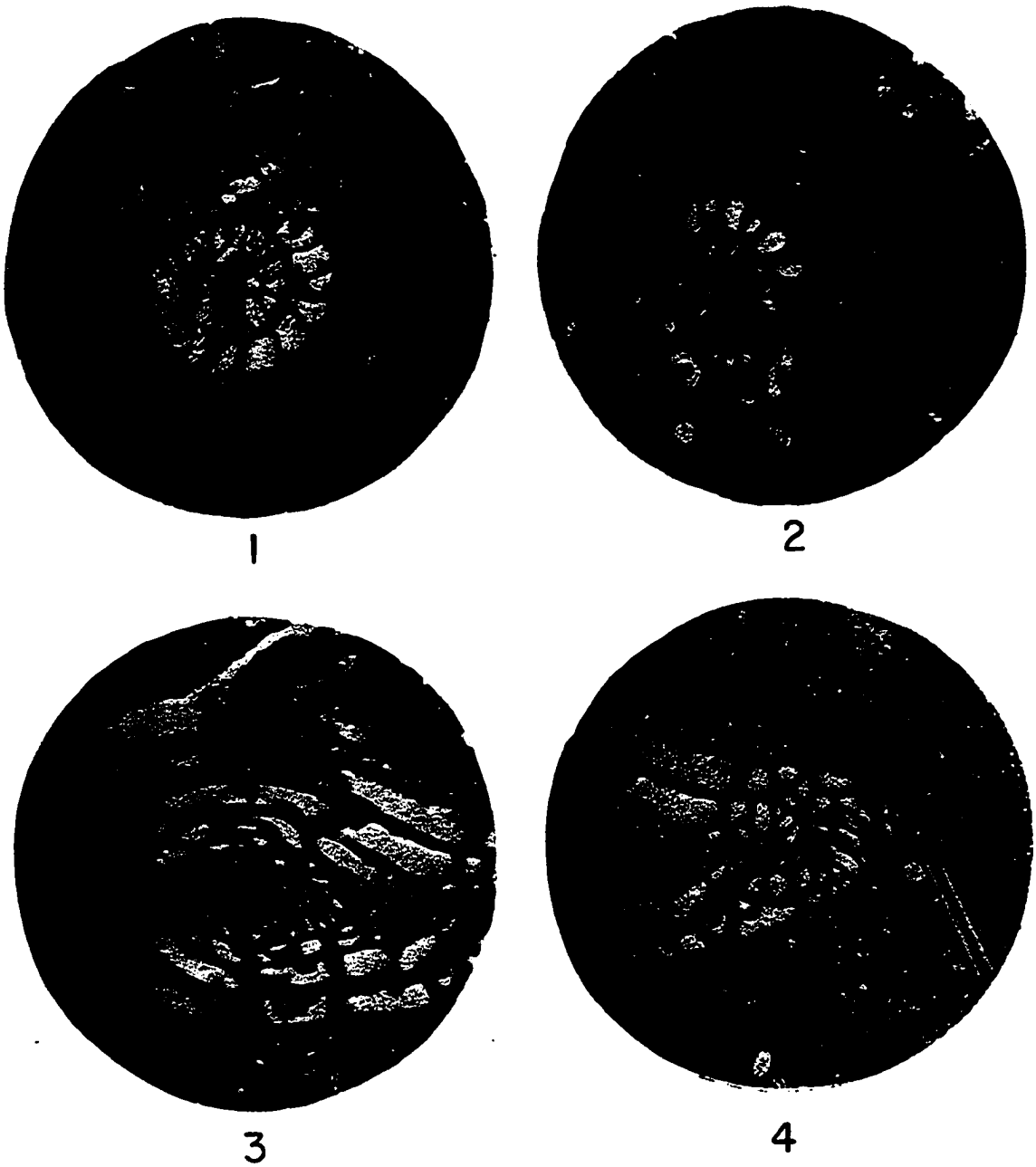

1 2

3 4

PLATE 3

Description of Measured Sections

Heald (1916) considered the exposure of the Red Eagle Limestone southwest of Foraker as the type section. This outcrop only represents the middle portion of the Red Eagle Limestone. Better outcrops are found to the south of Foraker and about two miles east of Burbank. The exposure north of Highway 60 was considered by McCrone (1963) as typical Red Eagle Limestone. A similar but larger outcrop is found south of Highway 60, in the SE 1/4 section 25, T. 26 N., R. 5 E., in a quarry. The quarry is a few acres in area and still active. This outcrop represents an excellent exposure of the Red Eagle Limestone in the area.

The contact of the Red Eagle Limestone with the overlying Roca Shale is sharp (pl. 2, fig. 2) and conformable. The lower portion of the formation is not exposed. The outcrop represents about 7/8 of the total Red Eagle Limestone thickness. The Red Eagle Limestone consists of limestone beds ranging in thickness from a few inches to three feet interbedded with laminae of shale. The limestone beds are variable in thickness, thicker in the upper part of the section. The rocks are gray in the lower part of the section and light brown in the upper few beds. The contrasting light brown color is due to the presence of iron stain on the upper beds, which was probably derived from the overlying Roca Shale.

Two facies are recognized in this measured section. A microsparite facies comprises the lower and middle portions of the section. Fossils are the main allochemical grains in this facies. Burrows are common and mostly filled with white, clear sparry calcite. Fragmentation of the fossils was probably done by burrowing organisms. The microsparite facies comprises about 3/4 of the stratigraphic section. The microsparite grades upward into a sparry calcite facies. This facies has an irregular thickness. The allochemical grains in the lower portion of the sparry calcite facies consists of fragments of crinoids and some brachiopods. Such fragmentation was also probably done by burrowing and scavenger animals. Pellets are the main allochemical constituents in the overlying beds of this facies. The pellets are probably of algal origin (pl. 13, fig. 1 and 2). A trace amount of dolomite is detected on all X-ray patterns. However, dolomitization is not observed in the examined thin sections, and only a few isolated dolomite rhombs are found dessiminated in some thin sections. Burrowing is characteristic of the Red Eagle Limestone at this outcrop. Burrows filled with sparry calcite are easily confused with recrystallized algae. Some algal tubes, which are filled with sparry calcite, are oriented parallel to the bedding. Recrystallization of some of the matrix can be seen in all the thin sections of the Red Eagle Limestone. Although

recrystallization is more abundant in the microsparite facies, it is also seen in the unwinnowed matrix of the sparry calcite facies. No significant amount of silicification is observed in the thin sections. In general, the amount of insoluble residue increases downward with the increase in the number and thickness of the interbedded shale units. The insoluble residue consists mainly of clays and minor amounts of silt-size grains. Quartz is the main constituent of the silt-size fraction. The clay minerals, identified mainly from x-ray diffraction patterns, consist mainly of illite, chlorite, and a trace amount of montmorillonite.

Algae, which consist of Osagia and other encrusting varieties, are the most abundant fossils in this measured stratigraphic section. Crinoids, bryozoans, foraminifera, and brachiopods are also common. The microforaminifera, such as Tetrataxis, Ammobaculitus?, Nodosaria and Textularia, can be seen in a few thin sections.

The next measured section (R_1) is in section 22, T. 32 S., R. 8 E., along Highway 38, about two miles west of the Cowley-Chautauqua County line in Cowley County, Kansas. This stratigraphic section is measured along the northern side of the road cut. The section represents an excellent exposure of the Red Eagle Limestone in the area.

The boundary of the Red Eagle Limestone with the underlying Johnson Shale is gradational and can be

recognized on the basis of the occurrence of the fusulinid limestone bed at the base of the Red Eagle Limestone. The upper few beds of the formation are eroded, thus the nature of the upper contact of the Red Eagle Limestone with the overlying Roca Shale cannot be studied.

The Red Eagle Limestone consists of limestone beds ranging in thickness from a few inches to three feet interbedded with laminae of shale. The limestone beds are thicker in the upper part of the measured section. The weathered surface of the rock has a light gray color. The color of the fresh limestone surface is light brownish gray.

A microsparite facies comprises about 3/4 of the measured stratigraphic section. Isolated patches of white, clear calcite are common is this facies. Fossil fragments are scattered throughout the rock as seen in thin section. Fragmentation is believed to be done by burrowing organisms. The allochemical grains in this facies are totally made up of fossils. In many places, the fossil cavities are filled with a recrystallized matrix. This microfacies grades upward into a sparry calcite facies. The allochemical grains of this facies consist of pellets with few intraclasts and fossil fragments. The intraclasts are probably of algal origin (pl. 7, fig. 2). Dolomitization of the Red Eagle Limestone in this measured stratigraphic section is sparse.

Only a trace of dolomite can be recognized in a few thin sections (R_1-5, 11, 12, 14, and 20). No evidence of silicification is noticed in the limestone beds. The amount of the insoluble residue shows no consistent pattern. Clay minerals are the main insoluble residue component in the limestone beds of the Red Eagle Limestone. Quartz grains of very fine silt size are sparse in a few samples.

Fusulinids are well preserved and are found only in the lower two feet of the measured section. Other fossils such as algae, bryozoans, crinoids, and brachiopods are common in the middle part of the Red Eagle Limestone at this outcrop.

The exposure of the Red Eagle Limestone in section 10, T. 26 N., R. 6 E., in Osage County, Oklahoma, was measured as stratigraphic section No. R_3. The section was taken at the top of the hill about 1,000 feet south of Phillips Lake.

The Red Eagle Limestone-Johnson Shale contact is covered at this place. The upper portion of the Red Eagle Limestone has been eroded, thus the nature of the upper contact cannot be investigated. The Red Eagle Limestone has a light gray color on the weathered surface and a light brown to grayish brown color on a fresh surface. The limestone is thin to medium bedded.

A microsparite facies comprises the lower and most

Plate 4

1. Crinoid, sparse biomicrosparite. A view of a crinoid plate and stem that have been compacted and thus appear as single fossil fragment. Note the line separating the two fragments. Plain light X25. Red Eagle Limestone (R_1-17)

2. Bryozoan, pellet, algae, sparse biomicrosparite. Recrystallization of the matrix has obliterated not only the matrix but some of the allochemical grains as well. Note the (Ammodiscus?) has been partially destroyed by recrystallization. Plain light 100. Red Eagle Limestone (R_5-12)

3. Algae, packed biomicrosparite. The white, elongated fragments consist of pseudospars with a mosaic texture. These are probably recrystallized algae. The original detailed features of the algae have been destroyed by recrystallization. The allochemical grains present in the photograph are mainly algae. Plain light X25. Red Eagle Limestone (R_3-6)

4. Brachiopod, ostracod, algae, packed biomicrosparite. An excellent illustration of a geopedal structure in a brachiopod shell. A recrystallization zone is present in the lower part of the photograph. Plain light X25. Red Eagle Limestone (R_1-7)

1

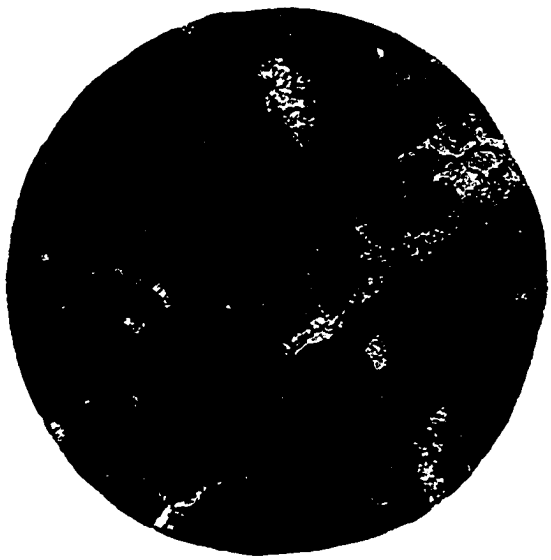

2

3

4

PLATE 4

of the upper part of the measured section. Recrystallization of the matrix is extensive. A totally recrystallized matrix can be seen in thin section (R_3-2). The intensity of the recrystallization decreases upward. Most of the fossil cavities are filled with pseudospar. Fossils are the only allochemical grains in the microsparite. The microsparite grades upward into a sparry calcite. The sparry calcite facies is thin at this outcrop. Fossil fragments and intraclasts, of probable algal origin, are the main allochemical grains in the sparry calcite facies. Voide filled with sparry calcite are also found in the microsparite facies and are difficult to differentiate from those of recrystallized algae (pl. 4, fig. 3). A trace of dolomite is detected from x-ray patterns of many of the samples. Also, dolomite rhombs are seen in a few thin sections. No significant amount of silicification is detected in any of the samples examined.

Algae, foraminifera, bryozoans, crinoids, and brachiopods are the main fossil types in the Red Eagle Limestone at the measured section.

The next Red Eagle Limestone exposure (R_4) was measured in a quarry about two miles east of the town of Burbank and 1/4 mile north of U.S. Highway 60 in section 25, T. 26 N., R. 6 E. Osage County, Oklahoma. The section was measured on the north side of the quarry.

The upper contact of the Red Eagle Limestone with the Roca Shale is sharp, but there is no physical evidence for

Plate 5

1. Burrowed, partially recrystallized, pellet, bryozoan, sparse biomicrosparite. Grain boundaries of microspars can be seen. The microspar has a similar grain size. No evidence that the microspars have originated from recrystallization in this particular slide. Plain light X250. Red Eagle Limestone (R_4-5)

2. Burrowed, partially recrystallized, ostracod, crinoid, bryozoan, sparse biomicrosparite. Microsparite originated by recrystallization. The dark spots are made up of very finely crystalline calcite. The boundaries of the white calcite grains are clear in the middle of the photographs where recrystallization is fully developed. The grains are smaller in the dark spots where the recrystallization process is not complete. Plain light X250. Red Eagle Limestone (R_4-5)

3. Crinoid, bryozoan, sparse biomicrosparite. Note floating fragments of matrix in pseudospars. Note the gradation in size of the cavity filling sparry calcite. Plain light X25. Red Eagle Limestone (R_4-6)

4. Crinoid, bryozoan, brachiopod, fusulinid, packed biomicrosparite. An example of microsparite where the recrystallization process has only partially contributed to the origin of the microspar. Plain light X250. Red Eagle Limestone (R_1-3)

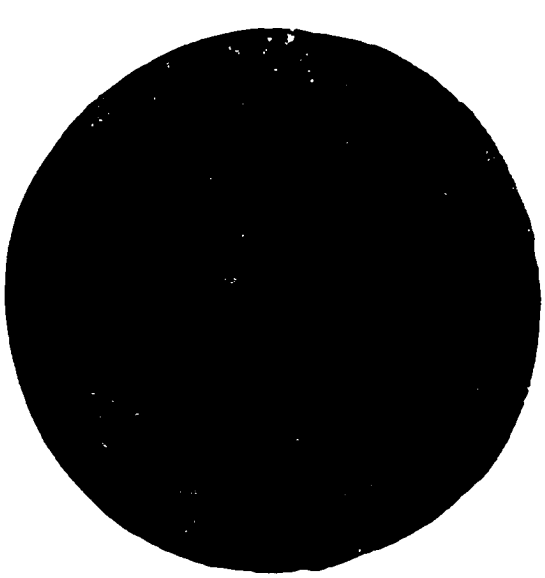

1

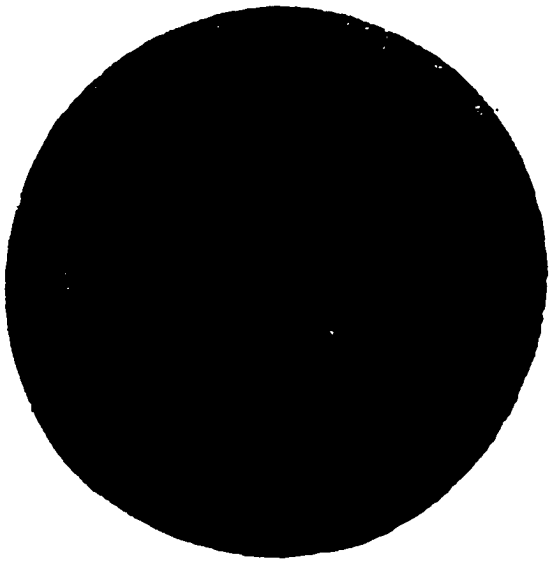

2

3

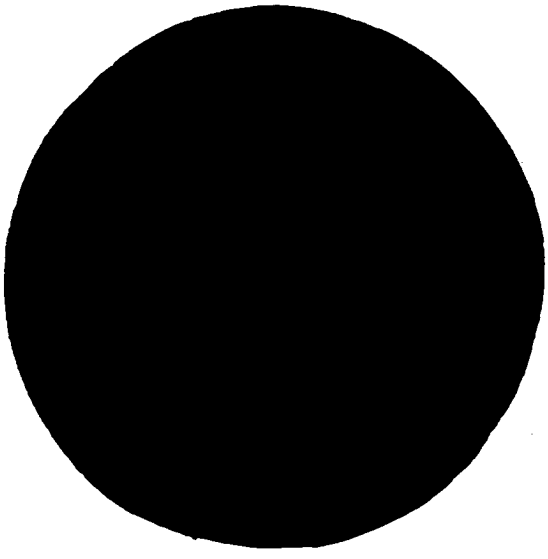

4

PLATE 5

an unconformity. The lower portion of the formation is not exposed at this outcrop. The number of interbedded shale laminae is great at this exposure. The shale contnet of the Red Eagle Limestone decreases downward in the section. The weathered surface of lower portion of the exposure is gray in color and the fresh surface of the limestone has a light gray color. Patches of iron stain are found on the weathered surface of the limestone beds in the upper part of the outcrop. The source of the iron stain is probably from the overlying Roca Shale.

The microsparite facies is about twenty feet thick at this measured section. Recrystallization of the matrix, although it is common, is less extensive than in the previous measured section. White, clear patches of sparry calcite are noticeable in the field in a few places. Algal tubes which have later been filled with sparry calcite are generally oriented parallel to the bedding planes. The sparry calcite facies is about seven feet thick and the allochemical grains are pellets. Dolomitization is not significant. Only a trace amount of dolomite is detected on a few x-ray diffraction patterns. Silicification is completely lacking. Clay minerals compose most of the terrigenous fraction of the Red Eagle Limestone at this outcrop. Only a few quartz grains of very fine silt size are found scattered through the rock as seen in a few thin sections. There is no consistent

pattern in the percentage of the insoluble residue fraction.

Fossils are sparse in the lower part and are more abundant in the middle part of the exposure. The most common fossils are: algae, crinoids, bryozoans, foraminifera, and brachiopods. Osagia and other encrusting varieties are the main algal types. Foraminifera are commonly represented by Tetrataxis, Textularia, and Nodosaria. Fragmentation of fossils in the microsparite facies probably has been done by burrowing organisms.

The Red Eagle Limestone (R_6) in section 29, T. 22 N., R. 5 E. was measured on the east side of a road cut on State Highway 18. This outcrop is about two miles north of the town of Pawnee in Pawnee County, Oklahoma.

The exposure is only six feet thick and consists of medium to thin limestone beds. The Red Eagle Limestone samples have a light brown color on the fresh surface and a darker brownish color on the weathered surface. Only the lower part of the Red Eagle Limestone is represented at this outcrop. The lower contact with the Johnson Shale is conformable. There is no physical evidence of an unconformity.

The Red Eagle Limestone at this outcrop consists entirely of the sparry calcite facies. The allochemical grains are composed of skeletal fragments which reveal some evidence of reworking and sorting. The insoluble

residue consists mostly of fine sand size quartz grains. The quartz grains are the straight extinction type. No significant amount of dolomitization and/or silicification was detected.

The fossils which make up the allochemical grains are fragments of crinoids, bryozoans, ostracods, and foraminifera.

The Red Eagle Limestone (R_8) which crops out in section 28, T. 20 N., R. 5 E., is exposed in a quarry on the south side of a dirt road about one mile east of the intersection with Highway 18. The limestone beds exposed here represent only the lower-middle part of the Red Eagle Limestone. The lower contact with Johnson Shale is not exposed. The limestone beds are thin and have a light brownish gray color on the weathered surface. The interbedded laminae of shale have irregular thicknesses.

The Red Eagle Limestone beds are completely dolomitized at this outcrop. Dolomitization is believed to be of a secondary replacement origin. Crinoid fragments are more resistant to dolomitization than any other allochemical constituents in the Red Eagle Limestone. Unaltered crinoid fragments can be observed in the thin sections studied from samples taken at this measured section. Only a few of the crinoid spicules and plates are partially replaced by dolomite rhombs. The quartz grains are much coarser than in the previous measured section.

Silicification is an important characteristic of this exposure. Chalcedonic chert is scattered through the examined thin sections in irregular patterns. Sponge spicules are common in the silicified limestone beds and are considered to be the main source of the silica in the Red Eagle Limestone.

Crinoids and sponge spicules are the only two types of fossils recognized at this outcrop.

The exposure of the Red Eagle Limestone in section 25, T. 28 N., R. 6 E., was measured on the south side of an east-west road along a 1/4 mile exposure, about two miles west of the town of Foraker.

The limestone at this outcrop is medium to thin bedded and is light brown in color on the weathered surface. The fresh surface of the limestone is a brownish gray color. The limestone beds are fractured and broken into irregular slabs on the surface. The rocks at this exposure represent only the middle portion of the Red Eagle Limestone.

A microsparite facies composes most of the measured section. This grades upward into a thin sparry calcite facies. Burrows are common in the microsparite facies. Dolomitization is sparse in the thin sections. A trace amount is detected on all the x-ray diffraction patterns. Silicification is completely absent, and the insoluble residue consists mainly of clay minerals.

Algae, bryozoans, crinoids, and brachiopods are the most abundant fossils in the Red Eagle Limestone at this outcrop. Algae is more common in the lower part, whereas other fossils are abundant in the upper portion.

The southernmost measured section is in section 2, T. 17 N., R. 4 E., in Payne County, Oklahoma. This stratigraphic section was measured along the north and south sides of a road cut on State Highway 33, about 2 miles east of the intersection with Highway 18.

The lower contact of the Red Eagle Limestone with the Johnson Shale is well exposed at this outcrop. This contact is sharp but there is no physical evidence of an unconformity. The limestone beds are grayish brown in color on the weathered surface. The fresh surface of the limestone is a light gray color.

The limestone at this locality is completely dolomitized. The dolomite rhombs are coarse to medium size. No significant amount of silicification is seen in the limestone beds. The dolomite is believed to be of secondary replacement origin.

Fusulinids are the only identifiable fossils in the rocks. The fusulinids have been completely dolomitized (pl. 14, fig. 2). The dolomite rhombs inside the shell are generally coarser than the average dolomite grains in the matrix outside the shell. The result is that each fusulinid appears as a single geode.

Figure 3

STRATIGRAPHIC SECTION OF THE RED EAGLE LIMESTONE
IN
SOUTHERN KANSAS AND NORTH-CENTRAL OKLAHOMA
by
Hashim Al-Khersan, January 1969

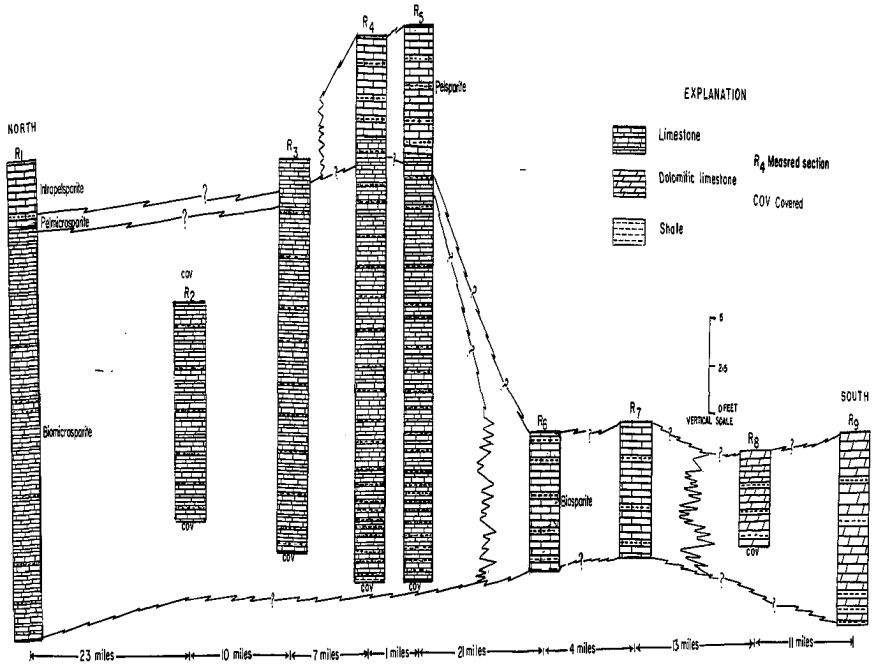

CLASSIFICATION OF CARBONATE ROCKS

Unlike other sedimentary rocks, carbonates are susceptible to major mineralogical and textural changes during diagenesis. These rocks have a complex origin and show rapid variations in texture and composition. Thus, there is no satisfactory classification which includes all carbonate rock types. There are many classifications with each emphasizing certain specific characteristics. In this study Folk's classification (1959, with minor modification, 1962) was used, because of its simplicity and application to more carbonate rock types than any other classification. Folk's carbonate classification, although basically descriptive, may be given certain genetic interpretations. According to Folk, carbonate rocks resemble other sedimentary rocks in their mode of deposition and like the terrigenous sedimentary rocks they will be affected by the environment of deposition, to the extent that they are subject to winnowing, sorting, and reworking. This classification is a combination of three parameters: 1) allochemical grains, 2) microcrystalline calcite or micrite, 3) sparry calcite or sparite (see diagram in fig. 4).

I. Allochemical grains

Folk recognized four types of allochems: 1) intraclasts, 2) oolites, 3) pellets, and 4) fossils.

1- Intraclasts: These are carbonate rock fragments which have been derived penecontemporaneously from semilithified carbonate sediments within the basin of deposition. These intraclasts are difficult to differentiate from similar carbonate rock fragments that have been derived from outside the basin of deposition.

2- Oolites: These are formed in a shallow water environment and require continuous reworking. Oolites commonly show both a concentric and a radial structure. They normally range in size from 0.1 to 1.0 mm.

3- Pellets: These are homogenous aggregates of microcrystalline calcite and they range in size from 0.03 to 0.2 mm. Pellets are well rounded and well sorted. According to Folk most are fecal pellets of invertebrate animals. In this dissertation three types of pellets were recognized. These are: 1) pellets which occur as isolated lumps in a recrystallized matrix, 2) pellets of probable

algal origin, and 3) fecal pellets (for further detail, refer to page 63).

4- Fossils: These are the most important and abundant constituents of virtually all carbonate rocks. In the Red Eagle Limestone fossil fragments are common. Fragmentation of fossils may be accomplished by either physical abrasion or by burrowing organisms. The evidence from this study indicates that most of the fragmentation of fossils in the Red Eagle Limestone was accomplished by burrowing organisms. Well preserved shells of fusulinids, bryozoans and ostracods are also present.

II. Microcrystalline calcite (micrite)

Folk uses 3.5 microns as the boundary limit between micrite and microsparite. The microcrystalline calcite is more abundant than microsparite or sparry calcite cement in the rock of the Red Eagle Limestone. The microcrystalline calcite probably originates as the result of direct precipitation from sea water, from abrasion of fossil fragments, and by secretion by bacteria and algae during photosynthesis. Micrite is equivalent to the clay matrix in sandstones. Although micrite is contemporaneously deposited with the allochemical

grains, it is not necessarily formed at the site of deposition. It could be transported from other parts of the basin (Folk, 1959).

III. Sparry calcite cement (sparite)

This is the clear calcite that fills the pore spaces between the allochemical grains. Sparry calcite is commonly mistaken with other visible and clear calcite types of different origin. Bathurst (1958) gave many criteria for the recognition of void filling calcite. The three important ones are: a) there is an increase in the grain size away from the wall of the void, b) the boundaries between the grains are plane surfaces, and c) crystals near the walls of the voids are oriented perpendicular to the wall. (For details on the sparry calcite, see page 45).

According to Folk (1959) eight carbonate types originate from the combination of the four allochemical grains with micrite and/or sparite (for further details, see Folk 1959 and 1962). In this study another carbonate rock family is added. This new carbonate family consists of the combination of the four allochemical grains and microsparite. Although the process of origin is not clear, recrystallization from micrite may not be the prime reason for the presence of microsparite in the Red Eagle Limestone. In the described thin sections of the Red Eagle

Limestone, microspars comprise either all or most of the carbonate matrix. Thus, it is necessary to include the term microspar in the specific name of the rock for a better representation of the rock. Microspar ranges in size from 3.5 to 30 microns (Folk, 1965). However, Bathurst put the lower limit at five microns. In the examined thin sections of the Red Eagle Limestone almost all show a size range of the microspar in excess of five microns and, thus, there is no problem of separation. Pseudospar which include a recrystallized matrix is also considered as a separate component in the present study. The distinction between pseudospar and other type of calcite is thought necessary in any carbonate petrographic analysis where the process of recrystallization is intense. Thus a fourth carbonate family which includes both pseudospar and allochemical grains is also suggested (See fig. 4).

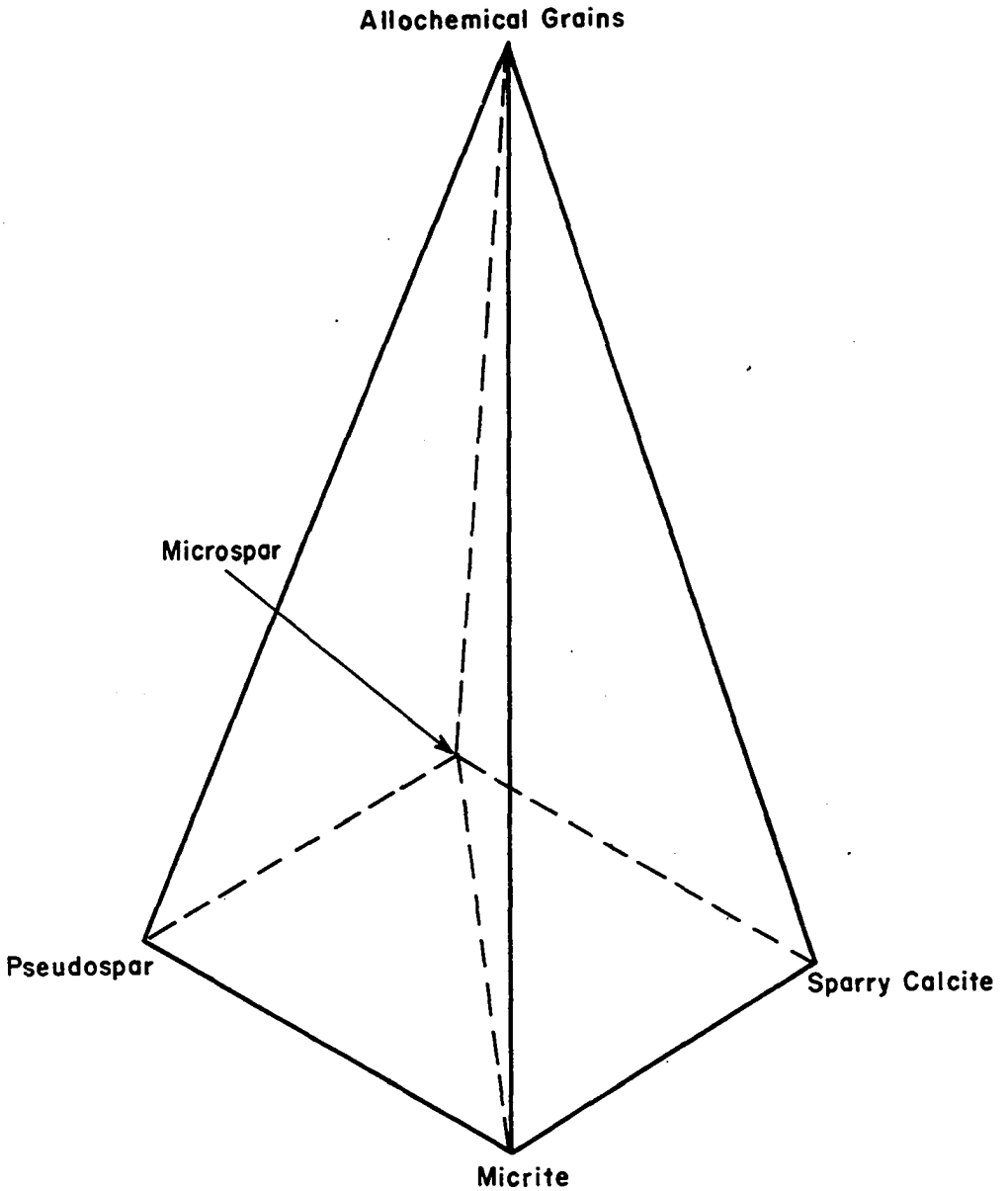

CARBONATE PYRAMID (AFTER FOLK, 1962)

Figure 4

PETROLOGY OF THE RED EAGLE LIMESTONE

The Red Eagle Limestone is consistent in its gross lithology throughout the studied area. The unit is primarily composed of carbonate, which is, in many places, interbedded with layers of shale. The Red Eagle Limestone shows little or no changes in its overall mineralogy in southern Kansas and north-central Oklahoma. However, in the extreme southern part of the area studied, the limestone beds are dolomitized. Thus, the main emphasis of this study is devoted to a petrographic study of the carbonate rocks. Other techniques such as x-ray diffraction, staining methods, and trace element analysis are also necessary for other aspects of the study.

Eighty thin sections were made mostly of the carbonate units but a few were made from samples of the shale beds. The carbonate constituents of the Red Eagle Limestone are: microspar, sparry calcite, micrite and various allochemical grains. The terrigenous constituents of the Red Eagle Limestone are either very thin layers of shale interbedded with the carbonate beds or concentrated in the carbonate beds as insoluble residue. The shale layers lack any evidence of current features. The amount of insoluble

Plate 6

1. Burrowed, recrystallized, bryozoan, pellet, crinoid, sparse biomicrosparite. Cavity filled with sparry calcite. Note the irregular shape of the calcite grains. There is an increase of grain size away from the wall of the cavity. Plain light X25. Red Eagle Limestone (R_4-3)

2. Burrowed, algae biomicrosparite. An example of microspar. Grains are unequal in size and have sharp boundaries. Plain light X500. Red Eagle Limestone (R_1-12)

3. Burrowed, recrystallized, bryozoan, pellet, crinoid, sparse biomicrosparite. Recrystallized matrix has developed a granular calcite. Grain size decreases inward in contrast to that shown in Figure 1 of this plate. Plain light X25. Red Eagle Limestone (R_4-3)

4. Burrowed, partially recrystallized, pellet, bryozoan, sparse biomicrosparite. An excellent example of an ostracod filled with sparry calcite in a recrystallized matrix. Note the gradation in grain size of the pseudospars. Note syntaxial overgrowth on crinoid plate. Bryozoan autopors are filled with both pseudospars and sparrycalcite. Plain light X25. Red Eagle Limestone (R_4-5)

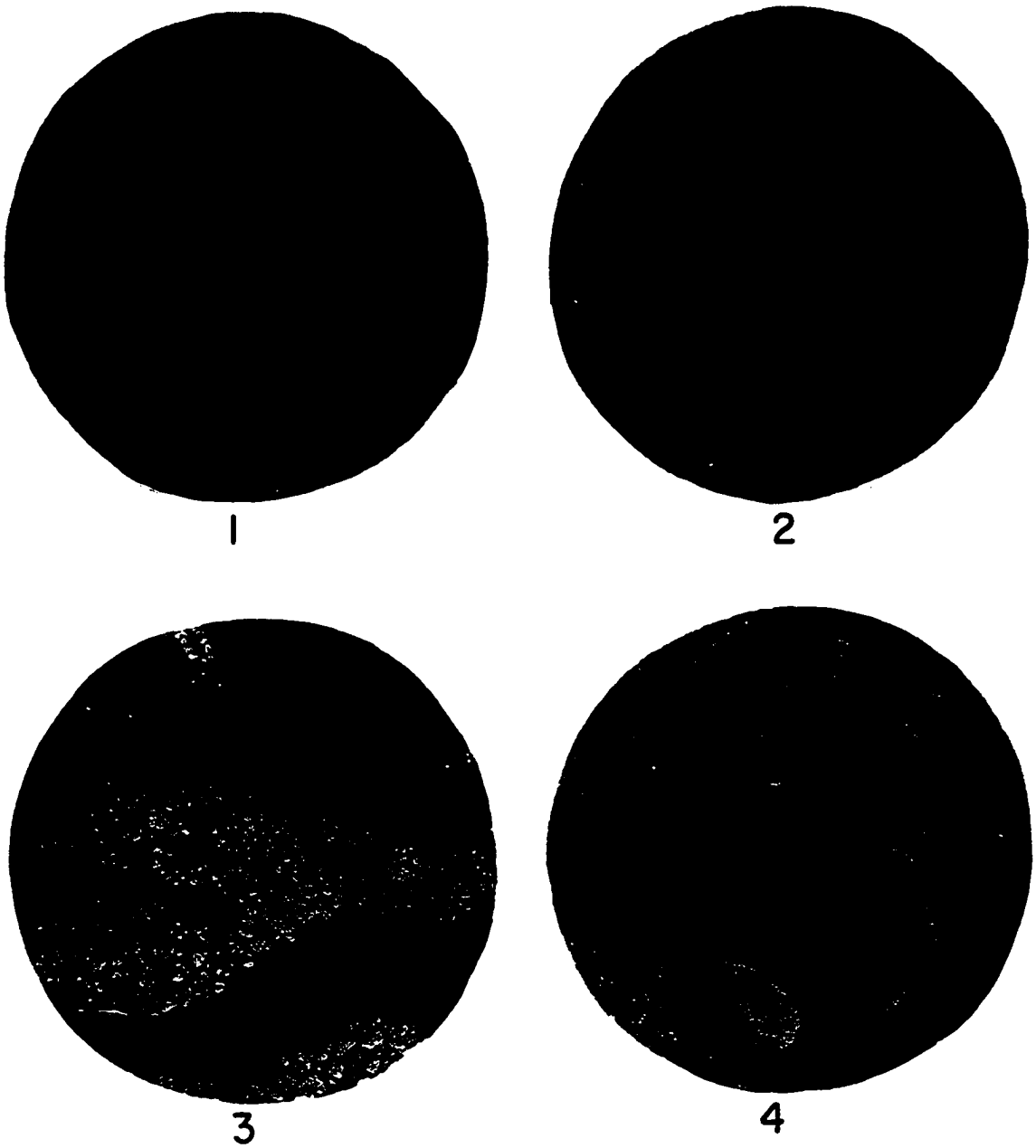

PLATE 6

residue ranges from 4.2 to 42 percent. Other beds that contain more than 50 percent insoluble residue are considered terrigenous rocks. The terrigenous fraction of the Red Eagle Limestone is composed mainly of clay minerals, silt, and very fine sand-sized quartz grains. One of the characteristics of the Red Eagle Limestone is the abundance of burrowing and recrystallization of the matrix. A completely recrystallized matrix into pseudospar has been observed in a few thin sections.

Constituents of the Limestone

In the following discussion, the various constituents of the Red Eagle Limestone will be evaluated in detail. Actually, in any limestone there are two major components: 1) Allochemical grains and 2) Orthochemical fraction. As previously stated, the allochemical grains are of four types. These types are: intraclasts, oolites, fossils, and pellets. The orthochemical components include the matrix (micrite, microspar, and pseudospar) and sparry calcite.

Sparry calcite

In the Red Eagle Limestone the sparry calcite facies is the uppermost facies. Although sparry calcite is commonly used by many people as synonymous to the cement in sandstone, the name is broad and cement is only one type of sparry calcite. Sparry calcite may precipitate

directly from solution in a pre-existing framework. The time of precipitation of the sparry calcite in the framework varies. The various types of sparry calcite arise from the variation in the nature of the pre-existing framework in the limestone and the time of precipitation. The following types of sparry calcite are recognized in the Red Eagle Limestone.

1. Sparry calcite cement: Sparry calcite cement fills in the pore spaces between the allochemical grains. This sparry calcite type is the main constituent of the sparry calcite facies except for the allochemical grains. The size of individual crystals ranges from few microns to a very coarse size. The very fine grained sparry calcite cement is commonly mistaken with the pseudospar grains which originate by the recrystallization of the matrix. Ten microns is considered by Folk (1962, p. 66), as the lower limit between sparry calcite cement and other orthochemical constituents (micrite). This, however, is an arbitrary limit for sparry calcite grains. However grains smaller than ten microns cannot be differentiated from other orthochemical constituents with certainty.

2. Void-filling sparry calcite: This type of sparry calcite is common mainly in the microsparite facies. The grains of this type of sparry calcite are characterized by their clear appearance and increase in grain size toward the center of the cavity. Although the grains may

have irregular shapes and size, they are commonly elongate with their long axis oriented perpendicular to the wall of the cavity (pl. 6, fig. 1).

3. Sparry calcite filling in shell cavities: Ostracod shells are the most abundant fossils which have their cavities filled with sparry calcite in the Red Eagle Limestone (pl. 4, fig. 4). In general, the davities are filled with coarse sparry calcite grains. In many places, the cavities are filled with a single grain. The cavities of other fossils such as brachiopods and bryozoan autopores are also filled with sparry calcite. The fossil cavities that are filled with sparry calcite must have been open voids at the time of deposition of the carbonate sediments. Later, solution saturated with calcium carbonate entered the shell cavities and precipitated the sparry calcite.

Microcrystalline calcite (micrite)

Microcrystalline calcite constitutes only a minor amount of the orthochemical constituents in the Red Eagle Limestone. Microcrystalline calcite according to Folk (1959) is the calcite with a size less than four microns. This variety of calcite constitutes the matrix in the limestone and corresponds in size to the clay minerals in sandstones. The micrite appears dark in color due to their fine size and the probable presence of impurities. The boundaries of individual grains cannot be easily seen under an ordinary petrographic microscope due to their extremely small size.

Microspar

This type of calcite is the most predominant orthochemical constituent in the Red Eagle Limestone. According to Bathurst (1959) microspar grains are larger than five microns. However, Folk (1965) considers 3.5 microns as the lower limit for this type of calcite. Under the ordinary petrographic microscope, grains of the size from 3 to 5 microns cannot be easily recognized. The matrix in the Red Eagle Limestone consists mostly of very fine crystalline calcite with an average grain size of ten microns (pl. 6, fig. 2). Very fine crystalline calcite with a grain size smaller than ten microns may well be microspar, but cannot be determined with great certainty.

Pseudospar

Pseudospar is used by Folk (1965) for calcite grains that form by recrystallization from calcite mud and/or by inversion of organic skeletons. In the Red Eagle Limestone recrystallization of the original matrix into pseudospar can be recognized in many places. A totally recrystallized matrix can be recognized in plate 6, figure 4. Recrystallization is extremely rare in the skeletal fragments of the Red Eagle Limestone and only noticeable on few algae and echinoderm fragments (pl. 9, fig. 4). Pseudospar that originates close to structural discontinuities is only found in a few places, and there forms a zone only a few millimeters thick (pl. 11, fig. 4).

In many places, pseudospar and sparry calcite cannot be easily differentiated in the Red Eagle Limestone. Mosaic textures and cross-cutting relationships with the allochemical grains are the most important criteria for recognizing most of the psuedospar. Isolated patches of original non-recrystallized matrix in a pseudospar is a good indication of recrystallization. For such types of pseudospar, Bathurst (1959) and Harbaugh (1961) believed in the idea of grain growth with progressive migration of the grain boundaries in the solid state. The exact mechanism by which pseudospar develops is not well understood. Pseudospar grains fill many shell cavities such as those of bryozoans and fusulinids (pl. 3, fig. 2). The process of the formation of pseudospar can take place at any time after the deposition of the Red Eagle Limestone.

Becuase microspars constitute more than 50 percent of all the examined thin sections of the microsparite facies, the term microsparite is used as part of the rock name in this study. This is consistent with the descriptive nature of the Folk carbonate classification which is used in this study. The same also holds for pseudosparite.

Allochemical grains

Fossils are the most abundant allochemical grains in the Red Eagle Limestone. Fossils are identified mainly from thin sections. Fossils are important indicators of

Plate 7

1. Brachiopod, ostracod, algae, packed biomicrosparite. A good example of a pisolite. Note the center of the pisolitic grain has been recrystallized. Fragment of algae is shown in the photograph. Plain light X25. Red Eagle Limestone (R_1-7)

2. Algae, bryozoan, crinoid intrasparite. This is a view of various algae grains which show partial recrystallization. Plain light X25. Red Eagle Limestone (R_4 8)

3. Silty, bryozoan, algae, sparse biomicrosparite. An example of the effect of structural discontinuity on recrystallization of the matrix. Note the bryozoan encrusted by algae at the upper right corner. Plain light X25. Red Eagle Limestone (R_5-10)

4. Burrowed, partially recrystallized, crinoid, algae sparse biomicrosparite. A large blue green algae. Plain light X25. Red Eagle Limestone (R_6-6)

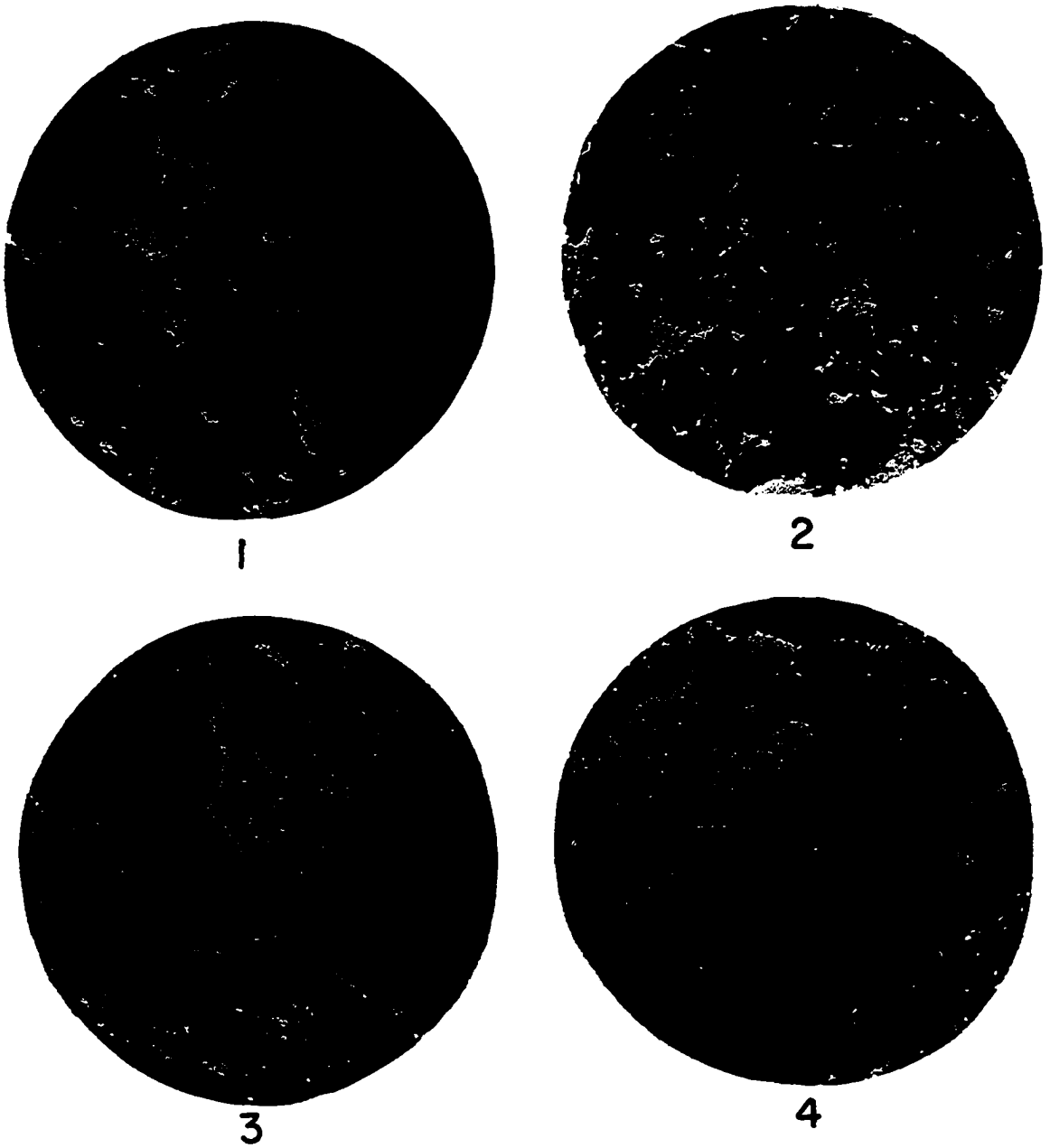

1 2 3 4

PLATE 7

the environment of deposition of the associated rock. In this study, fossils are grouped according to their major phyla. However, the order Foraminifera is described separately. Furthermore, the family Fusulinidae of the order Foraminifera is considered as separate group, because they are abundant in certain places, are important stratigraphic indicators in this part of the rock column, and they can be easily recognized.

Algae

Algae are abundant in the Red Eagle Limestone. Only a few of the examined thin sections show no evidence of algae. In the Red Eagle Limestone, algae can be divided into two major groups: 1) algal fragments, and 2) Osagia and other encrusting varieties.

1) The algal fragments which consist of white, clear calcite are generally oriented parallel to the bedding. Most of the original features of the algae have been obliterated by recrystallization and/or solution, and infilling by sparry calcite. The distinction between recrystallization and cavity filling is extremely difficult (pl. 4, fig. 3). These algae are probably of the genus Anchicodium?, McCrone (1963, p. 41).

2) The second type of algae consists of Osagia. Osagia was first described by Twenhofel (1919, p. 351). It is the most abundant type of algae in the Red Eagle Limestone. The algae is encrusting on a variety of nuclei

which consist mainly of fossil fragments (pl. 10, fig. 1 and 3). The thickness of the algal coating ranges from a few micron to several millimeters. The matrix of most samples examined has been significantly effected by recrystallization but the allochemical grains show little apparent alteration. Recrystallization of the allochems is mainly observed in some algal fragments (pl. 9, fig. 4).

Only a few rounded grains of algal origin are found in the Red Eagle Limestone. The algae that surround the nucleus may trap non-algal matter between the laminae. All the oncolites in the Red Eagle Limestone consist of blue-green algae. The occurrence of such grains in a microsparite matrix certainly do not reflect reworking by a high energy environment but more likely indicate a growth in place (pl. 9, fig. 1).

Fusulinids

Fusulinids are among the most easily recognizable fossils in the Red Eagle Limestone. In the Red Eagle Limestone most of the fusulinids are not well preserved except in the lowermost two feet of measured section (R_1). Thompson (1954, p. 14) reported three genera of fusulinids from the Red Eagle Limestone: Dunbarinella glenensis, n.sp. Triticites rockensis, n. sp. and Schwagerina campa. The last two genera were also reported by McCrone (1963, p. 36). The septal pores of the fusulinids are filled mainly with a recrystallized matrix (pl. 3, fig. 3). The

pseudospars inside the septal pores have a clear, white appearance and vary in grain size. The concentration of the microcrystalline calcite is high in the proloculus and inner septal pores. The intensity of recrystallization decreases outward and several of the terminal septal pores are filled with unaltered matrix (pl. 3, fig. 2). The effect of structural discontinuity on the recrystallization is apparent. The intensity of recrystallization inside the shell decreases away from the structural discontinuity. In the southernmost part of the area studied (measured section R_1) near Cushing, Payne County, Oklahoma, the fusulinids have been totally dolomitized. In this outcrop, the fusulinids are soft and cannot be easily thin sectioned. The internal structure of the fusulinids is completely obliterated by dolomitization (pl. 14, fig. 2). In other parts of the Red Eagle Limestone, the fusulinids are scarce and smaller in size. Without any exceptions, the fusulinids are concentrated in the carbonate beds and are lacking from the shale beds of the Red Eagle Limestone. In the carbonate beds the fusulinids are present only in the microsparite facies and are absent from the sparry calcite facies. No evidence of abrasion or reworking of the fossils is discernible and the destruction of some of the fusulinids is primarily a result of burrowing organisms and scavengers. There is no noticeable orientation of the fusulinids with respect to bedding. One of the many

excellent preserved fusulinids in the Red Eagle Limestone is Triticites rockensis which is shown in plate 1, figure 3 and 4.

Microforaminifera

There are many types of microforaminifera in the Red Eagle Limestone. In many places, the microforaminifera have either been partially or totally obliterated, because of their fragile and delicate shells. Many of the calcareous microforaminifera are partially recrystallized which makes identification extremely difficult. A partially recrystallized form is shown in plate 4, figure 2. This microforaminifera is probably Ammodiscus(?) in a microspar matrix. The microforaminifera are present in both carbonate and shale beds of the Red Eagle Limestone. Arenaceous microforaminifera are common in the limestone beds. Although the shells of such microforaminifera are made of very fine grains of various mineral types, the septal pores are mainly filled with pseudospars (pl. 12, fig. 3 and 4).

Most of the microforaminifera are associated with the microsparite facies. In many places, the microforaminifera are obliterated by the diagenetic process in the limestone beds. Also, they may have been transported for some distance from their original environment. Of the many microforaminifera present in the Red Eagle Limestone,

Plate 8

1. Bryozoan, algae, pellet, packed pelmicrosparite. An excellent example of a bryozoan with the autopores filled with pseudospars. Plain light X25. Red Eagle Limestone (R_5-8)

2. Burrowed, partially recrystallized bryozoan biomicrosparite. An example of bryozoan partially destroyed by recrystallization of the matrix. Note the autopores of the bryozoans which are filled with pseudospars. Plain light X25. Red Eagle Limestone (R_4-5)

3. Recrystallized, brachiopod, crinoid, bryozoan, sparse biomicrosparite. A bryozoan in a totally recrystallized matrix. In some places, the pseudospars have cut through the walls of the bryozoan. Plain light X25. Red Eagle Limestone (R_4-2)

4. Brachiopod, crinoid, bryozoan, sparse biopseudosparite. The same thin section as in No. 3 showing another variety of bryozoan. Plain light X25. Red Eagle Limestone (R_4-2)

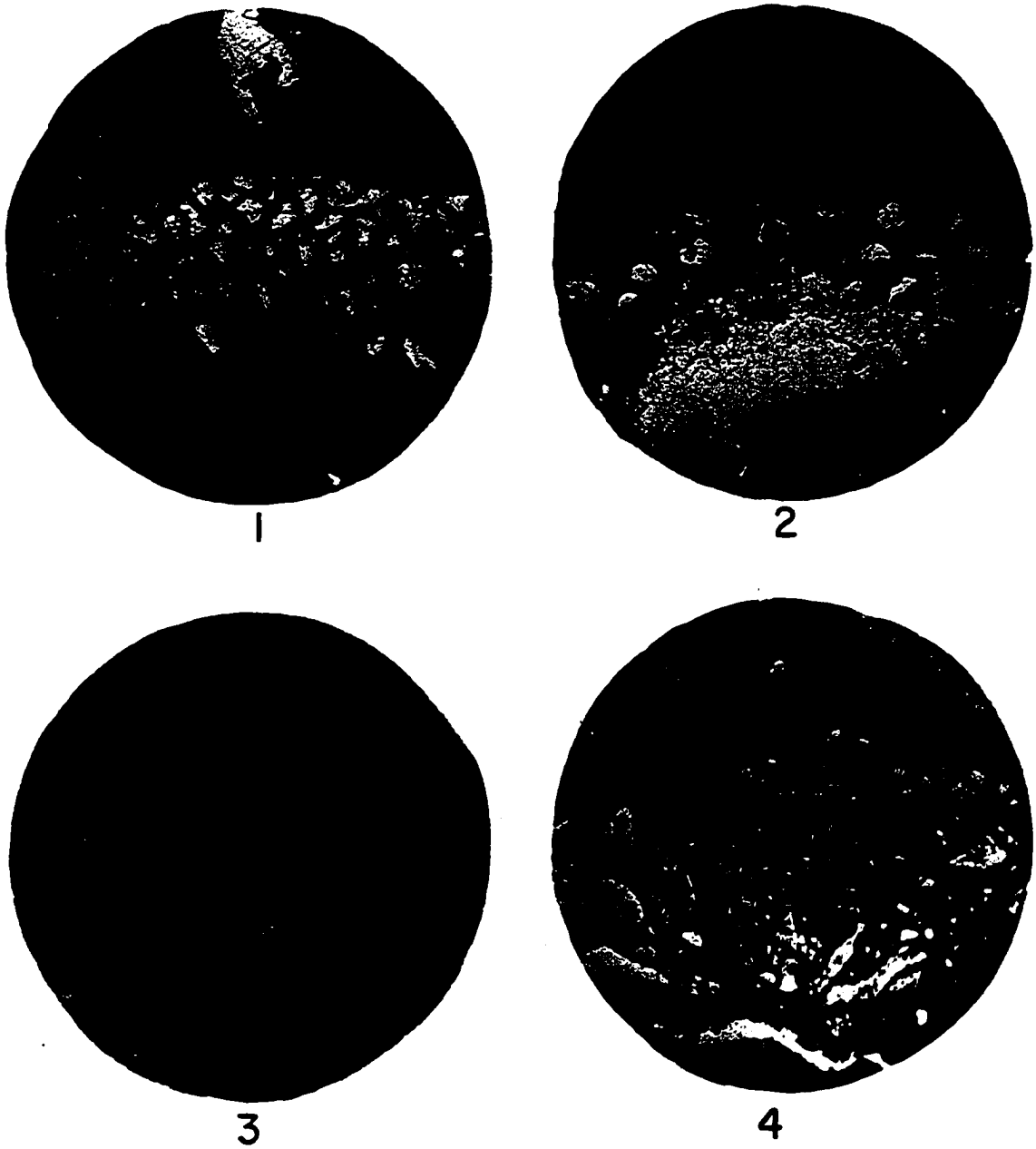

1 2 3 4

PLATE 8

Textularia, Ammobuculites and Nodosaria are the most common (pl. 12).

Bryozoans

Bryozoans are common in the Red Eagle Limestone. They are more abundant in the middle part of the formation and scarce in the upper and the lower parts. Fenestrate and ramose forms are the most common types of bryozoans (pl. 8, fig. 1, 2, 3 and 4). Encrusting bryozoans are extremely rare. Fragmented colonies of bryozoans are abundant and do not indicate reworking by currents. Many bryozoans are reported by Condra and Elias (1937), of which Rhombopora lepidodendroides, Bascomella and Caulostrepsis are the most important types. The bryozoans fragments, although they are common in the microsparite facies, are also found in the sparry calcite facies. Bryozoans fragments are the most abundant nuclei types for the oncolites. Of the fossil fragments encrusted by algae, bryozoans is the most abundant type. Bryozoans are not recognized in the dolomitized limestone. The bryozoan fragments completely lack evidence of any recrystallization. However, some of the fragments may have been cut by veins which are filled with sparry calcite. In many places, the autopores of the bryozoans are filled with matrix. In many of the pores the matrix is recrystallized to pseudospars. Autopores filled with sparry calcite are not common, and such autopores are difficult

to identify from the pseudospars. No evidence of silicification of the bryozoan fragments in the Red Eagle Limestone is observed. The bryozoan fragments are not restricted to one type of facies, but they are certainly more abundant in the microsparite facies. Bryozoans comprise as much as 25 percent of the allochemical grains in some places (R_5-13). They are also found in the shale beds. However, the bryozoans in the shale beds are not well preserved. The destruction of the bryozoans in the shale beds probably is the result of compaction.

Echinoderms

Echinoderms are widely distributed in the Red Eagle Limestone; they are observed in most of the examined thin sections. The echinoderm fragments comprise up to 30 percent of the rock in some thin sections (R_5-13, R_6-7 and R_7-2). They are common in both the microsparite and sparry calcite facies. They are the most abundant constituents of the sparry calcite in the Red Eagle Limestone. Echinoid stems are recognized in the field in many places. Nearly all the examined fragments of echinoderms in the thin sections are parts of crinoids and echinoids. These two types of echinoderms are difficult to differentiate. In the Red Eagle Limestone, the echinoderm fragments are more resistant to recrystallization and dolomitization than the rest of the allochemical grains. They are among the few fossil fragments that can be identified

in the dolomitized limestone (pl. 4, fig. 10). Only in a few places do the crinoid fragments show syntaxial overgrowth and/or recrystallized rims (pl. 4, fig. 1). Spicules of various geometrical shapes and sizes are also common.

Ostracods

The ostracods are not restricted to one carbonate facies. The shells in the sparry calcite facies are well preserved. This may indicate that the current was only strong enough to winnow the matrix. Ostracods are also found in the shale beds of the Red Eagle Limestone. They are scarce in the southernmost part of the studied area. They are completely absent from the dolomitized limestone beds. Bairdia and Carvenilla are abundant in some samples. The filling of the ostracod cavities by sparry calcite is characteristic of the fossils in many places; it is present in almost all the examined thin sections. The time of filling of the cavities of the ostracod shells cannot be determined. The ostracods comprise as high as 10 percent of the total allochemical grains in many samples (R_6-9, R_1-2).

Brachiopods

Both articulate and inarticulate brachiopods are present in the Red Eagle Limestone. Many genera including Lingula, Orbiculoidea, and Neospirifer were identified in

the field. However, such identification cannot be readily made in thin section.

More brachiopod genera are listed in McCrone (1963, p. 36). In general, brachiopod fragments are not abundant; however they comprise as much as three percent in several thin sections and up to 30 percent in one thin section (R_7-1). They also make up to 13 and 20 percent in R_1-2 and R_4-2 respectively. Only brachiopod shells show geopetal structures (pl. 15, fig. 1) in the Red Eagle Limestone. In the microsparite facies, the brachiopod fragments are not abraded and they probably were fragmented by burrowing organisms and other scavengers. Recrystallization is completely lacking from the shells and some of the fragments show the typical fibrous structure of the brachiopod shell (pl. 9 , fig. 3). The centers of a few brachiopod spicules are slightly recrystallized. Some of these spicules are encrusted by algae. Brachiopod fragments are totally absent from the dolomitized limestone beds.

Mollusca

The mollusca are represented in the Red Eagle Limestone by abundant fragments. Only small spiral-shaped gastropods are found in some samples. Mollusca comprise of only trace amounts of the allochemical grains. Many of the molluscan fragments have a mosaic calcite texture and are therefore difficult to differentiate from

recrystallized algal fragments. Most of the molluscan shells probably consisted of aragonite which later was converted to calcite. This may be the main factor in the obliteration of the shell structure. In the Red Eagle Limestone, pelecypods and gastropods are the main types of molluscs. The fragments are found in both the microsparite and sparry calcite facies.

Pellets

Pellets are aggregate of microcrystalline calcite (pl. 11, fig. 2). These are the most abundant nonskeletal allochemical constituents in the Red Eagle Limestone. Although the term "pellets" seems to be used primarily in a descriptive manner by many workers, some consider they have similar origin. This arises mainly from their similar size, shape, and high degree of sorting and roundness. The pellets are characterized from other nonskeletal allochemical grains by having no internal structure. Many carbonate petrographers consider them to be fecal pellets of worms and other invertebrate animals (Folk 1962, p. 65, following Hatch and Rastall 1938, in Folk 1962).

Pellets cannot be recognized in the field or under the binocular microscope because of their small size (0.03 to 0.15 mm). Grains which have a similar appearance but are larger in size are considered as intraclasts whether they show internal structure or not. In this paper the

term "pellet" is used descriptively for any nonskeletal grains within the size range of 0.03 to 0.15 mm. In the Red Eagle Limestone, the pellets can be divided into at least three types according to their probable origin.

Fecal pellets, these grains are better sorted and better rounded than the average pellets in the Red Eagle Limestone and have oval to subspherical shapes. They are probably the product of worms and invertebrate animals. They have a light to dark brownish color due to the presence of organic matter and very small grains of various mineral constituents. These and other pellet types are difficult to recognize in the microsparite facies except for their appearance. Such pellets which are common in the geologic record are also abundant in many carbonate sediments at the present time. Eardley (1938, p. 1401) noticed the association of some rodlike, very well sorted pellets in the Great Salt Lake of Utah associated with the shrimp Artemia gracilis. Eardley believes that those pellets are the product of the shrimp in the lake.

Pellets may originate from the process of recrystallization of the carbonate matrix. These pellets are less rounded and not as well as sorted as the first type. The process of recrystallization, in many places, effects both the matrix and the pellets. The time of recrystallization cannot be predicted exactly but it must have

occurred before the filling of the pore space with sparry calcite (pl. 11, fig. 1). The sparry calcite in these pore spaces lacks any evidence of recrystallization.

The third type of pellets are probably of algal origin. The external appearance, lack of internal structures, and association of these pellets with algae are the main reasons for believing in their algal origin. They range in shape from elongate, rodlike forms to short oval and subspherical shapes. These pellets are rounded and better sorted than the above-mentioned type (pl. 13, fig. 1).

Intraclasts

Intraclasts are the other nonskeletal grains in the Red Eagle Limestone. The origin of the intraclasts is not well understood by many workers in carbonate petrology. This confusion arises mainly from the adaptation of many terms. In the terminology of Folk (1959), intraclast grains are pieces of carbonate fragments which are locally reworked and are slightly older than the carbonate beds in which they are found. There are actually no definite criteria by which we can tell how much older the intraclasts are than the enclosing beds. Intraclasts are of various origins and they are, in many places, confused with pellets except for their size. In the Red Eagle Limestone, the intraclasts comprise a trace amount of the total allochemical grains. However, they make up

as much as 25 percent of the total allochemical grains in thin section R_6-10. Intraclast grains which are surrounded by pseudospars originate by recrystallization. These intraclasts have various sizes and irregular shapes. Other grains which are better sorted and better rounded, are probably of algal origin.

The intraclasts do not comprise an important facies in the Red Eagle Limestone.

Other allochemical constituents

The other grains in the Red Eagle Limestone are composed mainly of various fossil fragments. These are not important and only comprise a trace amount of the total allochemical grains. Spicules are the most abundant of these constituents. They vary in shape and size and probably belong to more than one faunal assemblage. The spicules are randomly oriented and they are mainly restricted to the carbonate beds of the Red Eagle Limestone.

Two types of spicules are found in the limestone. The calcareous type compose up to three percent of one sample (R_6-9). The siliceous spicules are found mainly in the dolomite facies of the Red Eagle Limestone. The siliceous spicules are the most probable source for the silica in the rock (R_8-2).

Other constituents are mainly fragments of unknown vertebrates. McCrone (1963, p. 36) has reported several

Plate 9

1. Pellet bryozoan, algae biomicrosparite. An example of a pisolite made up of blue-green algae. Recrystallization of the matrix is extensive. Also note that the structural discontinuity of the pisolite grains has locally affected the recrystallization of the matrix. Plain light X25. Red Eagle Limestone (R_1-8)

2. Algae, packed biomicrosparite. The star shape in the middle part of the photograph is recrystallized matrix into pseudospars. Bryozoan autopores are filled with pseudospars in the upper right side of the picture. Plain light X25. Red Eagle Limestone (R_1-5)

3. Fusulinid, packed biomicrosparite. An excellent example of a brachiopod fragment with the fibrous structure of the shell easily seen. Notice the small fusulinid by the brachiopod fragment. Plain light X25. Red Eagle Limestone (R_1-1)

4. Algae, packed biomicrosparite. Although recrystallization is common in the matrix, it is not completely lacking in the allochemical grains. In the middle of the photograph, recrystallization has obliterated a large portion of the algae. Plain light X25. Red Eagle Limestone (R_1-5)

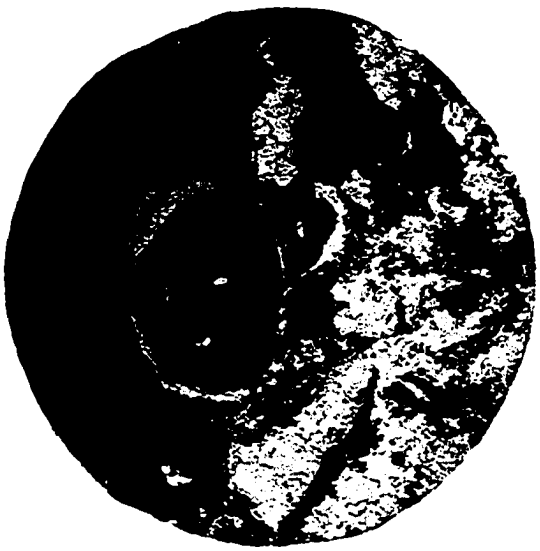

1

2

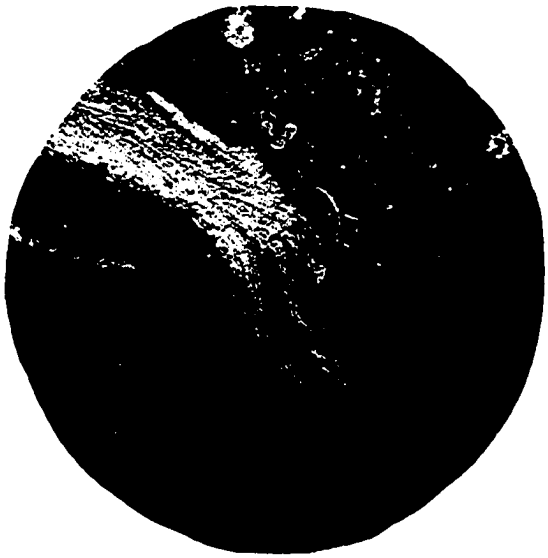

3

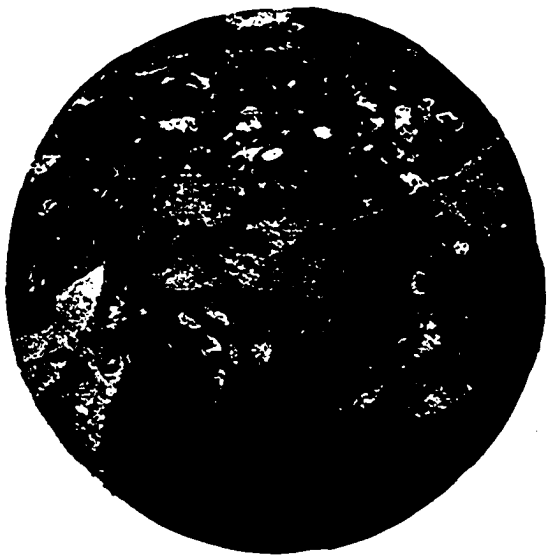

4

PLATE 9

Plate 10

1. Sandy, bryozoan, crinoid biosparite. Large crinoid grains well rounded and coated with algae. Also very fine sand grains which are sorted but not rounded. The sand grains consist of quartz. The allochemical grains are not sorted. Plain light X25. Red Eagle Limestone (R_7-2)

2. Silty, bryozoan, crinoid, packed biomicrosparite. An excellent example of crinoid stems. Also many fragments of crinoid plates. One fragment at the top of the photograph shows a syntaxial overgrowth. All the silt grains are quartz. Plain light X25. Red Eagle Limestone (R_5-13)

3. Foraminifera, bryozoan algae crinoid biosparite. Fragments of crinoids with some syntaxial overgrowths and many algae fragments. Note the vein in the middle that cut through many of the allochems is filled with sparry calcite. Very poorly sorted allochemical grains. Plain light X25. Red Eagle Limestone (R_6-7)

4. Dolomitized, crinoid biosparite. A crinoid stem in the center. All the cement has been replaced by dolomite. The crinoid is only partially dolomitized. Plain light X25. Red Eagle Limestone (R_9-2)

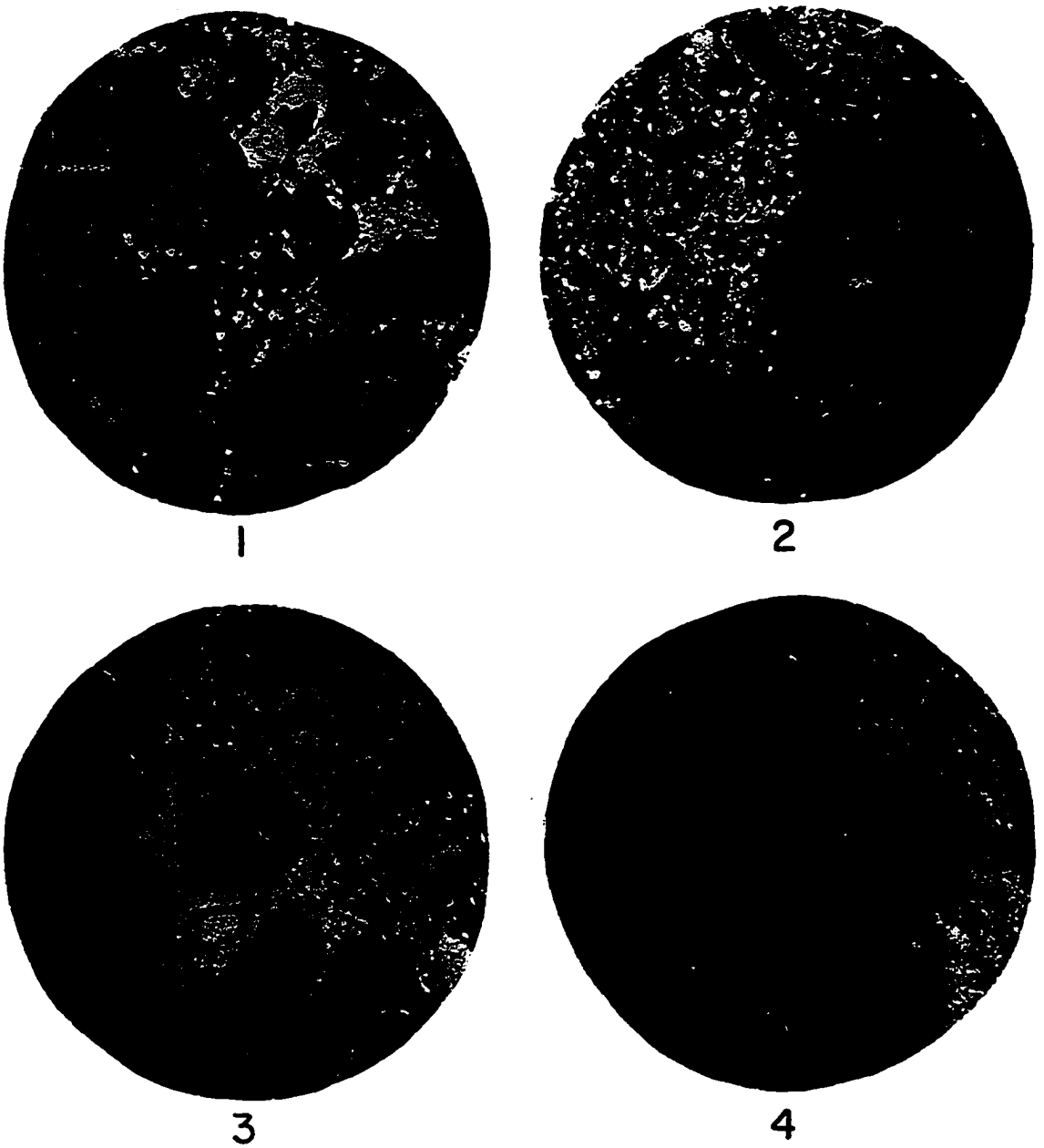

PLATE 10

types of conodonts and shark teeth in the Red Eagle Limestone.

Terrigenous Constituents

The terrigenous constituents in the Red Eagle Limestone consist mainly of quartz. The quartz grains range in size from 22 to 260 microns. They are angular and, in many places, not well sorted. The quartz grains are of the straight extinction type. The homogeneity in the quartz types may arise from their very small grain size where the other types cannot be recognized. Also many of the composite grains break down to individual extinction units which have straight to slightly undulose extinction. The grains are generally disseminated through the limestone and show no evidence of concentration along any certain horizon or laminations. The percentage of quartz grains ranges from a trace amount to as much as 20 percent in some places (R_5-3 and R_7-2). No significant amount of feldspar or other types of coarse detrital minerals are found in the Red Eagle Limestone.

Clay minerals in the Red Eagle Limestone cannot be adequately identified with the petrographic microscope. The clay minerals, in many places, comprise the major part of the terrigenous constituents in the carbonate beds. X-ray diffraction techniques were used for the study of the clay minerals in the limestone beds and in the shale which is interbedded with the limestone.

DIAGENETIC PROCESSES

There is no satisfactory agreement among geologists on the definition of diagenesis. There appears to be no sharp break or boundary between diagenetic processes on the one hand and metamorphic processes on the other. Diagenesis and metamorphism are considered by some geologists as one continuous process which starts immediately after the deposition of the sedimentary unit. However, the most accepted definition for diagenesis is the one used by Twenhofel (1939, p. 254) and later adopted by Krumbein (1942, p. 111) which states:

> Diagenesis includes all modifications that sediments undergo between deposition and lithification under conditions of pressure and temperature that are normal to the surface or outer part of the crust, and in addition, those changes that take place after lithification under the same temperature and pressure which are not katamorphic in character so that the effect is delithification...

In this dissertation, this definition is used. Some of the changes in the Red Eagle Limestone such as silicification, dolomitization, cavity filling, and geode formation are considered diagenetic changes occurring after the deposition of the Red Eagle Limestone.

Silicification

In the Red Eagle Limestone silicification is scarce in most of the formation and is significant only in one locality in southern Pawnee County (R_8). There is no nodular chert in any part of the limestone except at that outcrop. The chert there consists of chalcedony which is disseminated throughout the rock as seen in thin section. The chert is mainly of two types: (1) microcrystalline quartz and (2) chalcedonic quartz.

The chalcedonic quartz is characterized by a fibrous structure and brownish color which is absent in the microcrystalline quartz (Folk and Weaver, 1952). From electron microscopic studies, Folk and Weaver (1952) concluded that the basic difference between the two types of chert is the abundance of minute water-filled cavities in the chalcedonic type. This is considered to be the main reason for the spongy appearance and brownish color under reflected light and for its low specific gravity. The recent work of Monroe (1964) also confirmed that conclusion reached by Folk and Weaver (1952).

In the Red Eagle Limestone, the chalcedonic chert is found only in a dolomitized bed. The boundary between the dolomite and the chalcedony is irregular. Crinois plates and stems are the only megafossils in the chert. Fossils can be seen only after a thorough examination. No other calcareous fossils are present in the dolomite or the

chert. The only other abundant fossils in the rock are the siliceous sponge spicules. They are randomly oriented and, in many places, are partially dissolved and difficult to resolve.

Although the origin of silica in carbonate beds is intensely debated and there are several theories for its origin, it is reasonably clear from this study that the chalcedonic chert of the Red Eagle Limestone has a replacement origin. The replacement origin of the chert in the Red Eagle Limestone is evident from the presence of floating dolomite rhombs in the chert. Also, some of the crinoid plates and stems are completely surrounded by silica and partially silicified in the dolomitized bed. The sponge spicules are the most obvious source for such localized chalcedonic chert. The silica in the sponge spicules is amorphous and therefore has a higher degree of solubility than ordinary quartz (Pittman, 1959). These spicules during burial of the sediment and during an increase of the pH will bring about the solution, migrating and precipitation of the silica (Rankama and Sahama, 1950, p. 555-556). Calcite responds to a fluctuation of the pH in the sediment in the opposite manner (i.e., an increase in the pH will cause silica to be dissolved and bring the deposition of calcite, whereas a decrease in the pH causes the precipitation of calcite and solution of the silica).

Plate 11

1. Pellet intrasparite. The intraclasts may not have been transported but probably formed in place. Note recrystallization at the boundary of some of the grains. Many of the black spots are composed of pellets closely packed. The allochemical grains are probably of algal origin. Plain light X25. Red Eagle Limestone (R_6-10)

2. Bryozoan, pellet, crinoid, sparse biomicrosparite. This portion of the slide shows some algae in a recrystallized matrix. The ostracod is filled with sparry calcite. Plain light X25. Red Eagle Limestone (R_5-15)

3. Bryozoan, algae, packed biomicrosparite. An excellent example of algae encrusting bryozoans. Plain light X25. Recrystallization of the matrix into pseudospars is extensive in the right side of the photograph. Plain light X25. Red Eagle Limestone (R_1-10)

4. Burrowed, bryozoan, algae, packed biomicrosparite. Excellent example of the effect of structural discontinuity on recrystallization. Note the brachiopod spicule in the center of the photograph which is surrounded by a thin zone of recrystallized matrix. Plain light X25. Red Eagle Limestone (R_1-13)

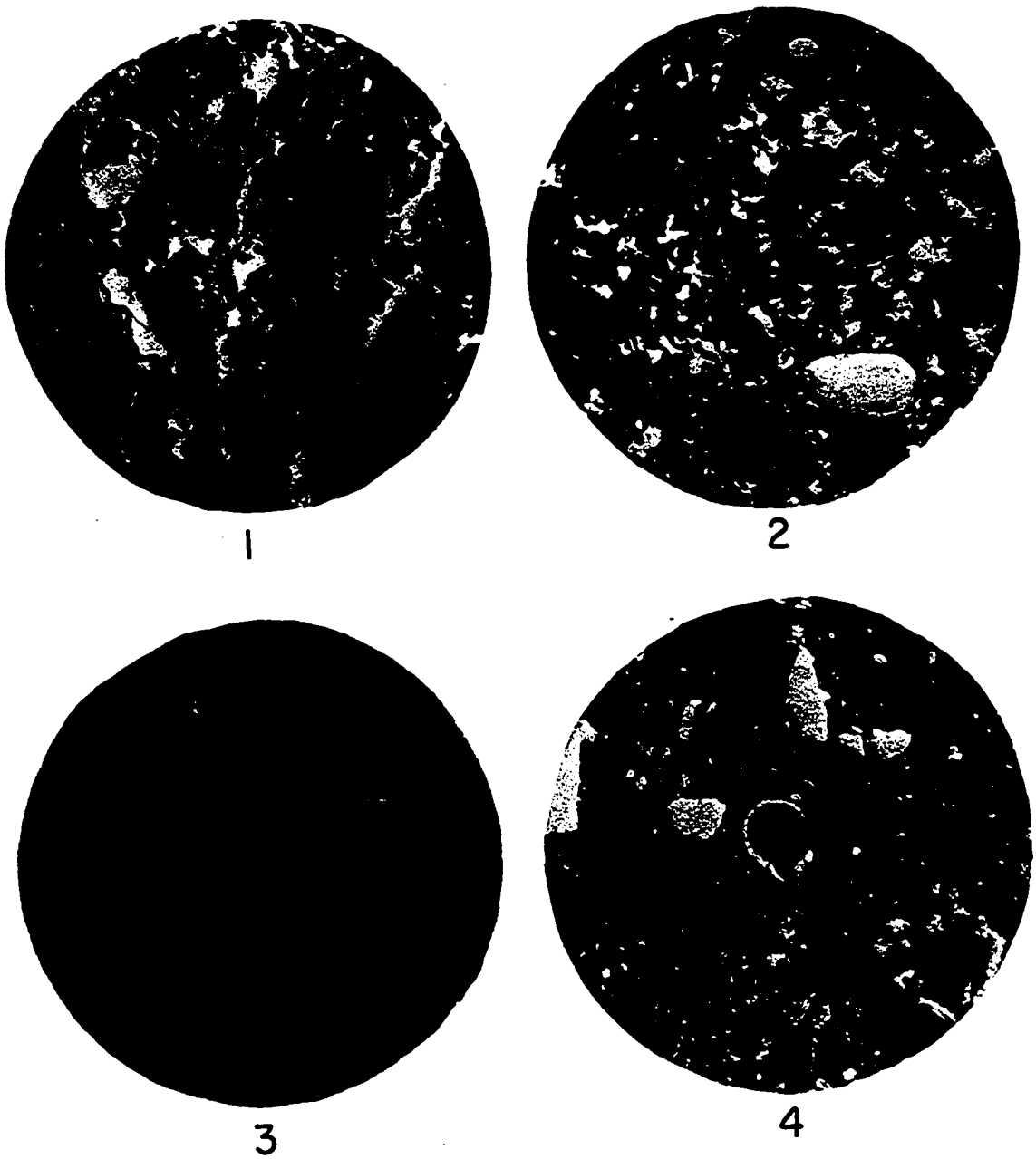

PLATE II

According to Rankama and Sahama (1950), fluctuation in the pH can be attributed to the activities of bacteria. Pittman (1959, p. 132) has suggested that whereas there is an increase in the pH and silica will be dissolved at one place, there must be silica precipitated elsewhere. Thus a trap for silica will be set in that particular place as long as the pH gradient remains constant. Therefore, the silica will be concentrated in one place which results in the formation of chert.

The time of the precipitation and formation of the chalcedonic chert cannot be predicted exactly, but it is certain that it occurred after the dolomitization in the Red Eagle Limestone because of the presence of floating dolomite rhombs.

Dolomitization

The recent discoveries of dolomite precipitating in several places such as in Bonaire of the Netherland Antilles (Deffeyes et al., 1965), on the Bahama Banks (Shinn et al., 1965), and in the Arabian Gulf (Illing et al., 1965) have shed some light on the long controversial problem dolomite formation. Actually, the mineral forming at the above indicated localities consists mainly protodolomite. It is also protodolomite that has been synthesized in laboratories. Siegal (1961) has precipitated protodolomite under temperature and pressure not much different from normal conditions. This has led geologists

Plate 12

1. Slightly silty, ostracod, crinoid, sparse biomicrosparite. Good example of foraminifera (Textularia). There is no evidence of recrystallization. Plain light X25. Red Eagle Limestone (R_5-1)

2. Burrowed, partially recrystallized, bryozoan, ostracod, algae, crinoid, sparse biomicrosparite. An example of Textularia? Note the pisolite grain at the upper left corner. Only partial recrystallization of the matrix. Plain light X25. Red Eagle Limestone (R_6-2)

3. Partially recrystallized ostracod, foraminifera, algae, packed biomicrosparite. The foraminifera in the middle of the photograph has been slightly obliterated by the recrystallization of the matrix in the septal pores. Plain light X25. Red Eagle Limestone (R_1-14)

4. Partially recrystallized crinoid, pellet, bryozoan, algae, packed biomicrosparite. A view of extensive recrystallization of the matrix. Note the microforaminifera in the center (Ammobuculites?). A few fragments of algae. Plain light X25. Red Eagle Limestone (R_1-5)

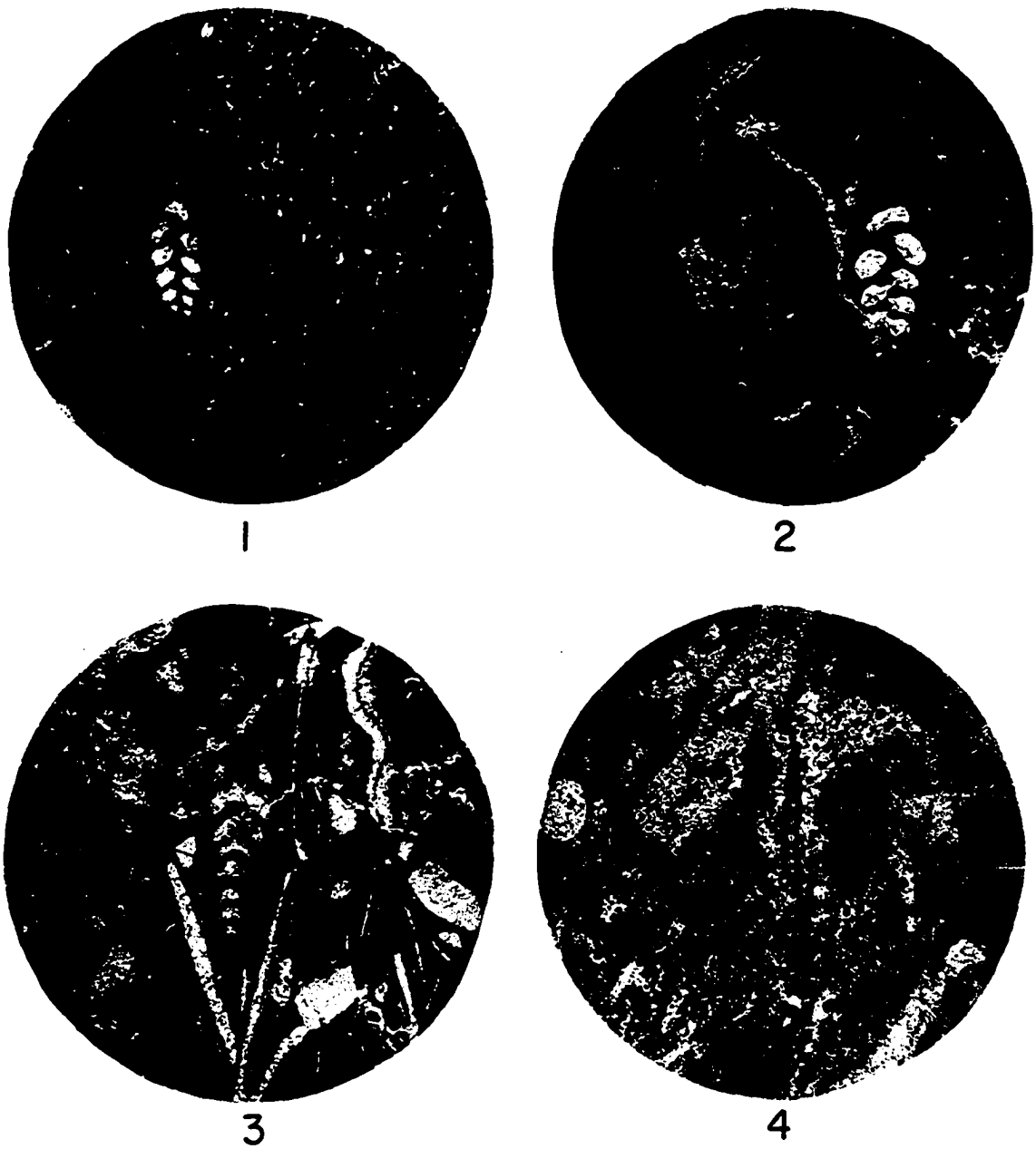

1 2 3 4

PLATE 12

to believe that protodolomite has to pass through some diagenetic changes in order to convert to dolomite. X-ray diffraction analyses of the carbonate sediments in the places investigated by the above authors indicate the occurrence of some true dolomite in those recent sediments. According to those several authors continuous evaporation of sea water brings about the concentration of magnesium relative to that of calcium. Thus dolomite forms at the expense of the pre-existing soft sediment carbonates. This magnesium rich solution will cause diagenetic changes in the recent carbonate sediments and bring about the formation of dolomite. The most recent dolomite reported from these places is found to be about 2500 years old by carbon-14 dating methods. Thus, it seems evident that dolomite has to pass through some diagenetic change to reach its final form. However, the question of time has not been answered and such changes do not necessarily have to occur long after the cessation of deposition. It can take place penecontemporaneously with the deposition of the aragonite and/or calcite.

X-ray diffraction patterns, staining with alizarine red S and petrographic studies of the thin sections have shown that a trace of dolomite is present in many places in the Red Eagle Limestone. X-ray diffraction techniques are the most effective methods for determining the presence of dolomite.

Plate 13

1. Pelsparite. Pellets are of algal origin. No winnowing or sorting is evident. Plain light X25. Red Eagle Limestone (R_4-14).

2. Pelsparite. An example of pellets cemented with sparry calcite. Many pellets are compacted. A few foraminifera can be recognized. Plain light X25. Red Eagle Limestone (R_4-18)

3. Pelsparite. In this example, microforaminifera can be easily recognized among the pellets. Plain light X25. Red Eagle Limestone (R_1-20)

4. Pelsparite. Note the spicules of unknown origin pellets are probably of algal origin. Plain light X25. Red Eagle Limestone (R_5-9)

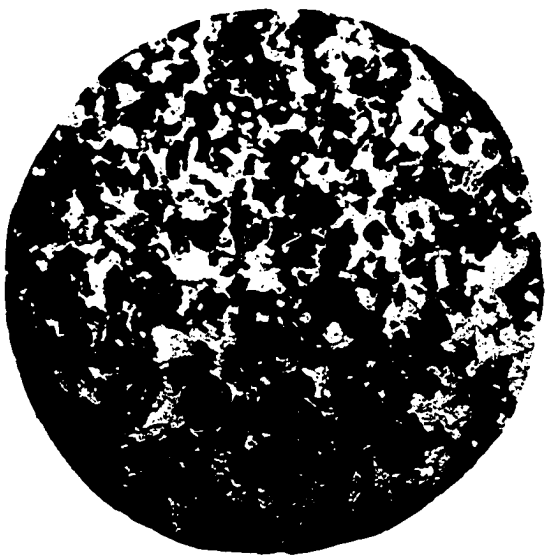

1

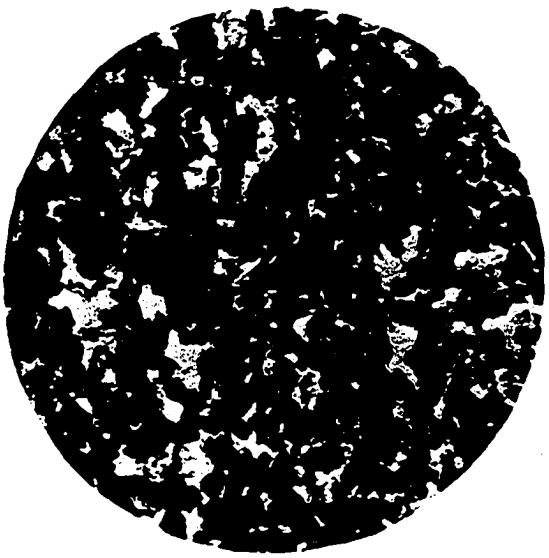

2

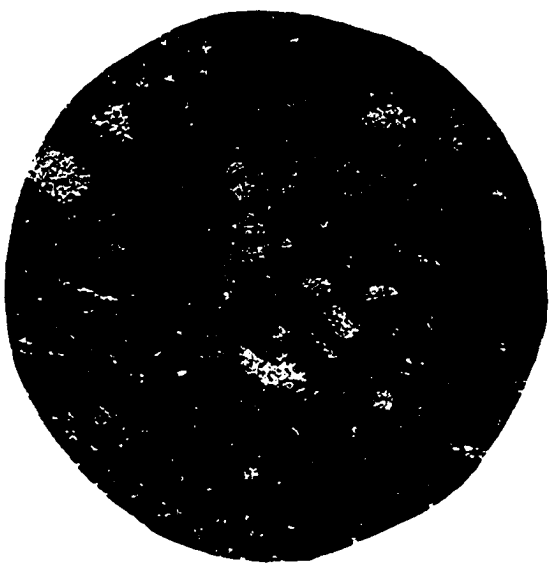

3

4

PLATE 13

Dolomite in the Red Eagle Limestone is scarce in the northern and central parts of the studied area. In these places, dolomite primarily has been detected on the X-ray patterns and seldom as scattered grains in the thin sections and/or in stained samples. The southernmost two measured sections (R_8 and R_9) appeared to be totally dolomitized. The dolomite comprises more than 90 percent of the examined specimens. The dolomite grains range from very coarse to very fine in size and have euhedral to subhedral shapes.

Crinoid fragments and fusulinids are the only two allochemical grains recognized in the dolomitized rocks. The fusulinids are more susceptible to dolomitization than crinoid plates and spicules. The fusulinids in one measured section (R_9) are totally replaced by dolomite. In general, the dolomite grains inside the fusulinid septal pores are coarser than the average dolomite grains in the matrix. The crinoids are only partially effected by the process of dolomitization.

The origin of the dolomite in the Red Eagle Limestone is evident from the nature and types of the fossils preserved in the dolomite. Crinoids and fusulinids are good indicators of the replacement origin of the dolomite. The time of the replacement cannot be predicted, but it is evident that it took place after the deposition of the Red Eagle Limestone and before the silicification (large fragments of dolomite float in the chalcedonic chert).

Recrystallization

The recrystallization process is present in most of the examined thin sections. Some of the thin sections are totally recrystallized (pl. 8, fig. 3). The recrystallization effects the matrix more than the allochemical grains. Of the many allochemical grains, algae are the most susceptible to recrystallization followed by microforams and intraclasts. The obliteration of algal structures on many algal fragments, which consists of white, clear, fine grain-size calcite which has a mosaic texture, is believed to be a result of recrystallization and/or by solution and filling by calcite. Such early stages of recrystallization are actually shown on very few Osagia fragments (pl. 9, fig. 4). Other fossils that are effected by recrystallization are very rare. Only a few echinoderm fragments possess syntaxial recrystallized rims (pl. 10, fig. 3).

The septal pore and autopores of bryozoans are, in many places, filled with a white, clear pseudospar (pl. 8, fig. 2 and 3). Such a gradation in the process of recrystallization can be shown in many of the fusulinid septal pores (pl. 3, fig. 1 and 3). The inner septal pores are always filled with coarse grain calcite and the recrystallization decreases outward away from the proloculus chamber. The structural discontinuity is the main reason for the apparent presence of the pseudospars inside the

Plate 14

1. Bryozoan crinoid biosparite. Fragments of crinoid and bryozoan. Note the foraminifera "fusulinid in the center of the photograph. A major portion of the matrix is not winnowed. Plain light X10. Red Eagle Limestone (R_6-7)

2. Dolomitized fusulinid biosparite. An excellent example of a cross section of a fusulinid completely replaced by dolomite. The ground mass is composed of dolomite grains which are smaller than the dolomite grains replacing the allochemical grains. Plain light X25. Red Eagle Limestone (R_9-2)

3. Dolomitized limestone. Dolomite grains of various size. The grains have not yet developed perfect rhombs. Plain light X25. Red Eagle Limestone (R_9-3)

4. Burrowed, recrystallized, bryozoan, pellet, crinoid, sparse biomicrosparite. Burrows and veins are filled with sparry calcite. Note microforaminifera (Nodosaria?). Plain light X10. Red Eagle Limestone (R_4-3)

1

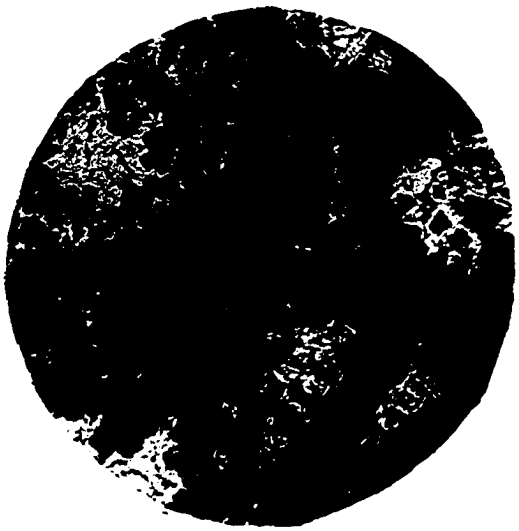

2

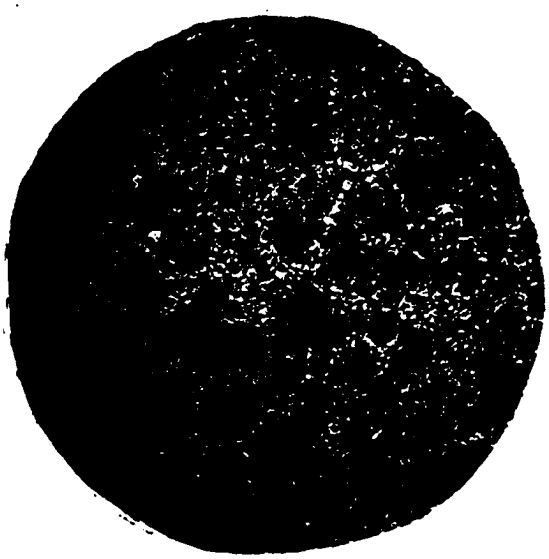

3

4

PLATE 14

autopores. Structural discontinuity has only a limited effect in a few places on the recrystallization of the matrix outside the fossil cavities (pl. 11, fig. 4). Generally, fossil and matrix contacts are the most important structural discontinuities. The size of the pseudospar grains is always coarser near the wall of the shell and decreases toward the matrix. The zone of recrystallization, in many places, is only a fraction of a millimeter in width. Recrystallized calcite grains have a white, clear appearance which makes them difficult to differentiate from similar grains of a different origin. Harbaugh (1961, p. 94) has recognized four types of visibly crystalline calcite in Late Paleozoic limestones: (a) grain-growth calcite, (b) blade calcite, (c) encrusting calcite, and (d) void-filling calcite. The first two types are thought to form through recrystallization. Such criteria for recognizing the grains of a recrystallized origin from those formed by direct precipitation are well described by Bathurst (1959), Harbaugh (1961), and by Orme and Brown (1963). Of the several criteria which characterized grain growth, coarse mosaic texture, irregular grain boundaries, and heterogeneity and irregularity of grain size are the most important.

In the Red Eagle Limestone the gradation in grain size from coarse outside the cavity to very small size inside is characteristic of grain growth calcite in the

matrix. Allochemical grains are commonly found floating in the recrystallized matrix. The cement of the sparry calcite facies in the northern part of the area studied is composed of fine-grained calcite. This makes it difficult to recognize any such recrystallization effect in the cement.

The time of recrystallization in the Red Eagle Limestone cannot be predicted from petrographic studies. Such diagenitic processes could have taken place immediately after the deposition of the Red Eagle Limestone or at any subsequent time.

Cavities

Cavities in the Red Eagle Limestone are common and they are either cavities formed by solution of shells or produced by burrowing organisms. Thus, the second type of cavities are formed before the lithification of the sediment. According to the types of carbonate sediment which fills the cavities, they are divided by Orme et al. (1963, p. 57) into two types: 1) cavities with basal sediments; 2) cavities without basal sediments. In this study four types of cavities are recognized. The first two types are similar to those of Orme's, whereas the other types are cavities with pseudospars, and cavities which are filled only with matrix.

The first type of cavity is the so-called "geopetal" structure. This type of cavity in the Red Eagle Limestone

is associated only with brachiopod shells. In this situation, the shells are filled with matrix after death of the animal. According to Orme et al. (1963, p. 57), the upper part of the matrix in such cavity types is leached away by solution and a layer of sparry calcite fills the void. Mankin (personal communication) suggested that, as a result of either compaction or incomplete filling, a void in the upper part of the cavity can be formed which is filled with a layer of sparry calcite. Actually, the irregular nature of the basal layer does not necessarily indicate leaching as suggested by Orme et al. (1963, p. 57). The irregularities in the upper surface of the basal layer can also form as a result of modification by crystal growth in the upper cavity (Mankin, personal communication). The upper roof of one brachiopod shell is fractured. Although the fractures can result from pressure resulting from crystal growth, fracturing here is believed to originate before the filling of the void by sparry calcite. The evidence for this conclusion is from the lack of any effect of fracturing on the coarse-grained calcite. The straight surface of one calcite grain can be seen extending immediately under the fracture without displacement or disturbance (pl. 4, fig. 4). The collapsed shell may indicate a substantial lithification of the sediment before deposition of sparry calcite in the cavity. Some of the sparry calcite grains in the cavity are as

Plate 15

1. Partially recrystallized, ostracod, foraminifera, brachiopod, algae packed biomicrosparite. Brachiopod partially filled with matrix and the upper portion filled with sparry calcite. Good illustration of geopedal structure. The white area is a burrow filled with sparry calcite. Plain light X25. Red Eagle Limestone (R_1-13)

2. Burrowed, partially recrystallized, algae, sparse biomicrosparites. An example of microspar under high magnification. Plain light X500. Red Eagle Limestone (R_5-5)

3. Bryozoan, sparse biomicrosparite. An example of a bryozoan in microspar. The autopores and the channels of the bryozoan are filled with recrystallized matrix. Note the almost complete absence of recrystallization of the matrix in the ground mass. Plain light X25. Red Eagle Limestone (R_3-2)

4. Burrowed, partially recrystallized, bryozoan, algae pellets, packed pelmicrosparite. Styrolite and fragments of bryozoans. Note the bryozoan to the right side is totally encrusted by osagia. Plain light X25. Red Eagle Limestone (R_1-6)

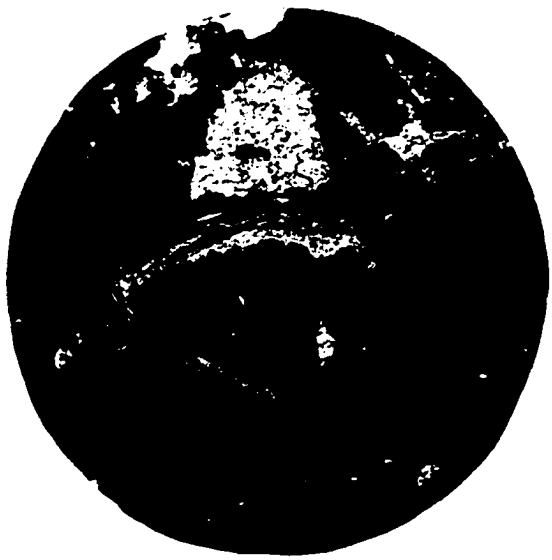

1

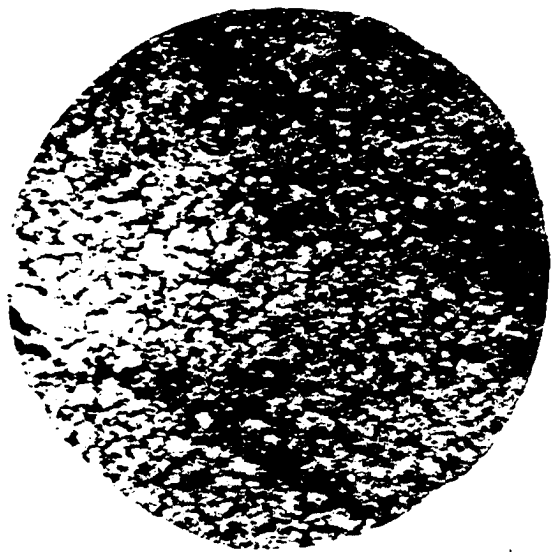

2

3

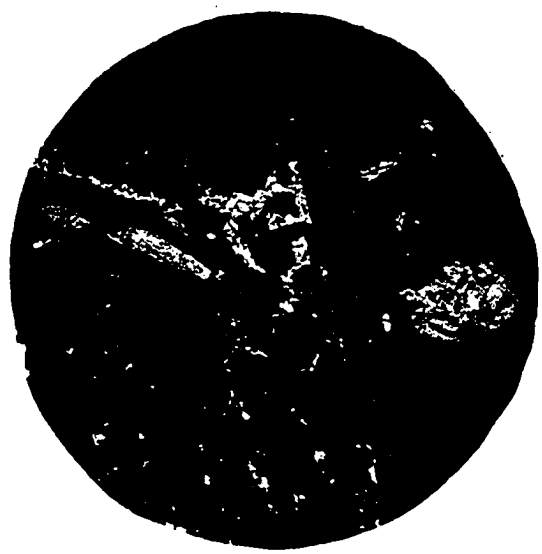

4

PLATE 15

much as 0.8 mm in length.

According to Orme et al. (1963), the second type of cavity is one without basal sediment and these are filled with either a fibrous and/or a sparry calcite mosaic.

In the Red Eagle Limestone burrows and fossil cavities such as brachiopod and ostracod shells are of this type. The time of deposition of sparry calcite is subsequent to burial and probably after lithification of the sediments. Many of the ostracod cavities are filled with a large single grain of sparry calcite which shows a structural continuity with the shell wall.

Filling of cavities with a basal sediment only and without sparry calcite must be penecontemporaneous with the deposition of the Red Eagle Limestone. This cavity type is the least important and lacks evidence of any diagenetic change after the deposition of the Red Eagle Limestone.

The fourth type of cavity is also filled with basal sediment but these have undergone some diagenetic changes. The foraminifera septal pores (pl. 3) and bryozoan autopores (pl. 8) are the most representative of these cavity types. Isolated patches of the original matrix can be seen in many of these cavities. Also the gradation in grain size can be recognized between the pseudospar and the matrix (pl. 3, fig. 3). The pseudospars have a white, clear appearance, and consist of a fine-grained calcite mosaic. The process of recrystallization has taken place

after deposition of the matrix in the cavity, but the exact time for the neomorphism process cannot be determined with certainty.

Burrowing

Burrowing by organisms in the Red Eagle Limestone is common. Such activities are mainly prevalent in the microsparite facies. Fragmentation of the various fossils is believed done by burrowing organisms. This process is observed in many thin sections. In this rock type the fossil fragments are randomly oriented in the carbonate sediment. The fragments are angular and of various sizes. The effect of burrowing and scavenger invertebrate animals in recent carbonate sediments is well discussed by Emery (1953) and Ginsburg et al. (1958). Obliteration of original sedimentary structures by burrowing organisms can be seen in many examples (pl. 15, fig. 4). Many of the cavities in the Red Eagle Limestone which were later filled with white, clear sparry calcite are believed to be formed by burrowing organisms prior to the lithification of the carbonate sediment. But, in many places, these cavities are difficult to recognize from similar patches of calcite of algal origin.

INSOLUBLE RESIDUE

The weight percent of the terrigenous constituents in the Red Eagle Limestone was the main objective of the insoluble residue analysis. Forty-eight samples were selected for this purpose. Thirty-gram samples were crushed to sand size. The samples were dissolved in cold, ten percent hydrochloric acid. The samples were digested for a period of 48 hours. The samples were stirred to aid in the complete digestion of the carbonate minerals. Also, heating is necessary to assure the digestion of dolomite. After four hours, the solution was filtered through no. 30 filter paper. The filter paper was dried for at least 12 hours in a low temperature (78°C) oven to prevent ashing. Each of the insoluble residue samples was weighed and the weight percent obtained. These data are presented in tables 1 and 2.

The insoluble residue was studied under the binocular microscope for particle morphology and x-rayed for the determination of the mineral constituents. In addition, special techniques were employed for the analysis of the clay minerals.

Quartz constitutes more than 95 percent of the silt

Table 1

Weight Percent of Insoluble Residues

Sample	Percent	Sample	Percent
R_1-3	10.00	R_3-4	23.00
R_1-5	9.85	R_3-5	29.00
R_1-8	6.35	R_3-6	18.00
R_1-10	4.50	R_4-1	9.35
R_1-14	0.90	R_4-2	4.82
R_1-19	2.00	R_4-3	4.68
R_1-20	5.60	R_4-4	6.66
R_1-21	9.00	R_4-7	5.00
R_3-1	12.00	R_4-8	4.82
R_3-2	36.90	R_4-9	5.35
R_3-3	5.00	R_4-10	7.40

Table 2

Sample	Percent	Sample	Percent
R_5-1	26.22	R_6-6	19.70
R_5-3	7.32	R_6-8	19.40
R_5-5	63.80	R_6-9	54.00
R_5-6	23.00	R_6-10	20.70
R_5-9	34.00	R_6-11	10.05
R_5-10	25.80	R_6-13	21.80
R_5-12	27.18	R_7-1	25.70
R_5-16	29.00	R_7-2	30.70
R_5-17	22.40	R_8-1	14.00
R_5-18	12.50	R_8-2	36.00
R_6-1	42.00	R_9-1	12.70
R_6-3	27.00	R_9-2	6.20
R_6-5	25.20	R_9-3	10.00

and sand-sized fractions. Other minerals such as feldspar are present only in trace amounts in the southern part of the studied area. Sponge spicules are locally abundant (R_8-2).

There is no consistent pattern of change in the percentage of insoluble residue in most of the measured stratigraphic sections. This is apparently due to the fluctuation in the environment of the deposition between the carbonate and non-carbonate components. In a general manner, there is an increase in the percentage of the terrigenous constituents in a southward direction.

The highest percentage of insoluble residue is 63.5 in sample R_5-5. Those samples which had an insoluble residue content of more than 50 percent are classified as terrigenous rocks (Folk, 1959). In such samples, the insoluble residue is primarily clay minerals. They are therefore classified as calcareous shales. The amount of coarse terrigenous grains increases southward. From the petrographic study of thin sections and the analysis of the insoluble residues with the binocular microscope, only clay and fine silt make up the bulk of the insoluble residue in the north and north-central parts of the studied area.

The average amount of insoluble residue in the microsparite facies is greater than that in the sparry calcite facies in southern Kansas and northern Oklahoma. The

terrigenous consitutents in these two facies consist mainly of clay minerals and very fine silt-size quartz. Although the sparry calcite facies is a very thin unit, it is the best developed of the two facies in some localities (R_6 and R_7). The sparry calcite facies in these localities contains a considerable amount of insoluble residue which consists of fine-grained terrigenous quartz and lesser amounts of clay minerals. In measured section R_8, which is a totally dolomitized limestone, authegenic chalcedonic quartz comprises most of the insoluble residue. The clay minerals as they have been analyzed by x-ray diffraction techniques consist mainly of illite with minor amounts of chlorite. This is, however, a consistent feature with the clay minerals of the shale beds in the Red Eagle Limestone. The quartz grains are angular and, in many places, they are poorly sorted. In the limestone, except in a few places, the quartz grains are homogenously distributed throughout the rock.

The following general conclusions can be drawn from the study of the insoluble residue of the Red Eagle Limestone:

1. The lack of a consistent pattern of increase or decrease in the insoluble residue in an individual measured section is due mainly to a fluctuation of the depositional environment.

2. There is a general increase in the amount of the

insoluble residue from Kansas to Oklahoma.

3. The size of the terrigenous constituents increases southward.

4. Except for the chalcedonic quartz and sponge spicules in measured section R_8, the insoluble constituents are terrigenous grains of various sizes and mineral composition.

5. Illite and chlorite minerals constitute most of the clay-size fraction, and quartz is the major constituent of the silt- and sand-size fractions.

6. The microsparite facies contains more insoluble residue than the sparry calcite facies in many places of the area studied.

X-RAY DIFFRACTION

One of the primary values of x-ray diffraction in a study of carbonate petrography is the determination of the presence of dolomite. In the Red Eagle Limestone, dolomitization is abundant in the extreme southern part of the studied area (measured section R_8 and R_9). In these measured sections the dolomite can be seen with the patrographic microscope and with staining techniques. Such methods become inadequate when dolomitization is present in trace amounts as it is in southern Kansas and northern Oklahoma. A trace of dolomite is present in many of the examined samples but it can only be detected on the x-ray diffraction patterns.

Each sample is crushed into very fine powder which is concentrated by sieving through an 80 mesh sieve. The sample then is dusted on a vaseline-coated glass slide and x-rayed using Cu K-alpha radiation, with a Norelco x-ray diffraction unit at a setting of 35 Kv and 18 ma. The various intensities of the first-order diffraction peaks of calcite, dolomite, and quartz are at 3.00A, 2.89A, and 3.34A respectively. Figure 5 and 6 are x-ray diffraction patterns showing patterns of these minerals. Notice the

complete absence of dolomite in sample R_6-6 (fig. 5) and the complete absence of calcite from the pattern of sample R_8-1 (fig. 6).

X-ray diffraction analysis was also used as a supplementary method for the study of the insoluble residues, although the petrographic and binocular microscopes were the basic tools used. X-ray diffraction gives a rapid method of determination of the various constituents present. It is also the most effective method available for the analysis of the clay-size fraction of the insoluble residue. The insoluble residue is ground to a fine powder and concentrated by spreading the powder on a vaseline-coated slide and x-rayed under the conditions previously described. Quartz was found to be the main constituent of the insoluble residues (fig. 7).

The clay minerals of the Red Eagle Limestone were determined by x-ray diffraction. Thirty samples from the shale intervals were ground to a fine powder. Approximately one gram of each sample was dispersed in distilled water. The suspension was then placed in an ultrasonic transducer for 20 minutes. Two sedimented slides were prepared for each sample; one slide was treated with ethylene glycol for 24 hours at temperature of 60°C. Fifteen samples of the insoluble residues were treated in a similar manner to identify the clay minerals.

Figure 5 and 6

X-RAY DIFFRACTION PATTERNS OF SOME CARBONATE SAMPLES FROM THE RED EAGLE LIMESTONE.

X-ray diffraction patterns of powder samples from the Red Eagle Limestone illustrating the diffraction maxima of calcite, dolomite and quartz. Note the complete absence of the dolomite peak in sample R_8-1. Cu K-alpha radiation, Ni filtered at a setting of 35 Kv and 18 ma.

Figure 5

A. Measured Section R_6, six feet from the base of the Red Eagle Limestone exposure.

B. Measured section R_1, 20 feet from the base of the Red Eagle Limestone exposure.

C. Measured section R_3, 5 feet from the base of the Red Eagle Limestone exposure.

Figure 6

A. Measured section R_4, 16 feet from the base of the Red Eagle Limestone exposure.

B. Measured section R_8, 3 feet from the base of the Red Eagle Limestone exposure.

C. Measured section R_8, one foot from the base of the Red Eagle Limestone exposure.

DEGREES 2θ

Figure 5

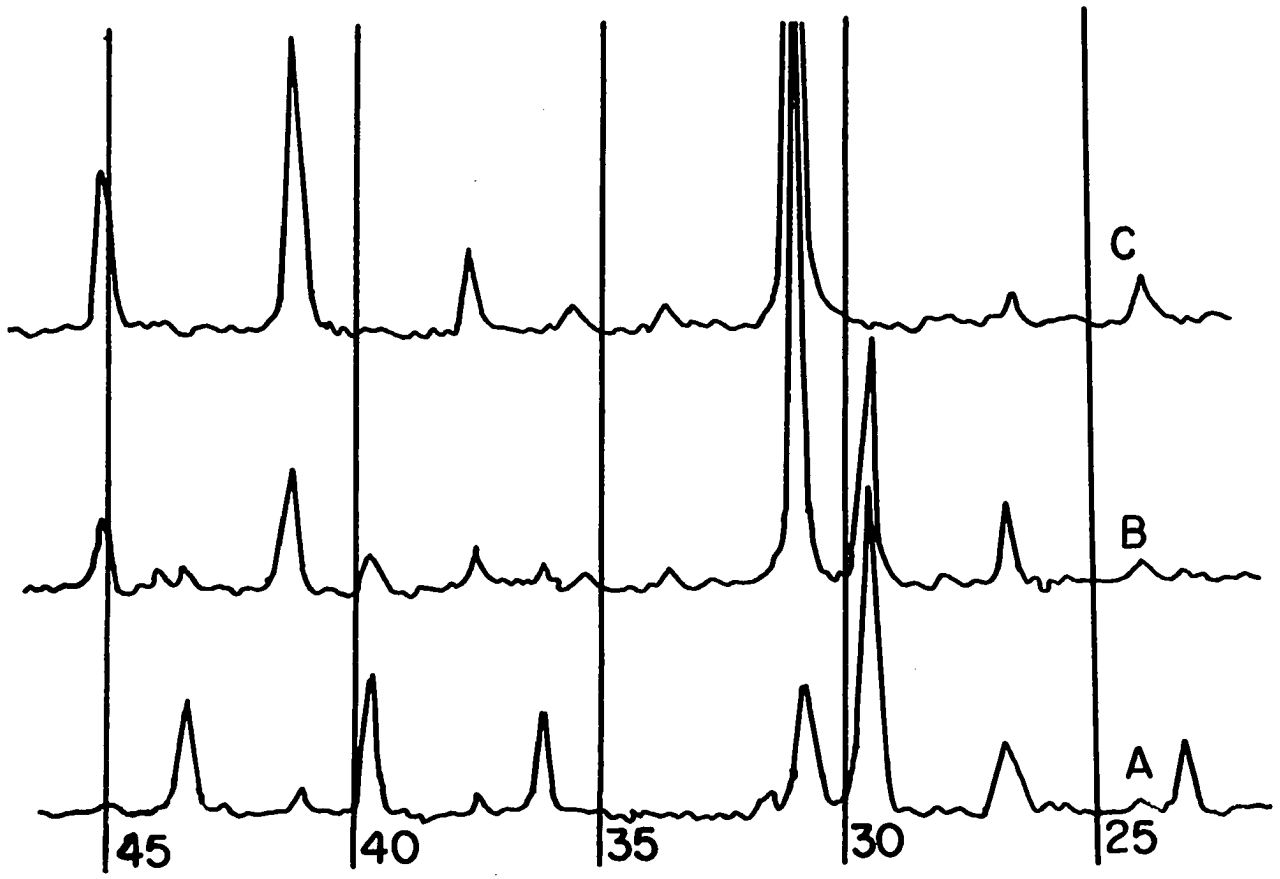

Figure 6

Figure 7

X-RAY DIFFRACTION PATTERNS OF SOME INSOLUBLE RESIDUE SAMPLES FROM THE RED EAGLE LIMESTONE

Powder samples of some insoluble residue samples illustrating the diffraction maxima of quartz which is the most common terrigenous mineral other than clays in the Red Eagle Limestone beds. Cu K-alpha radiation, Ni filtered at a setting of 35 Kv and 18 ma.

A. Measured section R_1, 9 feet from the base of the Red Eagle Limestone exposure.

B. Measured section R_3, 3 feet from the base of the Red Eagle Limestone exposure.

C. Measured section R_6, 7 feet from the base of the Red Eagle Limestone exposure.

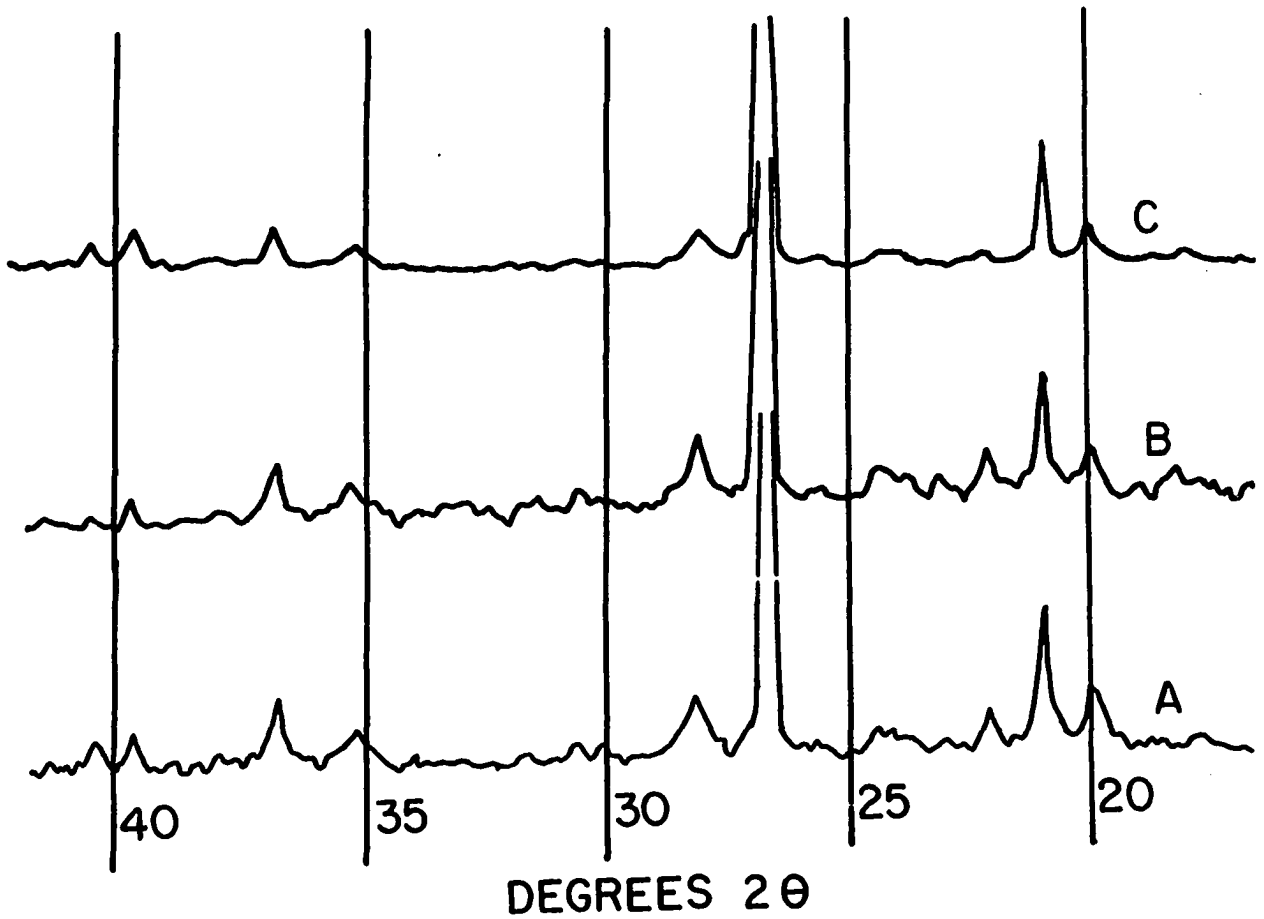

Figure 7

Illite

Illite is the most abundant clay mineral in the interbedded shaly laminae of the Red Eagle Limestone. Basal reflections from (001), (002), and (003) are approximately at 10A, 5A, and 3.3A. These are characteristic of the mineral illite on x-ray diffraction patterns (fig. 8). Illite is found in all the examined samples of the shales. In southern Kansas and northern Oklahoma, illite is the most important mineral constituent of the terrigenous rocks of the Red Eagle Limestone. Illite is also found as the major mineral constituent of the clay fraction in the insoluble residues.

The 10A reflection is an assymetrical peak which is an indication of a degraded illite. The presence of mixed-layers of illite-montmorillinite and chlorite-montmorillinite contribute to the asymmetry of the (001) reflections.

Chlorite

Chlorite is the second most important clay mineral in the shaly beds. Chlorite is present in many but not all of the examined samples. In the insoluble residue, the relative intensities of the (001 and 002) chlorite peaks vary in different samples. This is probably due to the fact that chlorite is slightly soluble in hydrochloric acid. However, these chlorite peaks are present in some of the insoluble residue diffraction patterns. The diminution of the 7A peak and increase in the intensity of the

Figure 8

X-RAY DIFFRACTION PATTERNS OF CLAY MINERALS IN SOME OF THE INSOLUBLE RESIDUE SAMPLES FROM THE RED EAGLE LIMESTONE

X-ray diffraction pattern illustrating diffraction maxima of illite and chlorite clay minerals in some insoluble residue samples. Cu K-alpha radiation, Ni filtered at a setting of 35 Kv and 18 ma.

A. Measured section R_4, 15 feet from the base of the exposure of the Red Eagle Limestone.

B. Measured section R_2, 4 feet from the base of the exposure of the Red Eagle Limestone.

C. Measured section R_5, one foot from the base of the exposure of the Red Eagle Limestone.

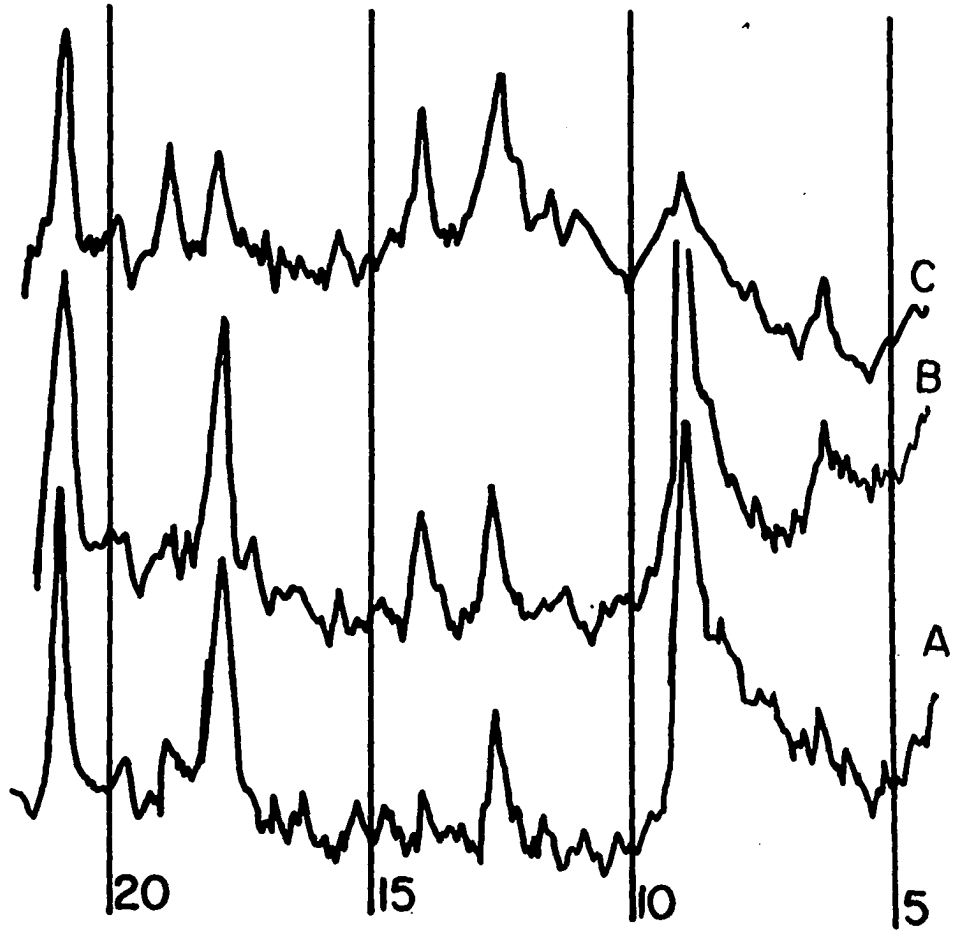

Figure 8

Figure 9

X-RAY DIFFRACTION PATTERNS SHOWING CLAY MINERALS OF THE RED EAGLE LIMESTONE

Sedimented slides showing diffraction maxima of illite and chlorite. Cu K-alpha radiation, Ni filtered, at a setting of 35 Kv and 18 ma.

A. Measured section R_3, four feet from the base of the exposure of the Red Eagle Limestone.

B. Measured section R_4, four feet from the base of the exposure of the Red Eagle Limestone.

C. Measured section R_5, four feet from the base of the exposure of the Red Eagle Limestone.

D. Measured section R_8, three feet from the base of the exposure of the Red Eagle Limestone.

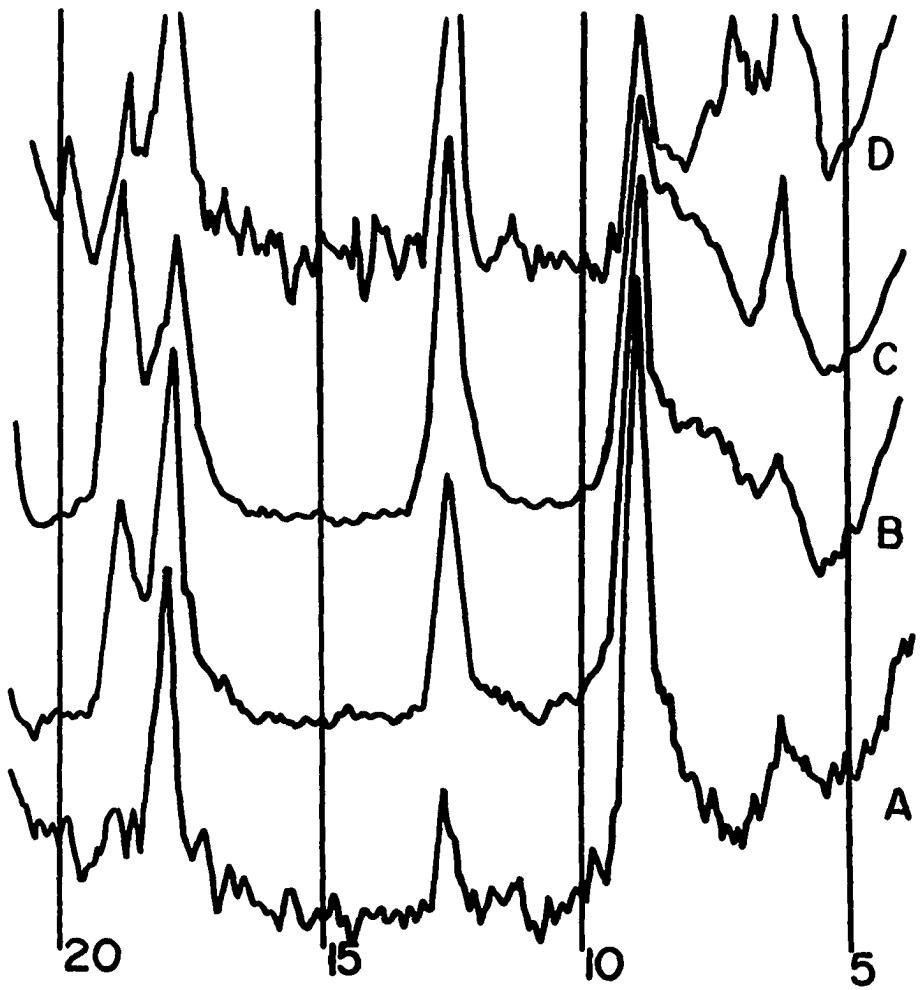

Figure 9

Figure 10

X-RAY DIFFRACTION PATTERNS OF CLAY MINERALS FROM THE RED EAGLE LIMESTONE

(A) Slide heated, (B) glycolated and (C) sedimented to 550°C. Note the similarity of the illite peaks and the complete elimination of the 7A peak (002), and the increase in the intensity of the 14A peak (001) of chlorite on heating to the above temperature.

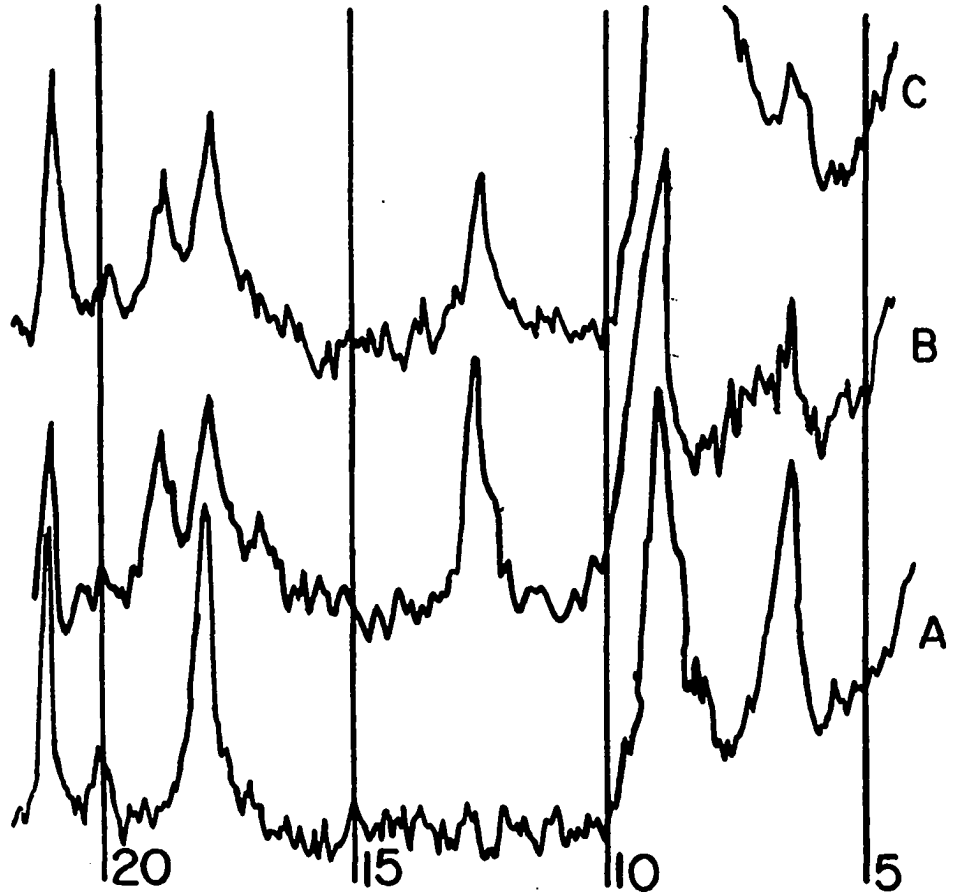

Figure 10

14A on the heating the sample in an oven at 550°C is a positive indication of chlorite as opposed to kaolinite. The lack of expansion of the 14A peak on treatment with ethylene glycol will differentiate chlorite from montmorillinite.

Montmorillonite

Montmorillonite is found only in trace amount. There is no consistent pattern to the distribution of montmorillonite; it is found in few samples in scattered localities. Other trace amounts of clay minerals such as mixed-layer illite-montmorillonite and chlorite-montmorillonite (R_8-3), are rare and are detected on few x-ray patterns.

TRACE ELEMENT ANALYSIS

Semi-quantitative spectrochemical analysis was carried out on 30 samples from the Red Eagle Limestone. The samples were selected from the petrographic study. The spectrochemical analyses were performed with the assistance of Mr. Kenneth Sargent, graduate student at the University of Oklahoma.

The samples were ground to less than 200 mesh (74 u). Each sample was diluted 1:9 with spectrographic grade graphite and homogenously mixed on an automatic shaker. Ten milligrams of each sample were loaded on a spectrographic graphite electrode and burned to completion in a DC arc of 5 ampers. A Jarrel-Ash, 1.5 meter, Elbert mount spectrograph was used in the analyses. The spectra was recorded on 35 mm film and read on a Jarrel-Ash microphotometer. The spectra of the samples were compared with standard film which was made for this purpose.

Trace elements which are thought to be important for the study were selected after a thorough scanning of a few carbonate samples from the Red Eagle Limestone. In this manner only trace elements which can be read from the spectra were selected for the study. The abundance of these trace elements is recorded in table 3.

Table 3

Sample	Concentration of the elements in parts per million										
	B	Ga	Ti	Sn	V	Cu	Zr	Ni	Sr	Mn	Cr
R_1-3	12	ND	360	18	ND	ND	1	1	ND	ND	ND
R_1-6	ND	3	240	52	12	8	1	ND	500	135	2
R_1-5	31	30	340	28	1	1	21	18	300	340	7
R_1-8	ND	6	580	110	16	9	3	20	500	390	9
R_1-10	ND	2	140	10	4	ND	ND	ND	650	375	3
R_1-20	ND	3	760	ND	17	ND	3	ND	510	460	6
R_2-1	ND	2	600	50	5	10	1	ND	510	128	1
R_2-2	ND	5	660	94	2	ND	3	16	560	570	1
R_2-4	105	33	ND	8	1	10	114	26	510	250	16
R_2-5	28	4	ND	14	23	5	3	13	500	450	8
R_3-1	ND	4	210	45	27	13	4	10	590	500	5
R_3-4	ND	6	64	12	6	2	ND	17	550	194	1
R_3-6	ND	1	180	22	8	1	1	16	520	225	4
R_3-7	ND	ND	25	8	5	3	2	10	540	300	4
R_3-9	ND	2	158	46	10	212	1	ND	510	280	1
R_4-7	158	47	ND	16	2	5	108	31	530	156	39
R_4-8	35	3	ND	5	12	89	16	23	150	370	14
R_4-11	32	21	ND	16	17	3	17	19	100	390	16
R_4-13	38	3	ND	9	5	11	1	ND	540	188	4
R_4-18	ND	1	290	ND	ND	ND	1	ND	60	155	ND
R_5-2	ND	2	510	170	11	58	3	22	500	207	5
R_5-3	57	6	1000	56	27	11	49	12	820	445	20
R_5-7	45	18	ND	9	10	2	7	18	100	265	12
R_5-10	170	9	ND	787	10	23	9	20	1000	308	42
R_5-12	32	4	ND	27	7	67	1	ND	820	159	3
R_5-15	ND	4	1000	225	19	7	410	62	650	1000	14
R_8-1	155	9	ND	1	6	51	1	10	410	280	4
R_8-2	ND	4	2000	52	18	32	5	16	150	1000	9
R_8-3	ND	10	750	120	13	39	34	52	200	1000	10
R_8-4	ND	8	1420	21	1	39	1	ND	250	1000	3

ND: Not detected

The main purpose of the semi-quantitative spectrographic analyses was for the determination of the relation of the trace elements to diagenetic processes and ad possible indicators for the environment of deposition.

Boron

The boron content in the Red Eagle Limestone ranges from zero to 70 ppm and the average amount is 31 ppm. Boron has been used in the determination of the paleosalinity and thus the environment of deposition of the sedimentary rocks (Keith et al., 1959, p. 45). Marine sedimentary rocks are found to contain more boron that similar fresh water deposits (Keith, 1959). This is explained by the higher concentration of boron in the ocean. However, unlike other sedimentary rocks, marine carbonate sediments contain a very small amount of boron (Goldschmidt, 1962, p. 287). According to Goldschmidt, the average amount of boron in limestone is 10 ppm and it may reach as low as 5 ppm in dolomite rocks. No boron was detected in the dolomite rocks of the Red Eagle Limestone (R_9-1, 2 and 3). The low boron content in the carbonate rocks is thought to be mainly due to leaching of boron with time (Goldschmidt, 1962, p. 287).

Plotting the relation between the boron content and the amount of insoluble residue (fig. 11) shows a linear relationship between the two in the Red Eagle Limestone. Thus, it is apparent that the boron content of the Red

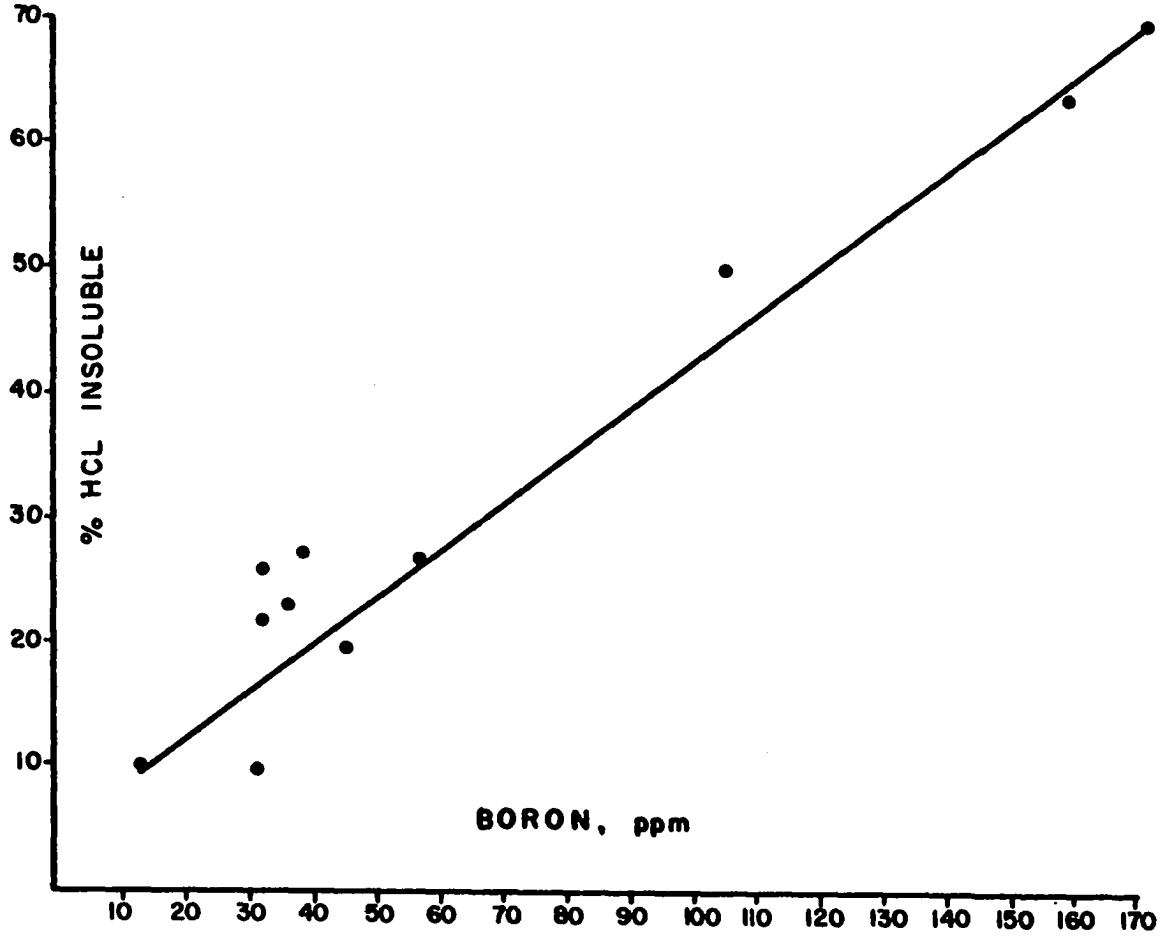
70
60
50
40
30
20
10
% HCL INSOLUBLE
BORON, ppm
10 20 30 40 50 60 70 80 90 100 110 120 130 140 150 160 170

Figure II

Eagle Limestone is concentrated in the insoluble residue fraction (clay minerals). Because the present analyses were not made on the clay mineral fraction alone, the amount of the boron in the clay fraction cannot be predicted with accuracy. Boron is absorbed mainly on clay surfaces and only minor amounts are substituted for the aluminum in the silica tetrahedral layer of illite (Degens, 1964, p. 40).

Copper

The amount of copper ranges from less than one to 212 ppm. The average amount is 24 ppm; about 83 percent of the samples contain less than 50 ppm. In the Red Eagle Limestone there is no relationship between the amount of copper and the insoluble residue.

Copper may be adsorbed by clay minerals and quartz (Heydenann, 1959) and the adsorption capacity of clay increases with an increase in pH as well as copper concentration in the environment. Copper also has the ability to combine with organic matter in the protein hemocyanic and various other organic functional groups. An increase in copper content in the sediment with a decrease in the particle size was noticed by Ginsburg et al. (1960).

Riley (1937 in Goldschmidt, 1962, p. 187) studied the relation of copper to various organic groups. According to Riley, copper can be removed from sea water by organic matter, and during periods of production a very large

fraction of copper may be bound with organic matter. Thus, the concentration of copper from place to place within the Red Eagle Limestone, may be related to variations in the organic content.

Gallium

Gallium is currently being investigated as an environmental indicator (Keith et al., 1959). Unlike boron, the total amount of gallium in sea water is low. Thus, sediments being deposited in marine environments would be expected to contain a minor amount of gallium.

Goldschmidt (1962, p. 328) indicated that the amount of gallium in marine carbonates is low with an average of 5 ppm, and the main distribution of gallium in such rocks is concentrated in the associated hydrolysate sediments. The mean value of the gallium in the Red Eagle Limestone is 8.2 ppm which is slightly above the value predicted by Goldschmidt. Migdisov and Borrisenok (1965) indicated that the content of the gallium is directly proportional to the clay content. The presence of a high amount of clay in the Red Eagle Limestone probably is the main reason for the high gallium content.

Manganese

One of the important studies in the area of the geochemistry of manganese was done by Ronov and Ermishkina (1959). According to Ronov and Ermishkina there will be

an increase in the amount of manganese from sandstone to clay and to carbonate. Such variations in the amount of the manganese is well demonstrated in a humid climate. Humid climate solutions are highly acid due to high concentrations of organic matter. All the manganese that can be removed from the continent during weathering can be carried and transported seaward. Rivers that discharge into the sea are able to dilute the sea water for a greater distance during intervals of humid climates. Thus, there will be a gradual change in the pH to an alkaline condition and thus manganese is concentrated seaward. However, in arid climates, the divalent manganese will be oxidized and converted into immobile trivalent manganese (Mn^{+3}) which cannot be carried away due to low stream discharge. Thus, carbonate rocks formed in arid climates will contain smaller amounts of manganese than those formed in humid climates. The analyses of 30 samples show ranges in the amounts of manganese from zero to 1000 ppm, with an average of 381 ppm.

The average of manganese in humid climates as reported by Ronov (1959) for 3,967 carbonate rock samples was found to be 810 ppm, whereas 6,000 carbonate samples from arid climates were found to be 320 ppm. The value of 381 ppm obtained for thirty samples of the Red Eagle Limestone is about 60 ppm higher than the value reached by Ronov and Ermishkina. Such a discrepancy could arise from

the smaller number of analyzed samples.

In the Red Eagle Limestone the maximum value of 1000 ppm is found only in four samples which are either totally or partially dolomitized. A higher manganese concentration in dolomitized rocks is also reported by Mogharabi (1966). In carbonate sediments, Mn^{2+}(0.81 A) may become enriched in the sediment due to the replacement of Ca^{2+}(1.08 A) ions (Rankama and Sahama, 1950, p. 648).

Such an ordered compound between Ca^{2+} and Mn^{2+} such as Kutnahurite ($CaMn(CO_3)_2$) is well established (Frondel and Bauer, 1955, p. 757). They also concluded that such ordering is possible between Mg^{2+} and Mn^{2+} because the radius difference between the last two is very similar to that of Ca and Mg. However, Palache et al. (1951) indicated that in such binary system of manganese and magnesium, manganese is more likely to be substituted, because it has a larger radius. Thus it is not possible to suggest that the high content of manganese in the dolomite beds of the Red Eagle Limestone results from substitution of manganese for the magnesium. It is quite possible that manganese has replaced the calcium in the dolomitized beds.

Strontium

Strontium has received more attention in the study of carbonate geochemistry than any other trace element. This

arises from the controversial calcite-aragonite problem. The great abundance of aragonite in recent carbonate mud and its almost complete absence in ancient carbonate rocks has led some geologists to over emphasize the role of strontium on the stability and precipitation of aragonite at the present time. Fyfe (1965, p. 6) on a thermodynamic basis has indicated that impurities such as strontium favor the formation of aragonite over calcite, because it has the least free energy and thus it is more stable than calcite. The orthorhombic structure of aragonite is more favorable for the large strontium radius (1.27) than the rhombohedral calcite. It is not certain whether the presence of strontium ions in the environment is the main reason for the formation of aragonite or the presence of the aragonite mineral is the main factor for the incorporation of the strontium its suitable structure. Degens (1965, p. 114) has suggested that certain trace constituents such as strontium have no controlling influence on the primary mineralogy, and the presence of greater amounts of strontium in the crystal lattice of aragonite as compared to calcite has presumably structural reasons because strontiumite ($SrCO_3$) is isostructural with aragonite.

The loss of strontium during diagenesis with the transformation of aragonite to calcite is a well established fact from several analyses made on recent and old carbonate rocks (Vinegradov et al., 1956, p. 42; Turekian,

et al., 1956, p. 293; Kahla, 1965, p. 849).

In the Red Eagle Limestone, the amount of strontium calculated from the present analyses range from 60 to 1000 ppm. Only one sample (R_5-10) contains 1000 ppm of strontium.

Recrystallization of very finely crystalline calcite to pseudospar is present in all the examined thin sections of the Red Eagle Limestone. This makes it difficult to visualize the relationship between strontium and the process by recrystallization. Therefore, no definite conclusions can be drawn from the present analyses.

Vinogradov et al. (1952, in Craft, 1960, p. 35) indicated a loss of Sr^{++} from fossils during recrystallization in rocks from the Russian platform. Also, Sternberg et al. (1959, p. 81) found a significant difference between the strontium content in a recrystallized (Back-Reef) and nonrecrystallized (Fore-Reef) calcite. In the Red Eagle Limestone, recrystallization is found mostly in the matrix and only trace amounts of intraclasts and algae have shown minor amounts of recrystallization. However, Kahle (1965, p. 854) found no trend between the amount of strontium and recrystallization in 200 analyzed samples. Such a conclusion was also reached by Mogharabi (1966, p. 126). Such negative relationships between strontium and diagenesis may be apparent for the Red Eagle Limestone, but it is difficult to confirm.

The few analyzed dolomite samples have shown a smaller content of strontium than the average limestone. Goldschmidt (1962, p. 248) has indicated that the amount of strontium in dolomite is small due to the process of dolomitization of the original limestone where strontium ions are more effectively being replaced by magnesium than calcium, because of their larger radius. Dolomite which contains a large amount of celestite has larger amounts of strontium concentrated in the salt. Celestite was not detected on the x-ray patterns nor noticed in the thin sections of the Red Eagle Limestone.

Titanium

The titanium content of the Red Eagle Limestone ranges from less than 25 ppm to more than 2000 ppm. The mean value for titanium is 381 ppm. According to Ostroumov (1956) the distribution of titanium in sediments is controlled mainly by the amount of titanium delivered to the sea in clastic minerals. Degens (1965, p. 90) has indicated that the bulk of titanium in the sediment is incorporated in the clay minerals and also may be incorporated in various other minerals such as rutile, anatase, and brookite. In the Red Eagle Limestone there is no positive relationship between the percentage of the insoluble residue and titanium. This could be related to local concentration of some titanium-bearing minerals and as inclusions in quartz.

Vanadium

The vanadium content of the 30 analyzed samples from the Red Eagle Limestone ranged from less than one to 27 ppm with an average of 10.5. There is no significant difference in the vanadium content of the dolomite and limestone samples.

As indicated by Goldschmidt (1962, p. 498), the amount of vanadium in limestone is low except where clay or bituminous substances are present. The average amount of vanadium in the Red Eagle Limestone is equal to the (10 ppm) vanadium average given by Jost (in Goldschmidt, 1962, p. 468) for limestones. The vanadium content of the Red Eagle Limestone is probably concentrated in the clay minerals.

Zirconium

The average amount of zirconium in the Red Eagle Limestone samples is 27 ppm. The zirconium content ranges in amount from less than one to 410 ppm. Most of the zirconium is believed to be concentrated in the insoluble residue. The relation between the percentage of insoluble residue in the limestone and the amount of zirconium is illustrated by Adams and Weaver (1958) as a linear relationship; such a relationship is also confirmed by Mogharabi (1966). In both places, the relationship between the amount of zirconium and the percentage of insoluble residue is based on only eight analyzed samples in the first case

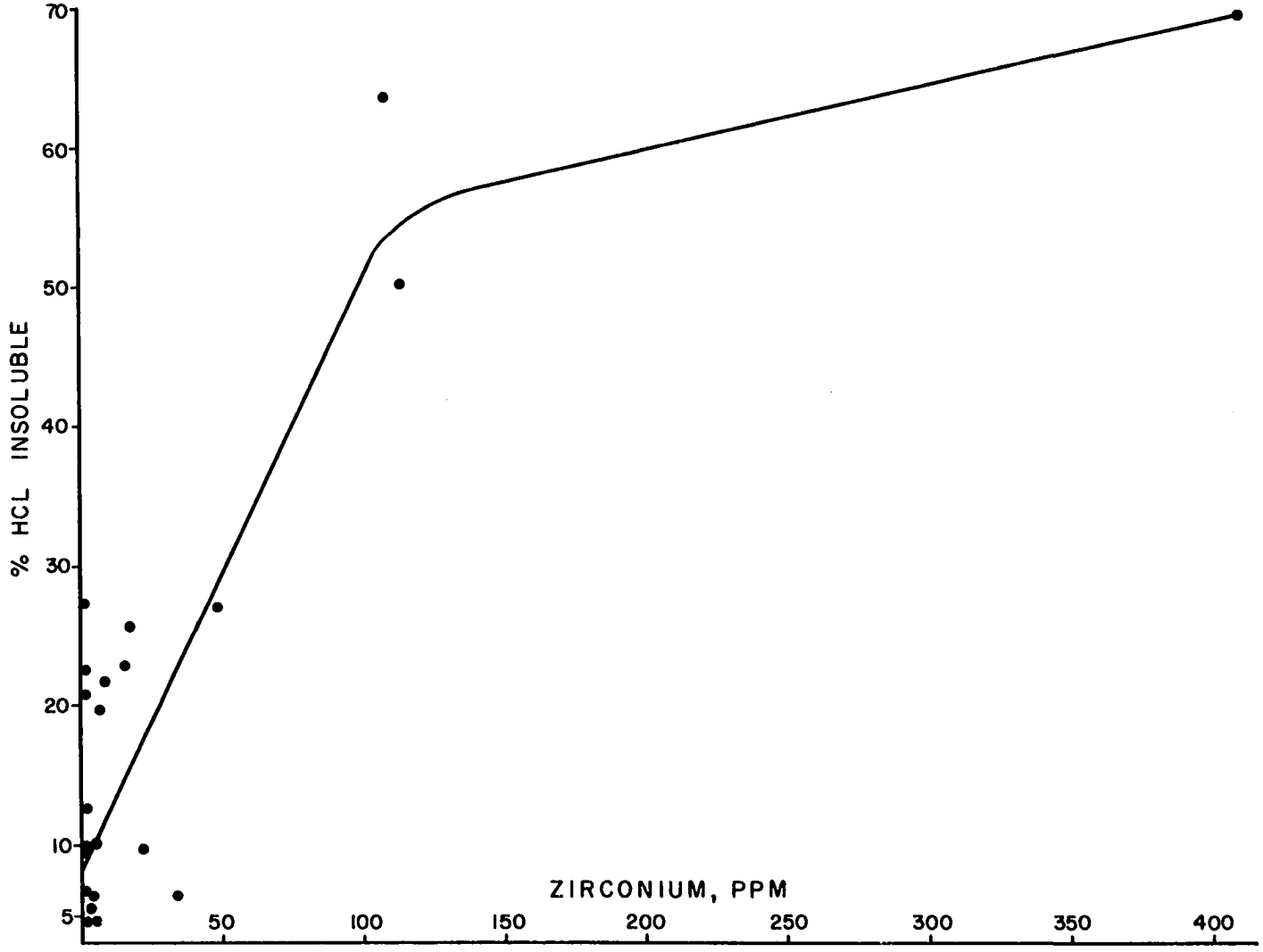
70
60
50
40
30
20
10
5
% HCL INSOLUBLE
50
100
150
200
250
300
350
400
ZIRCONIUM, PPM

Figure 12

and five in the other. Mogharabi has ignored many of the samples with insoluble residues as high as 53 percent and contained no significant amount of zirconium. Of the analyzed samples of the Red Eagle Limestone, 85 percent contained less than 25 ppm of zirconium. Most of these samples contain less than 25 percent insoluble residue. Although there is a relationship between the amount of zirconium and that of the insoluble residue, there is some scatter of points. Plotting of a large number of points by the Geological Survey of Great Britain (in Graf, 1960) has shown a wider scatter of points, and that region of high zirconium content and low insoluble residue percentage is essentially free of points (i.e., at 0 percent insoluble residue and 25 percent zirconium, and at 20 percent insoluble residue and greater than 150 ppm zirconium).

Of the present analyses one can see that 0-4 percent insoluble residue zirconium is completely absent and samples which have insoluble residue values of 4-26 contain no greater than 50 ppm of zirconium. Zirconium greater than 100 ppm is found only in samples which have greater than 50 percent insoluble residue (fig. 12 and 13). The entire zirconium content of the carbonate rocks is apparently concentrated in the insoluble residue in the clay minerals, zircon, Zr-bearing rutile, sphene, and apatite (Degenhardt, 1957). In the Red Eagle Limestone, zirconium is believed to be concentrated in the clay minerals, because of the

Figure 13

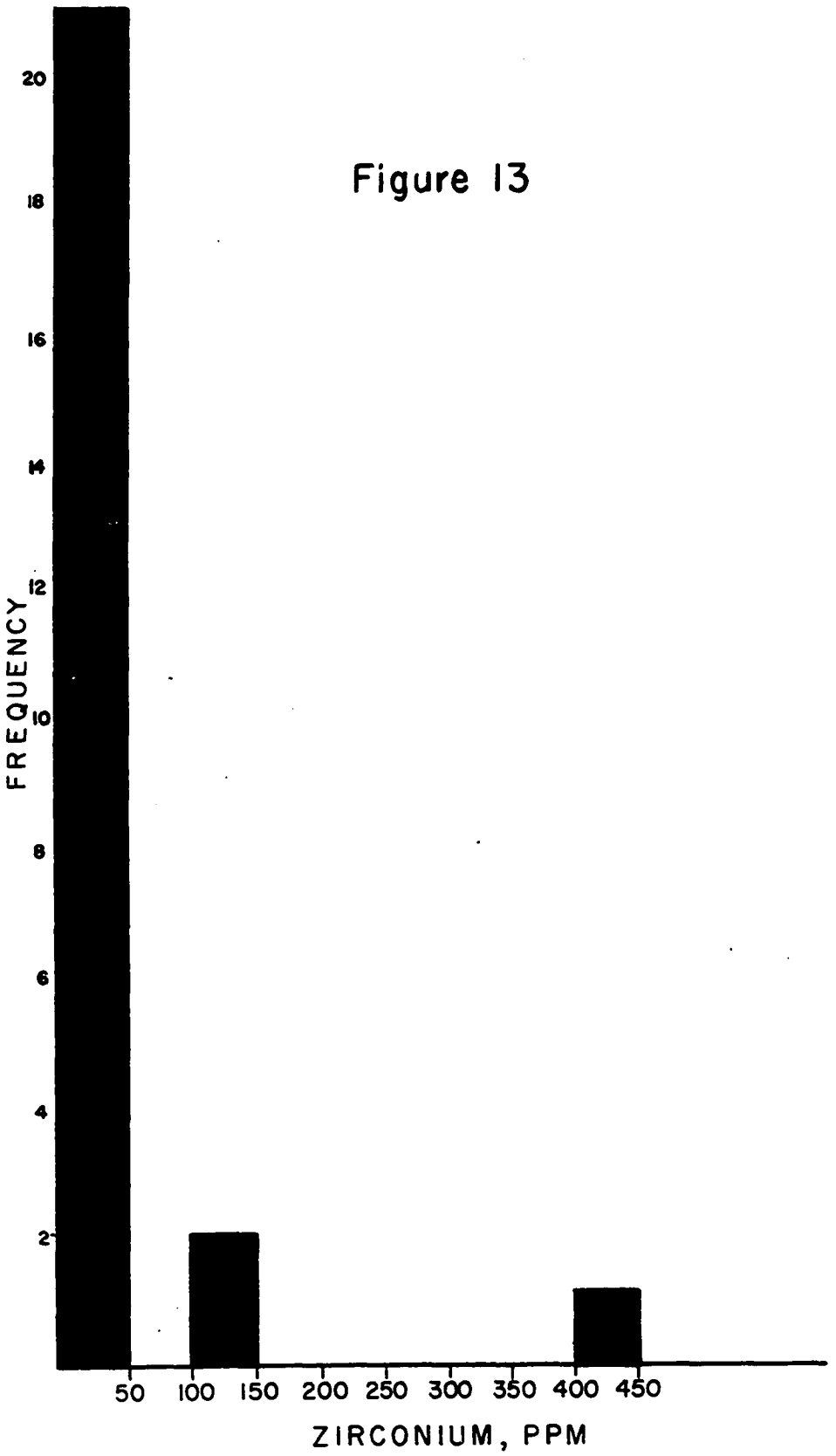
FREQUENCY
20
18
16
14
12
10
8
6
4
2
50
100
150
200
250
300
350
400
450
ZIRCONIUM, PPM

lack of other zr-bearing minerals. Adsorption on the clay minerals is the most probable mechanism for the concentration of the zirconium in the insoluble residue.

Other trace elements such as nickel and chromium have an average of 14 and 9 respectively. The amount of these trace elements from the present analyses of the carbonate rocks of the Red Eagle Limestone is close to the value reported by Craft (1960, p. 20 and 27). These elements are probably concentrated in the impurities with the insoluble residue, however, adsorption is excluded as a mechanism for pure concentration from sea water (Krauskopf, 1956, p. 7). There is no such relationship between nickel and dolomite in the present analyses. Such a positive relationship also has been answered in a negative fashion by Goldschmidt (1962, p. 676).

THE ORIGIN OF THE MICROSPAR

One of the most important characteristics of the Red Eagle Limestone is the presence of microspar as a major constituent of the limestone. The origin of the microspar is still uncertain. The uncertainty arises mainly from the fact that aragonite and only a small amount of calcite constitute the bulk of the recent carbonate sediments. The changes that are associated with the transformation of aragonite to calcite are not yet fully understood.

Folk (1965, p. 40) observed microspar in many Pennsylvanian limestone rocks as isolated patches in a micrite matrix. As a result of this observation he predicted that the microspar originated as a product of neomorphism from the micrite. Although Folk did not commit himself to a position of accepting either recrystallization or transformation from aragonite, he obviously preferred the former mechanism (Folk, 1965). Folk (1965, p. 41) did disregard the possibility that the microspar was mechanically deposited as silt-sized calcite. Bathurst (1959, p. 516) has suggested that the microspar of the Lanchashire Reef was carried in suspension along with other skeletal fragments. Bathurst, however, gave no conclusive evidence to support

this idea. Throughout the entire microspar facies, the allochemical grains show evidence for recrystallization. Only one algal particle shows recrystallization. This, however, may indicate that the recrystallization process is more effective in the matrix than in the allochems.

In the Red Eagle Limestone, microspar makes up all limestone beds. The beds are thin and interbedded with laminae of shale. The insoluble residue in the carbonate beds ranges from less than one to about 50 percent. The insoluble residue of the microsparite facies consists of clay and a small amount of silt-sized quartz. This rather unusual association of the carbonate-bearing microspar with thin shale laminae was also recognized by Folk (1965). Although the microsparite facies of the Red Eagle Limestone consists almost entirely of microspar, there are scattered white, clear patches of relatively coarse spar. The origin of the microspar in these patches as Folk (1965) indicated, are from the recrystallization of the original matrix. Because of the lack of convincing evidence for recrystallization as the only mechanism responsible for the origin of the microspar, this mechanism is tentatively suggested as the main source for the microspar in the Red Eagle Limestone.

Micrite can be formed by two main processes: (1) from abrasion of shell fragments and (2) from direct precipitation from sea water. If geologists have accepted abrasion

and reworking of shell fragments as a possible source for the microcrystalline calcite (micrite), it would appear likely that such a process could contribute to the formation of microspar. Thus microspar could form from various shell fragments by abrasion on the sea floor. It would not be necessary for the microspar to form at the site of deposition but it could be brought in from outside the environment of the deposition by currents. Concentration of microspar thus can be done by winnowing the micrite.

Emmons (1928) experimentally has demonstrated that very fine calcite grains are deposited from a solution saturated with calcium carbonate. He also indicated that coarser grains are produced in an agitated environment. This clearly indicates that an agitated environment may favor the formation of microspar from direct precipitation from sea water. However, the main objection to this process is the fact that aragonite and not calcite is the main constituent of most recent carbonate sediments. If micrite originates from direct precipitation of calcium carbonate and passes through the transformation from aragonite to calcite without a change in its size, then this should also be true for microspar. The presence of a considerable amount of terrigenous material which is mainly clay-sized particles strongly suggests that the Red Eagle Limestone was not deposited in a completely quiet water environment. Thus, it is possible that low energy currents are

responsible for the deposition of microspar in the Red Eagle Limestone.

ENVIRONMENT OF DEPOSITION

The present analysis of the environment of deposition of the Red Eagle Limestone is based on the many available data obtained from the study of the carbonate and terrigenous rocks, paleoecology of the various fossils, and geochemical data from trace element analyses.

The Red Eagle Limestone is characterized by its homogeneity throughout the area studied and like most other carbonate units, is characterized by its fossil content as the major allochemical constituent. Such fossil variations along with other variations in the matrix, cement, sorting, and texture are used in dividing the Red Eagle Limestone into several arbitrary facies. The environment of deposition of each of these facies is analyzed separately from other facies and the resulting general picture is based on these conclusions.

Unsorted microsparite facies with fusulinids and few algae comprises the lowermost part of the Red Eagle Limestone. The unit is extremely thin throughout the area with a maximum thickness of two feet. The fusulinid microsparite facies is found only in measured sections (R_1 and R_9). This unit is totally dolomitized in the

southern part of the area studied, but dolomite is minor in the northern part and has been detected only on x-ray diffraction patterns. Recrystallization of the matrix has been recognized in all the samples examined.

The fusulinids in this facies are well preserved, and they lack any evidence of abrasion or fragmentation. Although the exact environment of deposition of the microspar is not fully understood, the presence of a minor amount of insoluble residue with this facies indicates that the water must have contained little or no suspended terrigenous material.

Fossils other than fusulinids in this facies are extremely rare. Because of a paucity of fossils such as brachiopods, mollusca, and crinoids with fusulinids, Dunbar (1957) has concluded that other organisms avoided places which were inhabited by fusulinids. Dunbar (1957) also indicated that such places where the fusulinid shells are abundant and are unabraded or unbroken, the fusulinids must have lived and accumulated on a quiet sea floor far from currents which were capable of transporting their shells.

Elias (1937) deduced that fusulinids of the Big Blue Cyclothem thrived only where the water was 160 to 180 feet deep. Actually, such deductions were obtained by analogy to the environment of present-day large benthonic foraminifera.

The presence of Osagia in some of the samples of this facies may indicate that deposition was not below the zone of light penetration. According to Holms (1957, p. 120) about 95 percent of the sunlight energy which penetrates sea water is absorbed in the upper 50 meters of the sea. Thus it seems likely that the lower part of the Red Eagle Limestone was deposited on a shallow shelf at a depth not greater than 150 feet.

The second type limestone is an unsorted microsparite facies with algae, crinoids, and brachiopods. This facies is well developed in many places in the studied area, with a maximum thickness of 20 feet in northern Oklahoma. The carbonate beds are thin and interbedded with laminae of shale. Evidence of burrowing can be seen in all the samples of this facies. Recrystallization of the matrix is abundant and difficult to differentiate from algal tubes filled with sparry calcite. The environment of deposition of this facies is also difficult to interpret. The facies contains bryozoans and species of bryozoans are well represented in a variety of environments. Modern day forms are found from low tide down to a depth of 200 fathoms (Osburn, 1957). Most of the brachiopods and crinoids are reported in shallow marine environments. The higher percentage of algae in this unit indicates that the deposition actually took place in a shallow environment within the limit of the photosynthesis zone.

The lack of abrasion and sorting suggests that deposition of this facies occurred below the zone of active reworking and abrasion. According to Dietz et al. (1951) vigorous abrasion takes place up to a depth of about 30 feet. Fragmentation in this facies is believed to be done by burrowing organisms. The presence of a great number of calcareous algae may well indicate that deposition has taken place within the photosyntheses zone as suggested by Holms (1957) but at a depth greater than 30 feet.

The third type of facies is a sparry calcite facies. It is very thin and overlies the thick microsparite facies. This facies is found in only a few places. Sorting and reworking varies from place to place. Poorly-washed sparry calcite with poorly-sorted crinoid allochems are found in northern Oklahoma. This grades southward into a better-sorted crinoid and other fossil assemblage cemented by sparry calcite in the southern part of the area.

This unit may also be considered as two distinctive facies. The sparry calcite facies in the southern part of the area contains a considerable amount of quartz. The quartz grains, although they are not rounded, are sorted. This facies was probably deposited in a very shallow environment within the zone of abrasion and reworking in the southern part of the area. Current and waves were strong enough for winnowing all the matrix and reworking and sorting the allochemical and the terrigenous fractions.

A deeper environment is necessary for the apparent texture of the unit in the northern part of Oklahoma. The crinoid sparry calcite facies of northern Oklahoma was probably deposited below the zone of abrasion and reworking. The current was sufficient for winnowing a considerable amount of the matrix from the pore spaces which were later filled with sparry calcite.

The uppermost part of the Red Eagle Limestone consists of unreworked pellets and intraclasts of recrystallized algae cemented by fine-grained sparry calcite. This facies is found only in southern Kansas and northern Oklahoma. The pellet sparry calcite facies is about 8 feet thick in northern Oklahoma. The limestone beds are considerably thicker than those in the underlying units.

The allochemical grains are probably of algal origin. McCrone, although she considered this unit as an aphanitic limestone (1963), has indicated a probable algal origin for the allochemical grains.

Bottom communities such as algae can influence and control their physical environment (Ginsburg, 1958). The evidence for such control is not present in this facies. Currents may have been sufficient for winnowing the matrix from the pore spaces between the allochemical grains, where the fine-grained sparry calcite was later deposited. This unit probably was deposited in a shallow marine environment below the zone of active abrasion and reworking.

The dolomite facies which comprises the extreme southern part of the outcrop of the Red Eagle Limestone is of replacement origin. Fusulinids and crinoids can be seen replaced by dolomite in various samples of this facies. Thus, the dolomitized portion of the Red Eagle Limestone in the southern part of the area studied, is considered to be deposited in a normal shallow marine environment similar to that which prevailed in the north.

The amount of terrigenous material in the Red Eagle Limestone increases in a general way from southern Kansas to Burbank in northern Oklahoma where the amount and number of shale beds is the greatest. To the south of Burbank, the Red Eagle Limestone is very thin and either eroded and/or not exposed in many places in the area. The coarse fraction of the insoluble residue shows a positive increase in grain size and amount toward the south. Quartz grains are considered the only important constituents of the insoluble residue fraction. The quartz grains are of the straight extinction type and are angular.

Two possible source areas exist to the south, the Arbuckle and the Ouachita Mountains. The lack of carbonate rock fragments and a considerable amount of feldspar in the Red Eagle terrigenous constituents excludes the Arbuckle Mountains as a possible source. Probably the Ouachita Mountains contributed all or most of the terrigenous fraction. Mankin (personal communication) has suggested that

the lack of the chert grains from the insoluble residue probably may exclude the Ouachita Mountains as a main source, and may indicate another pre-existing sedimentary source for the terrigenous fraction of the Red Eagle Limestone.

The geochemical data obtained from the various trace element analyses also indicates a normal marine environment.

The Red Eagle Limestone has shown minor variations in facies which leads to some variation in the environment of deposition. But from all data obtained from the various analyses, the environment of deposition is believed to have been a broad, fluctuating shelf between terrigenous and carbonate deposition. Microspars may have been concentrated in the environment of deposition by low energy currents which were responsible for winnowing the micrite. The water probably was never clear or quiet. This is suggested by the high percentage of insoluble residues in most of the examined samples. Currents and suspensions may have been favorable for the deposition of the microspars.

CONCLUSION

The Red Eagle Limestone in southern Kansas and north-central Oklahoma consists of medium to thin limestone beds interbedded with thin laminae of shale. Two major carbonate facies are recognized in the carbonate beds--a sparry calcite and a microsparite facies. The microsparite facies comprises the lower and middle beds of the Red Eagle Limestone. This facies is well developed in the northern part of the area studied, and it is partially or totally absent in the southern part. Fossils are the main allochemical grain constituents in the microsparite facies. On the bases of variation in the fossils constituents, two microfacies are recognized within the microsparite facies--a fusulinid biomicrosparite and an algal biomicrosparite microfacies.

Burrowing and other scavenger animal activity is mainly responsible for fragmentation of the allochemical grains and other soft sediment features in the limestone beds. The fusulinids are common in the basal limestone beds which are exposed in only two measured sections. The algae biomicrosparite facies is a thick microfacies and well developed in all measured stratigraphic sections in

the northern part of the area. Other fossils such as bryozoans, brachiopods and ostracods are also common with the algae.

Pelsparite and biosparite are the two microfacies that have been recognized within the sparry calcite facies. The biosparite microfacies is better developed in the southern part of the area and the allochemical grains are moderately sorted which may indicate reworking by currents. The pelsparite microfacies is restricted to the northern part of the area studied. The limestone grades into dolomite in the extreme southern part of the area and the study suggests that the dolomite is of a secondary replacement origin. Chalcedonic chert is disseminated throughout the dolomitized beds and is of local origin. Siliceous sponge spicules are believed to be the main source of the silica.

The microspar in the Red Eagle Limestone may have been formed by more than one process, such as from abrasion of various shell fragments and/or direct precipitation from sea water. Microspar may indicate a slight current and agitation in the environment of deposition which would lead to the concentration of this particular type of calcite.

The trace element analyses indicate a linear relationship between boron and the amount of the terrigenous constituents in the Red Eagle Limestone. Although zirconium

is found to be concentrated in the terrigenous fraction, no such linear relationship between zirconium and the amount of the insoluble residue is found. Very high amounts of manganese are concentrated within the dolomite. This amount is slightly higher than that of arid climates as given by Ronov (1959). This may indicate strong leaching of manganese in the source area. The confidence obtained from the analysis of strontium is low and thus the relation of strontium, if any, with the various diagenetic processes in the limestone cannot be interpreted.

The terrigenous constituents of the interbedded shale and insoluble residue consists mainly of illite, chlorite, and quartz. The amount and size of the course fraction of the terrigenous constituents increase southward. The Ouachita Mountains are considered to be the main source area but the lack of detrital chert grains may indicate another sedimentary source. The Red Eagle Limestone was probably deposited in a fluctuating environment between carbonate and terrigenous components on a broad shelf within the zone of light penetration and photosynthetic process.

REFERENCES

Adams, J.A.A., and Weaver, C.E., 1958, Thorium to Uranium ratio as indicator of sedimentary process: Amer. Assoc, Petroleum Geologists, Bull., vol. 42, p. 387-430.

Baranov, V.I., Ronov, A.B., and Kunashova, K.G., 1956, Geochemistry of dispersed thorium and uranium in clays and carbonate rock of the Russian Platform: Geochemiya, no. 3, p. 227-235.

Bass, N.W., 1929, The geology of Cowley County, Kansas: Kans. State Geol. Survey, Bull. 12, 203 p.

Bathurst, R.G.C., 1959, The cavernous structure of some Mississippian stromatactis reefs in Lancashire, England: Jour. Geology, vol. 67, p. 506-521.

_____, 1964, Diagenesis and paleoecology. A survey, in Approaches to paleoecology, Imbrie, J. and Newell, N. (eds.): New York, John Wiley and Sons, p. 319-344.

_____, 1964, The replacement of aragonite by calcite in the molluscan shell wall, in Approaches to paleoecology, Imbrie, J. and Newell, N., (eds.): New York, John Wiley and Sons, Inc., p. 407-436.

Bayne, C.K., 1962, Geology and ground-water resources of Cowley County, Kansas: Kans. State Geol. Survey, Bull. 158, 219 p.

Berner, R.A., 1966, Diagenesis of carbonate sediments: Interaction of magnesium in sea-water with mineral grains: Science, vol. 153, no. 3732, p. 188-191.

Burton, J.D., Culkin, F. and Riley, J.R., 1959, The abundance of gallium and germanium in terrestrials; Geochim. et Cosmochim. Acta, vol. 16, p. 151-180.

Carrol, D., 1959, Ion exchange in clays and other minerals: Geol. Soc. America, Bull., vol. 70, p. 749-780.

Chanda, S.K., 1963, Cementation and diagenesis of the Lameta beds, Lametaghat, M.P. India: Jour. Sed. Petrology, vol. 33, p. 728-738.

_____, 1967, Petrogenis of calcareous constituents of the Lometa Group around Jabalpur; M.P. India: Jour. Sed. Petrology, vol. 37, p. 427-437.

_____, 1967, Selective neomorphism and fabric discontinuities: Jour. Sed. Petrology, vol. 37, p. 688-690.

Chilingar, G.V., 1956, Distribution and abundance of chert and flint as related to the Ca/Mg ratio in limestone: Geol. Soc. America, Bull., vol. 67, p. 1559-1562.

Condra, G.E., 1935, Geologic cross section, Forest City, Missouri, to DuBois, Nebraska: Nebr. Geol. Survey, Paper 8.

Cork, J.M. and Gerhard, S.L., 1931, Crystal structure of the series of barium and strontium carbonates: Amer. Mineralogists, vol. 16, p. 71-77.

Correns, C.W., 1950, Zur Geochemie der diagenese: Geochim. et Cosmochim. Acta, vol. 1, p. 49-54.

Deffeyes, R.S., Lucia, J., and Weyl, D.K., 1965, Dolomitization of Recent and Plio-pleistocene Sediments by marine evaporite waters on Bonaire, Netherlands Antilles, In Pray, L.C., and Murray, R.C., (eds.), Dolomitization and limestone diagensis, A Symposium: Soc. Econ. Paleontologists Mineralogists, Spec. Pub. 13, p. 71-88.

Degenhardt, H., 1957, Untersuchungen zur geochemischen verteilung des Zirkoniums in der Lithosphere: Geochim. et Cosmochim. Acta, vol. 11, p. 279-309.

Degens, E.T., 1965, Geochemistry of sediments: A brief survey: Englewood Cliffs, Prentice-Hall, Inc., N.J., 342 p.

Dietz, R.S. and Menard, H.W., 1951, Origin of abrupt change in slope at continental shelf margin: Amer. Assoc. Petroleum Geologists, Bull., vol. 35, p. 1994-2016.

Dunbar, C.O., 1956, Fusuline Foraminifera, in Treatise on marine ecology and paleoecology, vol. 2, Ladd, H.S., (ed.), Paleoecology: Geol. Soc. America, Mem. 67, Pt. 2, p. 753-754.

Eardley, A.J., 1938, Sediments of Great Salt Lake, Utah: Amer. Assoc. Petroleum Geologists, Bull., vol. 22, p. 1305-1411.

Elias, M.K., 1937, Depth of deposition of the Big Blue (Late Paleozoic) Sediments in Kansas: Geol. Soc. America, Bull., vol. 48, p. 403-432.

_____ and Condra, G.E., 1957, Fenestella from the Permian of West Texas: Geol. Soc. America, Mem. 70, 158 p.

Emery, K.O., 1953, Some surface features of marine sediments made by animals: Jour. Sed. Petrology, vol. 23, p. 203-204.

Emmons, R.C., 1938, Notes on the precipitation of calcium carbonate: Jour. Geology, vol. 36, p. 735-742.

Evumy, B.D., 1967, Dedomitization and development of rhombohedral pores in limestone: Jour. Sed. Petrology, vol. 37, no. 4, p. 1204-1215.

Fenoglia, A.F., 1957, Geology of Northeastern Payne County, Oklahoma: Okla. Univ., unpublished M.S. thesis.

Folk, R.L., and Weaver, C.E., 1952, A study of the texture and composition of chert: Amer. Jour. Science, vol. 250, p. 498-510.

Folk, R.L., 1959, Petrology of sedimentary rocks: Austin, Texas, Hemphill's Pub. Co., 154 p.

_____, 1962, Spectral subdivision of limestone types, in Ham, W.E., (ed.), Classification of carbonate rocks; A symposium: Amer. Assoc. Petroleum Geologists, Mem. 1, p. 62-84.

_____, 1965, Some aspects of recrystallization in ancient limestone, in Pray, L.C., and Murray, R.C. (eds.), Dolomitization and limestone diagenesis, A symposium: Soc. Econ. Paleontologists Mineralogists, Spec. Pub. 13, p. 14-48.

Friedman, G.H., 1959, Identification of Carbonate minerals by staining methods: Jour. Sed. Petrology, vol. 29, p. 87-97.

Frondel, C., and Bauer, L.H., 1955, Kutnahorite: A manganese dolomite Ca $Mn(CO_3)_2$: Amer. Mineralogists, vol. 40, p. 748-760.

Fyfe, W.S. and Bischoff, T.L., 1965, The calcite-aragonite problem, in Pray, L.C. and Murray, R.C., (eds.), Dolomitization and limestone diagenesis, A symposium: Soc. Econ. Paleontologists Mineralogists, Spec. Pub. 13, p. 3-13.

Ginsburg, R.N., 1959, Environment relationship of Grain size and constituent particles in some south Florida carbonate sediments: Amer. Assoc. Petroleum Geologists Bull., vol. 40, p. 2384-2427.

_____ and Lowenstam, H.A., 1958, The influence of marine bottom communities on the depositional environment of sediments: Jour. Geology, vol. 66, p. 310-318.

Ginzburg, I.I. and Mukanov, K.M., 1956, Distribution of Pb, Zn and Cu in different size ranges and density fractions of hill wash in two mineralized localities of central Kazakhstan: Gechimiya, no. 4, p. 390-397.

Goldschmidt, V.M., 1962, Geomchemistry: London, Oxford Univ. Press, 730 p.

Goldsmith, J.R., 1959, Some aspects of the Geochemistry of carbonates, in Research in geochemistry, Abelson, P.H., (ed.): John Wiley and Sons, Inc., Publ., New York, vol. 1, p. 336-358.

Graf, D.L., 1960, Geochemistry of carbonate sediments and sedimentary carbonate rocks, part III-Minor element distribution: Ill. State Geol. Survey, Circ. 301, 71 p.

Green, D.A., 1954, Permian and Pennsylvanian sediments exposed in central and west-central Oklahoma: Amer. Assoc. Petroleum Geologists Bull., vol. 20, p. 1454-1475.

Green, E.J., 1967, The stability of aragonite in sea-water: Thermodynamic influence of strontium: Geochim. et Cosmochim. Acta, vol. 31, p. 2445-2448.

Greig, P.B., Jr., 1959, Geology of Pawnee County, Oklahoma: Okla. Geol. Survey, Bull. 83, 188 p.

Grim, R.E., 1953, Clay mineralogy: New York, McGraw-Hill Co., Inc., 384 p.

Ham, W.E., 1951, Algal origin of the "Birdseye" limestone in the Mclish Formation: Okla. Acad. Science, Proc., vol. 33, p. 200-203.

Harbaugh, J.W., 1961, Relative ages of visibly crystalline calcite in Late Paleozoic limestone: Kans. State Geol. Survey, Bull. 152, pt. 4, p. 91-126.

Heald, K.C., 1916, The oil and gas geology of the Foraker Quadrangle, Osage County, Oklahoma: U.S. Geol. Survey, Bull. 641-B.

Heydemann, A., 1959, Adsorption aus sehr verdunnten Kupterlosungen an reinen tonmineralen: Geochim. et Cosmochim. Acta, vol. 15, p. 305-329.

Holms, R.W., 1957, Solar radiation, submarine daylight and photosynthesis, in Treatise on marine ecology and paleoecology, vol. 1, Heldpeth, J.W., (ed.), Ecology: Geol. Soc. America, Mem. 67, pt. 1, p. 109-128.

Illing, L.V., 1954, Bahama calcareous sands: Amer. Assoc. Petroleum Geologists, Bull., vol. 38, p. 1-95.

_____, Wells, A.J. and Taylor, J.C.M., 1965, Penecontemporaneous dolomite in the Persian Gulf, in Pray, L.C., and Murray, R.C. (eds.), Dolomitization and limestone diagenesis: Soc. Econ. Paleontologists Mineralogists, Spec. Pub. 13, p. 89-111.

Ingram, R.L., 1954, Terminology for the thickness of stratification and parting units in sedimentary rocks: Geol. Soc. America, Bull., vol. 65, p. 937-938.

Johnson, J.H., 1942, Permian lime-secreting algae from the Guadalupe Mountains, New Mexico: Geol. Soc. America, Bull., vol. 53, p. 195-226.

_____, 1945, Calcareous algae of the Upper Leadville limestone near Glenwood Springs, Colorado: Geol. Soc. America, Bull., vol. 56, p. 828-847.

_____, 1946, Lime-secreting algae from the Pennsylvanian and Permian of Kansas: Geol. Soc. America, Bull., vol. 57, p. 1087-1120.

_____, 1951, An introduction to the study of organic limestones: Colo. School of Mines, Quart., vol. 46, no. 2, 185 p.

_____, 1961, Limestone-building algae and algal limestone: Colorado School of Mines, 297 p.

Kahle, C.F., 1965, Possible roles of clay minerals in the formation of dolomite: Jour. Sed. Petrology, vol. 35, p. 448-453.

Keith, M.L. and Degens, E.T., 1959, Geochemical indicators of marine and fresh-water sediments: in Research in geochemistry, Abelson, P.H., (ed.): New York, John Wiley and Sons, Inc., p. 38-59.

_____, 1965, Strontium in oolitic limestone: Jour. Sed. Petrology, vol. 35, p. 846-856.

Klement, K.W. and Toomey, D.F., 1967, Role of the blue-green algae Girvanella in skeletal grain destruction and lime-mud formation in the Lower Ordovician of West Texas: Jour. Sed. Petrology, vol. 37, p. 1045-1051.

Krauskopf, K.B., 1956, Factors controlling the concentrations of thirteen rare metals in sea-water: Geochim. et Cosmochim Acta, vol. 9, p. 1-32b.

Krumbein, W.C., 1942, Physical and chemical changes in sediments after deposition: Jour. Sed. Petrology, vol. 12, p. 111-117.

Lane, N.G., 1958, Environment of deposition of the Grenola limestone (Lower Permian) in southern Kansas: Kans. State Geol. Survey, Bull., vol. 130, p. 117-164.

Logan, B.W., 1961, Cryptozoan and associate stromatolites from the recent, Shark Bay, Western Australia: Jour. Geology, vol. 69, p. 517-533.

Lowenstam, H.A. and Epstein, S., 1957, On the origin of sedimentary aragonite needles of the Great Bahama Bank: Jour. Geology, vol. 65, p. 364-375.

McCrone, A.W., 1963, Paleoecology and biostratigraphy of the Red Eagle Cyclothem (Lower) Permian in Kansas: Kans. State Geol. Survey, Bull. 164.

Migdisov, A.A. and Borrisenok, 1963, Geochemistry of gallium in sedimentation under humid conditions: Geochemiyo, no. 12, p. 1113-1128.

Mogharabi, A., 1966, Carbonate petrography of Foraker Formation (Lower Permian), north-central Oklahoma: Okla. Univ., Ph.D. dissertation, 189 p.

Monroe, E.A., 1964, Election optical observations of fine-grained silica minerals: Amer. Mineralogists, vol. 49, p. 339-347.

Nakayema, M.R., 1955, Geology of southeastern Payne County, Oklahoma: Okla. Univ., M.S. thesis.

Newell, N.D., Imbrie, J., Purdy, E.G., and Thurber, D.L., 1959, Organism communities and bottom facies, Great Bahama Bank: Amer. Mus. Nat. History, Bull., vol. 117, art. 4, p. 181-228.

O'Conner, H.G. and Jewett, J.M., 1952, The Red Eagle formation in Kansas: Kans. State Geol. Survey, Bull., vol. 96, p. 329-362.

O'Conner, H.G., 1963, Changes in Kansas stratigraphic nomenclature: Amer. Assoc. Petroleum Geologists, Bull., vol. 47, p. 1873-1877.

Orme, G.R., and Brown, W.W.M., 1963, Diagenetic fabric in the Avonian limestone of Derbyshire and north Wales: Yorkshire Geol. Soc., Proc., vol. 34, pt. 1, no. 3, p. 51-66.

Osburn, R.C., 1957, Marine bryozoa, in Treatise on marine ecology and paleoecology, vol. 1, Hedgpeth, J.W., (ed.), Ecology: Geol. Soc. America, Mem. 67, pt. 1, p. 1109-1112.

Ostrovmov, E.A., 1956, Distribution of titanium in sediments of the Okhotsk Sea: Geochemiya, no. 1, p. 89-96.

Pettijohn, F.J., 1957, Sedimentary rocks, 2nd ed.: New York, Harper and Bros., 718 p.

Pittman, Jr. J.S., 1959, Silica in Edwards limestone, Travis County, Texas, in Silica in sediment, A symposium: Soc. Econ. Paleontologists Mineralogists, Spec. Pub. 7, p. 121-134.

Powers, R.W., 1962, Arabian Upper Jurassic reservoir rocks, in Ham, W.E. (ed.), Classification of carbonate rocks, A symposium: Amer. Assoc. Petroleum Geologists, Mem. 1, p. 122-192.

Rankama, K., and Sahama, Th.G., 1950, Geochemistry: Chicago, Univ. Chicago Press, 912 p.

Ronov, A.B., and Ermishkina, A.I., 1959, Distribution of manganese in sedimentary rocks: Geochemiya no. 3, p. 206-225.

Ronov, A.B., Vainshtein, E.E. and Tuzova, A.M., 1961, Chemistry of hafnium, zirconium and some other hydrolyzate elements in clays: Geochemiya, no. 4, p. 343-355.

Shinn, E.A., 1968, Practical significance of birdseye structures in carbonate rocks: Jour. Sed. Petrology, vol. 38, p. 215-223.

_____, Ginsburg, R.N., and Lloyd, R.M., 1965, Recent supratidal dolomite from Andros Island, Bahama, in Pray, L.C., and Murray, R.E. (eds.), Dolomitization and limestone diagenesis: Soc. Econ. Paleontologists Mineralogists, Spec. Pub. 13, p. 112-123.

Siegal, F.R., 1961, Factors influencing the precipitation of dolomitic carbonates: Kans. State Geol. Survey, Bull. 152, pt. 5, p. 127-158.

Skinner, J.W., 1931, New Permo-Pennsylvanian Fusulinidae from northern Oklahoma: Jour. Paleontology, vol. 5, p. 16-22.

Stehli, F.G., and Hower, J., 1961, Mineralogy and early diagenesis of carbonate sediments, Jour. Sed. Petrology, vol. 31, p. 358-371.

Sternberg, T.E., Fischer, A.G. and Holland, H.D., 1958, Strontium content of calcium from the Steinplat Reef Complex, Australia: Abs. Geol. Soc. America, vol. 70, p. 1681.

Swett, K., 1968, Authigenic feldspars and chert resulting from dolomitization of illitic limestones, A hypothesis: Jour. Sed. Petrology, vol. 38, p. 128-135.

Taylor, R.C., 1953, The geology of the Foraker area, Osage County, Oklahoma: Okla. Univ., M.S. thesis, 108 p.

Thompson, M.L., 1954, American Wolfcampian fusulinids: Univ. Kansas, Paleont. Contr. no. 14, Art. 5, 226 p.

Turekian, K.K., and Kulp, J.L., 1956, The geochemistry of strontium: Geochim. et Cosmochim. Acta, vol. 10, p. 245-296.

Turekian, K.K., 1964, The marine geochemistry of strontium: Geochim. et Cosmochim. Acta, vol. 28, p. 1479-1996.

Twenhofel, W.H., 1919, Pre-cambrian and carboniferous algal deposits: Amer. Jour. Science, Ser. 4, vol. 43, p. 339-352.

_____, 1939, Principle of sedimentation: New York, McGraw-Hill Book Co., Inc., 673 p.

Vosburg, D.L., 1954, Geology of Burbank-Shidler area, Osage County, Oklahoma: Okla. Univ., M.S. thesis, 110 p.

Wade, B., 1926, The fauna of the Ripley formation of Coon Creek, Tennessee: U.S., Geol. Survey, Prof. Paper 137, 272 p.

Wolefenden, E.B., 1958, Paleoecology of the Carboniferous Reef Complex and shelf limestones in northwest Derbyshire, England: Geol. Soc. America, Bull., vol. 69, p. 871-898.

Wolf, K.H., 1964, Gradational sedimentary products of calcareous algae: Sedimentology, vol. 5, p. 1-37.

_____, 1965, Petrogenesis and paleoenvironment of Devonian algal limestones of New South Wales: Sedimentology, vol. 4, p. 113-178.

_____, 1965, Littoral environment indicated by open-space structures in algal limestones: Paleogeography, Palaeoclimatology, Paleoecology, vol. 1, p. 183-223.

Won, C.P. and Schot, E.H., 1968, Stylolites, their nature and origin: Jour. Sed. Petrology, vol. 38, p. 175-192.

Wyckoff, R.W.G. and Alexander, D., 1968, The strontium content of fossil teeth and bones: Geochim. et Cosmochim. Acta, vol. 32, p. 109-115.

APPENDIX A

THIN SECTION DESCRIPTION

The description of the carbonate rocks and a few terrigenous thin sections was obtained from the following:

1. A detailed study of thin sections with a petrographic microscope.
2. Analysis of the insoluble residue.
3. Qualitative x-ray diffraction study.
4. Quantitative trace element analysis.

The location, sample number, and stratigraphic position of each described thin section are given first. Rock name (underlined), other observational features, which include percent of each allochemical grain, structure and texture, various fossil types and their abundance, and diagenetic features are included. Thickness of beds are given in feet.

X-ray diffraction analysis was used to aid in the identification of the carbonate minerals and to identify the clay minerals.

The percentage of the terrigenous constituents was obtained from the insoluble residue analysis. The percent in each sample is designated by "IR".

Certain samples were analyzed for specific trace elements. The amount of these trace elements is given in parts per million (ppm) for each of the analyzed samples and designated with the letters (TE). For a detailed description of the exact location of each measured section, see Appendix B.

R_1-1, one-half foot above the base, brachiopod, crinoid, fusulinid, packed biomicrosparite; fusulinids (Triticites and Neoschwagarina?) 50%, microforaminifera 5%, crinoids 6%, brachiopods 6%. The slide shows some evidence of burrowing. Veins were later filled with sparry calcite. Fusulinid chambers are filled with finely crystalline calcite. There is only trace amounts of terrigenous constituents.

X-ray: Calcite and a trace of quartz.

R_1-2, one foot above the base, brachiopod, fusulinid, packed biomicrosparite; fusulinids 59%, brachiopods 4%. Fossils are homogeneously distributed. Fusulinid chambers are filled with finely crystalline calcite. The fossils are well preserved which may indicate the lack of any scavenger activities. Microspars have a mean grain size of 16 microns. A few veins cut through the matrix and some allochems were latter filled with sparry calcite.

R_1-3, one and one-half feet above the base, crinoid, bryozoan, brachiopod, fusulinid, packed biomicrosparite; fusulinids 55%, brachiopods 4%, bryozoans 3%, crinoids 3%. The rock is iron stained and fossils are broken, probably by burrowing organisms. Fusulinid chambers are filled with finely crystalline calcite which has a mozaic texture. Allochems are homogeneously distributed in the slide with no evidence of zonation. Microspars have a mean size of 14 microns. Neomorphism is evident in a small portion of the slide. Dolomitization is only minor with scattered rhombs present. Quartz is present in only trace amounts; most of the terrigenous constituents are clays.

X-ray: Calcite, trace of dolomite, and a trace of quartz.

IR: 10%.

R_1-4, three feet above base, burrowed, ostracod, pellet, brachiopod, algae, packed biomicrosparite; algae 30%, brachiopods 6%, pellets 10%, ostracods 4%, crinoid spines and plates 2%, bryozoans 1%. Allochems are oriented parallel to bedding. Burrows and algal tubes are filled with clear, sparry calcite. Fossil fragments are broken, probably by burrowing organisms. In many places, pellets are floating in a recrystallized matrix. Osagia and anchicodium(?) are the main types of algae. A few ostracod cavities are filled with sparry clacite.

X-ray: Calcite, trace of quartz.

R_1-5, four feet above the base, partially recrystallized, burrowed, pellet, bryozoan, brachiopod, algae, packed biomicrosparite; algae 40%, ostracods 5%, brachiopods 6%, bryozoans 4%, crinoids 2%, pellets 3%. Voids are filled with sparry calcite. Allochems are homogeneously distributed. There is no evidence of fossil zonation. There is intense recrystallization of the matrix into pseudospars, and no apparent effect of structural discontinuity on the recrystallization of the matrix. Microspars have a grain mean size of 17 microns. Terrigenous constituents consist mainly of clay; quartz is only a trace amount. Pellets seem to be floating in the pseudospars.

X-ray: Calcite, trace of dolomite, and a trace of quartz.

IR: 10%.

R_1-6, five feet above the base, partially recrystallized, burrowed, brachiopod, crinoid, algae, packed biomicrosparite; algae 30%, crinoids 7%, brachiopods 5%, microforaminifera 3%, ostracods 3%. Burrowing organisms seem to be the main factor in the disturbance and obliteration of the sedimentary structures in the slide. There is extensive recrystallization into pseudospars which, in many places, show a mozaic texture. Osagia is the main type of algae and only a few algae show some evidence of recrystallization into

finely crystalline calcite. Post-depositional veins which cut through some of the allochems were later filled with sparry calcite. A few of the crinoid plates have syntoxial overgrowths. Foraminifera (Tetrataxis and Nodosaria) chambers are filled with a recrystallized matrix.

X-ray: Calcite, trace of quartz.

TE (ppm): Ga 3, Ti 240, Sn 52, V 12, Cu 8, Zr 1, Mn 135, Cr 2, Sr 500.

R_1-7, seven feet above the base, burrowed, partially recrystallized brachiopod, ostracod, algae, packed biomicrosparite; algae 35%, ostracods 10%, brachiopods 6%, crinoids 5%, foraminifera 5%. There is no evidence of fossil zonation and allochems are homogenously distributed. Burrows are filled with sparry calcite. Pisolite grains are composed of Osagia and other encrusting algae have a mean grain size of 0.75 mm. Pseudospars and sparry calcite grade into each other and are difficult to distinguish. Microspars have a mean grain size of 20 microns and show intense recrystallization into pseudospars. Sparry calcite filling ostracod cavities shows structural continuity with the shell.

X-ray: Calcite.

R_1-8, eight feet from the base, burrowed, crinoid, ostracod, bryozoan, pellet, algae, packed biomicrosparite; Algae 30%, bryozoans 10%, pellets 10%, ostracods 5%, crinoids 4%. Allochems are homogeneously distributed. Burrowing organisms seem to be the main factor in breaking most of the shells. Burrows and algal tubes are filled with sparry calcite. A "birdseye" structure is a main feature of the slide. Osagia comprise most of the algae and pisolitic grains. In many places, pellets are isolated in a recrystallized matrix. Crinoid plates are perforated probably by algae. An excellent example of bryozoan-encrusting algae. The microspar matrix has a mean grain size of 18 microns. Clays comprise most of the terrigenous constituents and quartz constitutes less than one percent.

X-ray: Calcite, trace of quartz.

IR: 6.4%

TE (ppm): Ga 6, Ti 580, Sn 110, V 16, Cu 9, Ni 20, Mn 390, Cr 9, Sr 500.

R_1-9, nine feet above the base, burrowed, bryozoan, pellet, algae, packed biomicrosparite; algae 25%, ostracods 5%, pellets 20%, foraminifera 2%, brachiopods 1%. Osagia comprises most of the algae. Void-filling with sparry calcite is abundant. A few crinoid plates have syntaxial overgrowths. In most places, the recrystallized matrix (pseudosparite) shows a mosaic texture. Floating pellets in pseudospars is unusual. Other pellets are composed of very fine algae. Allochems are commonly oriented parallel to the bedding. Microspars have a mean grain size of 13 microns. Most fossil cavities are filled with partially or totally recrystallized matrix and ostracod cavities are filled with sparry calcite which shows structural continuity with the shell wall.

X-ray: Calcite, trace of quartz.

R_1-10, ten feet above the base, burrowed, partially recrystallized, crinoid, brachiopod, bryozoan, algae, packed biomicrosparite; algae 30%, bryozoans 10%, brachiopods 5%, crinoids 7%, ostracods 2%, foraminifera 1%. Osagia and other encrusting algae comprise most of the algae. White, clear calcite composes a large proportion of the slide and fills all voids and algal tubes. Allochemical grains are commonly parallel to bedding. A few scattered pisolites are present. There is only slight evidence of scattered silicification and structural discontinuities have no apparent effect on the recrystallization of the matrix.

X-ray: Calcite, trace of quartz.

IR: 4.5%.

TE (ppm): Ga 2, Ti 140, Sn 24, V 10, Cu 4, Mn 375, Cr 3, Sr 650.

R_1-11, eleven feet above the base, burrowed, partially recrystallized, crinoid, bryozoan, pellet, algae, packed biomicrosparite; algae 40%, pellets 10%, bryozoans 6%, foraminifera 2%, ostracods 2%, crinoids 3%. Pellets are probably algal in origin. An excellent example of bryozoan-encrusting algae. There is extensive recrystallization of the matrix into pseudospars

and burrows are filled with sparry calcite. Most pellet grains are floating in pseudospars. The microspars have a mean grain size of 16 microns. Ostracod cavities are filled with sparry calcite, and only a few algae show apparent recrystallization into very finely crystalline calcite.

X-ray: Calcite, trace of quartz, and a trace of dolomite.

R_1-12, twelve feet above the base, burrowed, partially recrystallized bryozoan, pellet, algae, packed biomicrosparite; algae 30%, pellets 20%, bryozoans 5%, crinoids 3%, ostracods 2%, foraminifera 1%. An excellent example of algal pisolite and bryozoan-encrusting algae. There is extensive recrystallization of the matrix into pseudospars, but only a few allochems (Osagia) show evidence of recrystallization into pseudospars. Void-filling sparry calcite is common. In many places, isolated matrix patches in pseudospars are the main type of pellets.

X-ray: Calcite, trace of quartz, and a trace of dolomite.

R_1-13, thirteen feet above the base, burrowed, partially recrystallized, brachiopod, bryozoan, pellet, algae, packed biomicrosparite; algae 40%, pellets 7%, bryozoans 10%, foraminifera 2%, ostracods 2%, brachiopods 4%, crinoid plates and spines 1%. Osagia and Anchicodium(?) are the main types of algae. A few brachiopods show geopedal structures. Burrowing is common and the recrystallized matrix shows a mosaic texture. There is no apparent evidence of fossil zonation.

X-ray: Calcite and a trace of quartz.

R_1-14, fourteen feet above the base, burrowed, partially recrystallized, spicule, bryozoan, pellet, algae, packed biomicrosparite; algae 20%, pellets 15%, bryozoans 12%, foraminifera 3%, spicules 5%, ostracods 3%. Burrows are filled with sparry calcite. There is extensive recrystallization of the matrix into pseudospars. White, clear calcite composes a large proportion of the slide. Sponge(?) spicules are abundant and have a random orientation. Floating pellets in a recrystallized matrix are common. Most of the shell fragments are coated with algae, and there are only a few pisolite grains.

X-ray: Calcite, trace of quartz, and a trace of dolomite.

IR: 0.9%.

R_1-16, fifteen feet above the base, burrowed, partially recrystallized, crinoid, ostracod, pellet, bryozoan, sparse biomicrosparite; bryozoans 15%, pellets 10%, ostracods 8%, crinoids 5%, pelecypods 2%. Bryozoan autopores and other shells are filled with a recrystallized matrix. Ostracod cavities are filled with a sparry calcite. The allochems are homogenously distributed. No algae are present, but burrows are common.

X-ray: Calcite.

R_1-17, eighteen feet above the base, burrowed, partially recrystallized, bryozoan, crinoid, sparse biomicrosparite; crinoids 7%, bryozoans 6%, foraminifera 4%, ostracods 2%, brachiopods 1%. Burrows are common. Microspars have a mean grain size of ly microns. Foraminifera (Tetrataxis?) chambers and bryozoan autopores are probably filled with a recrystallized matrix. Most of the ostracod cavities are filled with sparry calcite and burrows are also filled with clear, coarse-grained, sparry calcite.

X-ray: Calcite and a trace of quartz.

R_1-19, nineteen feet above the base, burrowed, recrystallized, foraminifera, bryozoan, sparse pelmicrosparite; pellets 25%, bryozoans 3%, foraminifera 5%, crinoids plates and spicules 3%. Burrows are common and recrystallization is more intense in the lower part of the slide. Veins cut through the matrix and some of the allochemical grains (bryozoan fragments) were filled later with sparry calcite. Only a few Osagia fragments are present. In many places, isolated matrix patches are floating in pseudospar. Microspars are of finely crystalline calcite.

X-ray: Calcite and a trace of quartz.

IR: 2%.

R_1-20, twenty feet above the base, partially recrystallized, crinoid, foraminifera, bryozoan, packed pelmicrosparite; pellets 35%, foraminifera 6%, bryozoans 7%, ostracods 2%, crinoids 5%. Foraminifera chambers and bryozoan autopores are filled with a recrystallized matrix with a mosaic texture. Only few burrows are present. Floating pellets in pseudospars are common. Terrigenous constituents consist mainly of clays with only a few scattered quartz grains. Microspars have a mean grain size of 16 microns.

X-ray: Calcite, trace of quartz, and a trace of dolomite.

IR: 5.6%.

TE (ppm): Ga 3, Ti 760, V 17, Zr 3, Mn 460, Cr 7, Sr 510.

R_1-21, twenty-one feet above the base, partially recrystallized, crinoid, bryozoan, pellet, algae, sparse biomicrosparite; algae 20%, pellets 10%, bryozoans 5%, ostracods 2%, crinoids 3%. Extensively recrystallized matrix into pseudospars is a prominent feature of the slide. Foraminifera chambers are filled with a recrystallized matrix. Only a few pisolite grains are present. Osagia is the main type of algae. Terrigenous constituents consist mostly of clays, with quartz grains comprising less than one percent. Microforaminifera and pellets, in many places, are floating in the recrystallized matrix.

X-ray: Calcite and a trace of quartz.

IR: 9%.

R_1-22, twenty-two feet above the base, crinoid, bryozoan, intrapelsparite; pellets 40%, intraclasts 10%, crinoids 6%, bryozoans 10%, foraminifera 2%, ostracods 1%. Almost all the intraclasts are partially or totally recrystallized into pseudospars. Voids within the intraclasts are filled with sparry calcite and the matrix between the allochemical grains is totally recrystallized into finely crystalline calcite. The intraclasts are probably of algal origin and fossil fragments are coated with algae. There is no evidence of reworking or sorting.

X-ray: Calcite and a trace of quartz.

R_3-1, two feet above the base, excessively burrowed, partially recrystallized, ostracod, crinoid, bryozoan, sparse biomicrosparite; foraminifera 2%, ostracods 3%, bryozoans 4%, crinoids 2%. Voids are filled with granular sparry calcite. Scattered dolomite rhombs replace the matrix. Recrystallization, with a coarse mosaic texture, to pseudospars composes a large portion of the slide. Bryozoan autopores are filled with pseudospars(?).

X-ray: Calcite, trace of quartz, and a trace of dolomite.

IR: 4.82%.

TE (ppm): Ga 4, Ti 210, Sn 45, V 27, Cu 13, Zr 4, Ni 10, Mn 500, Cr 5, Sr 590.

R_3-2, five feet above the base, partially recrystallized, burrowed, brachiopod, crinoid, bryozoan, sparse biomicrosparite; brachiopods 10%, bryozoans 20%, crinoids 5%, ostracods 2%. In many places, recrystallization is extensive. Microspars have a mean grain size of 10 microns. Syntaxial recrystallization on crinoid grains is common.

X-ray: Calcite, trace of quartz, and a trace of dolomite.

IR: 7.4%.

R_3-3, seven feet above the base, burrowed, recrystallized, bryozoan, pellet, crinoid, sparse biomicrosparite; pellets 4%, bryozoans 4%, feraminifera 2%, crinoids 5%, brachiopods 2%. There is an apparent fossil zonation. The slide appears to be homogeneous. In many places, pellets float in a recrystallized matrix. Foraminifera chambers (Tetrataxis?) and bryozoan autopores are filled with a mosaic of pseudospars(?). Burrows are filled with a granular, coarse, sparry calcite.

X-ray: Calcite, trace of quartz, and a trace of dolomite.

IR: 5.35%.

R_3-4, ten feet above the base, burrowed, partially recrystallized, pellet, ostracod, bryozoan, sparse biomicrosparite; intraclasts 1%, pellets 3%, ostracods 3%,

crinoids 2%, bryozoans 4%. Cavities are filled with sparry calcite. Crinoids have syntaxial recrystallized rims.

X-ray: Calcite, trace of quartz, and a trace of dolomite.

IR: 4.8%.

TE (ppm): Ga 6, Ti 64, Sn 12, V 6, Cu 2, Ni 17, Mn 194, Cr 1, Sr 550.

R_3-6, twelve feet above the base, burrowed, partially recrystallized, pellet, bryozoan, sparse biomicrosparite; bryozoans 25%, brachiopods 5%, foraminifera 1%, ostracods 2%, crinoids 3%. Pellets float in a recrystallized matrix. Bryozoan autopores are filled with a mosaic of pseudospars(?). Abundant ostracods and foraminifera are filled with sparry calcite. Microspars have a mean grain size of 14 microns.

X-ray: Calcite, trace of quartz, and a trace of dolomite.

IR: 6.6%.

TE (ppm): Ga 1, Ti 180, Sn 22, V 8, Cu 1, Zr 1, Ni 16, Mn 225, Cr 3, Sr 520.

R_3-7, fourteen feet above the base, burrowed, partially recrystallized, crinoid, bryozoan, sparse biomicrosparite; algae 2%, crinoids 5%, bryozoans 10%, foraminifera 1%. There is only slight recrystallization of the matrix into pseudospars. Void-filling sparry calcite is common.

X-ray: Calcite and a trace of quartz.

IR: 4.64%.

TE (ppm): Ti 25, Sn 8, V 5, Cu 3, Zr 2, Ni 10, Mn 300, Cr 4, Sr 540.

R_3-8, fifteen feet above the base, burrowed, partially recrystallized, bryozoan, sparse pelmicrosparite; bryozoans 3%, pellets 10%. Pellets have resulted from the recrystallization of the matrix. Microspars have a mean grain size of 18 microns. A large portion

of one slide consists of white, clear calcite. A few crinoids have syntaxial recrystallized rims.

X-ray: Calcite, trace of quartz, and a trace of dolomite.

R_3-9, sixteen feet above the base, algae, bryozoan intrapelsparite; crinoids 25%, bryozoans 15%, pelecypods 5%, brachiopods 5%, pellets 20%, intraclasts 10%. Allochemical grains are homogenously distributed. The original matrix is recrystallized to coarse pseudospars. Many of the fossil fragments are coated with encrusting algae. The allochems have a mean grain size of 0.3 mm.

X-ray: Calcite, quartz, and a trace of dolomite.

IR: 9.35%.

TE (ppm): Ga 2, Ti 158, Sn 46, V 10, Cu 212, Zr 1, Mn 280, Cr 1, Sr 510.

R_4-1, three feet above the base, slightly silty, clayey, ostracod, crinoid, sparse biomicrosparite; crinoids 20%, ostracods 4%, foraminifera 2%, brachiopods 1%. Only a few burrows are present. Ostracod cavities and burrows are filled with sparry calcite. Only a few fragments of Osagia are present. The slide is homogeneous with no apparent evidence of fossil zonation. Microforaminifera, such as Tetrataxis, Textularia and Ammodiscus, are present. In many places, the dark matrix is probably made of micrite. Microspars have a mean grain size of 13 microns. Partial recrystallization into pseudospars is common. Quartz has a mean grain size of 50 microns.

X-ray: Calcite and quartz.

IR: 26%.

R_4-2, five feet above the base, silty, clayey, algae, bryozoan, crinoid, sparse biomicrosparite; crinoids 20%, bryozoans 5%, algae 5%, pellets 3 %, foraminifera 2%, ostracods 2%, brachiopods 2%. Fossils are oriented parallel to bedding. There is no apparent evidence of recrystallization of the matrix into pseudospars. Microspars have a mean grain size of 14 microns. Voids are filled with sparry calcite.

X-ray: Calcite and quartz.

IR: 26.2%.

R_4-3, six feet above the base, clayey, spicule, algae, sparse biomicrosparite; spicules 3%, algae 4%, cinoids 2%, ostracods 2%, brachiopods 1%. The rock is slightly burrowed and only a small amount of recrstallization into pseudospars is evident. Algal tubes and voids are filled with sparry calcite.

X-ray: Calcite and a trace of quartz.

R_4-4, seven feet from the base, calcareous, fossiliferous, clay shale; crinoids 5%, foraminifera 2%, ostracods 3%. The rock is laminated and fossils are sparse. Silt-sized quartz grains compose 30% of the total terrigenous constituents. Quartz has a mean grain size of 60 microns. Illite is the main clay mineral.

X-ray: Illite, chlorite, quartz, and calcite.

R_4-5, nine feet above the base, burrowed, partially recrystallized, algae, packed pelmicrosparite; algae 10%, pellets 30%, crinoids 4%, foraminifera 1%. Pellets probably have originated as isolated matrix patches in pseudospar. Ostracod cavities are filled with sparry calcite which shows structural continuity with the shell. Recrystallization is more intense near the shell wall. The slide is homogeneous with no apparent evidence of fossil zonation. Bryozoan autopores are probably filled with a recrystallized matrix that has a mozaic texture. Bryozoan fragments are encrusted by algae (Osagia).

X-ray: Calcite, quartz, and a trace of dolomite.

IR: 7.3%.

R_4-6, ten feet above the base, partially recrystallized, crinoid, packed pelmicrosparite; pellets 60%, crinoids 3%. Pellets probably originated as a result of recrystallization of the matrix.

X-ray: Calcite and quartz.

R_4-7, twelve feet above the base, burrowed, partially recrystallized, bryozoan, algae, sparse pelmicrosparite; pellets 20%, algae 15%, bryozoans 6%. Burrows are filled with sparry calcite. Bryozoan autopores are filled with a recrystallized matrix. Pellets are common in the recrystallized matrix.

X-ray: Calcite, trace of quartz, and a trace of dolomite.

TE (ppm): B 158, Ga 47, Sn 16, V 2, Cu 5, Zr 108, Ni 31, Mn 158 and Cr 39, Sr 150.

R_4-8, thirteen feet above the base, bryozoan, algae, pellet, packed pelmicrosparite; pellets 30%, algae 12%, bryozoans 6%, crinoids 2%. The rock is only slightly burrowed. Pellets probably are of algal origin and algal tubes are filled with fine-grained, sparry calcite. Microspars have a mean grain size of 10 microns. Osagia and other encrusting algae are the main algal types. Bryozoan autopores are filled with pseudospar(?) which has a mosaic texture.

X-ray: Calcite and a trace of quartz.

IR: 23%.

TE (ppm): B 35, Ga 3, Sn 5, V 12, Cu 89, Zr 16, Ni 23, Mn 370, Cr 16, Sr 100.

R_4-9, fourteen feet above the base, algae, sparse pelmicrosparite; pellets 25%, algae 10%, crinoids 5%. The rock is only slightly burrowed. Burrows and algal tubes are filled with sparry calcite. Microspars are finely crystalline calcite. Microspars have a mean grain size of 12 microns. Pellets are probably of algal origin. Silt-size grains of quartz are only a trace amount.

X-ray: Calcite and a trace of quartz.

R_4-10, fifteen feet above the base, silty, bryozoan, algae, sparse biomicrosparite; bryozoans 6%, algae 10%. The slide shows current bedding. Burrows are filled with sparry calcite. Terrigenous constituents are concentrated in certain zones. Recrystallization of the matrix into pseudospars is common. Osagia and other encrusting algae are abundant. Silt consists

totally of quartz and has a mean grain size of 55 microns.

X-ray: Calcite, quartz, and a trace of dolomite.

IR: 34%.

R_4-11, sixteen feet above the base, partially recrystallized, pellet, algae, sparse biomicrosparite; algae 20%, pellets 8%, bryozoans 3%. Gervinela(?) is the main type of algae. In many places, recrystallization to pseudospars is extensive. Floating pellets in a recrystallized matrix is common. Algal tubes are filled with sparry calcite.

X-ray: Calcite and quartz.

IR: 25.8%.

TE (ppm): B 32, Ga 21, Sn 16, V 17, Cu 3, Zr 17, Ni 19, Mn 390, Cr 16.

R_4-12, seventeen feet above the base, silty, bryozoan, pellet, algae, sparse biomicrosparite; algae 15%, pellets 10%, bryozoans 5%, crinoids 2%. Algal tubes filled with sparry calcite are common. There are a few pisolite grains. Burrowing is common. Gervinalla(?) is abundant. Quartz has a mean grain size of 70 microns. Pellets probably formed from algae and from isolated matrix patches in pseudospars. Syntaxial overgrowths are present only on a few crinoid plates.

X-ray: Calcite, quartz, and a trace of dolomite.

R_4-13, eighteen feet above the base, silty, bryozoan, crinoid, packed biomicrosparite; crinoids 30%, bryozoans 19%, ostracods 1%, brachiopods 2%, pelecypods 1%. The rock is homogeneous and has no apparent evidence of fossil zonation. Fossil fragments are coarse and many of the ostracod cavities are filled with sparry calcite. Many of the crinoid plates show evidence of perforation. Algal grains are present only in trace amounts. Quartz has a mean grain size of 75 microns. Pellets are abundant in the recrystallized areas. Microspars have a mean grain size of 15 microns.

X-ray: Calcite, quartz, and a trace of dolomite.

IR: 28%.

TE (ppm): B 38, Ga 3, Sn 9, V 5, Cu 11, Zr 1, Mn 118, Cr 4, Sr 540.

R_4-19, nineteen feet above the base, foraminifera, algae pelsparite; pellets 60%, ostracods 2%, foraminifera 4%, crinoids 3%. Extensive recrystallization of the matrix into fine- and medium-grained pseudospars is evident. Sparry calcite is fine grained and cannot be easily distinguished from pseudospar. Pellets are probably of algal origin. Microforaminifera have the same size as the pellets. Pellets have a mean grain size of 0.23 mm. Crinoid fragments are coarse and all ostracod cavities are filled with sparry calcite. Foraminifera chambers are filled with a recrystallized calcite(?).

X-ray: Calcite and a trace of quartz.

R_4-15, twenty feet above the base, bryozoan, pellet, crinoid, sparse biomicrosparite; pellets 10%, crinoids 15%, bryozoans 7%. A few recrystallized intraclasts of probable algal origin are present. Pellets are concentrated in the lower portion of the bed and float in a recrystallized matrix. Only a few crinoids show syntaxial overgrowths. Microspars have a mean grain size of 18 microns.

X-ray: Calcite and a trace of quartz.

R_4-16, twenty-one feet above the base, intraclast pelsparite; intraclasts 5%, pellets 60%, ostracods 1%, bryozoans 1%, brachiopods 1%. Only a few patches of dolomite rhombs are present. There is no apparent evidence of sorting or reworking. The original matrix has been recrystallized into pseudospars. Micrite is found in few places. White, clear calcite is abundant and composes a large proportion of the slide. Pellets have a mean grain size of 0.33 mm.

X-ray: Calcite, quartz, and a trace of dolomite.

R_4-17, twenty-two feet above the base, algae, intraclast pelsparite; algae 3%, intraclasts 5%, pellets 60%. The rock is homogeneous and totally cemented by sparry calcite. Pellets are probably of both algal origin and from recrystallization. Pellets have a mean grain

size of 0.33 mm. A few, large dolomite rhombs are present.

X-ray: Calcite, a trace of quartz and dolomite.

IR: 29%.

R_4-18, twenty-three feet above the base, algae, intraclast pelsparite; pellets 60%, intraclasts 3%, algae 3%. The rock is iron stained and partially silicified.

X-ray: Calcite, a trace of quartz and dolomite.

IR: 22.4%.

TE (ppm): Ga 1, Ti 290, Zr 1, Mn 155, Sr 60.

R_4-19, twenty-four feet above the base, intraclast, pelsparite; pellets 66%, intraclasts 5%, ostracods 1%, brachiopods 1%, crinoids 2%. The rock is homogeneous and fossil fragments are more common than in lower units. Sponge(?) spicules are common.

X-ray: Calcite and a trace of quartz.

IR: 12.5%.

R_5-1, four feet above the base, burrowed, brachiopod, crinoid, sparse biosparite; brachiopods 3%, crinoids 4%, bryozoans 2%, ostracods 2%. The rock is intensively burrowed. No algae is present. The rock is homogeneous and has no apparent evidence of fossil zonation. Burrows are filled with granular, sparry calcite. Terrigenous constituents consist of clay and only a trace of quartz. A few crinoid grains show syntaxial recrystallization. Bryozoan autopores are probably filled with a recrystallized matrix which has a mosaic texture. There are only a few dolomite grains.

X-ray: Calcite, quartz, and a trace of dolomite.

IR: 42%.

R_5-2, six feet above the base, burrowed, partially recrystallized, foraminifera, bryozoan, ostracod, algae, crinoid, sparse biomicrosparite; crinoids 8%, algae 7%, bryozoans 6%, foraminifera 5%, ostracods 7%.

Burrows are filled with a granular, sparry calcite. There is extensive recrystallization of the matrix. A few veins cut through the matrix which were later filled with sparry calcite. Microspars comprise the bulk of the orthochemical fraction. Microspars have a mean grain size of 11 microns. Structural discontinuities have no apparent effect on the recrystallization of the matrix. Foraminifera chambers, ostracod cavities, and bryozoan autopores are filled with a recrystallized matrix. Only a few ostracods are filled with sparry calcite.

X-ray: Calcite, quartz, and a trace of dolomite.

TE (ppm): Ga 2, Ti 510, Sn 170, V 11, Cu 58, Zr 3, Ni 22, Mn 207, Cr 5, Sr 500.

R_5-3, eight feet above the base, clayey, ostracod, crinoid, sparse biomicrosparite; foraminifera 2%, bryozoans 4%, ostracods 6%, crinoids 7%. The slide shows current bedding. An excellent example of an ostracod cavity filled with fibrous, sparry calcite. A high percentage of clays. Quartz has a mean grain size of 60 microns. There is no apparent evidence of burrowing or algal remains.

X-ray: Calcite and quartz.

IR: 40%.

R_5-4, ten feet above the base, burrowed, bryozoan, crinoid, algae, sparse biomicrosparite; algae 15%, crinoids 8%, bryozoans 7%, ostracods 5%, brachiopods 2%. The matrix is partially recrystallized into pseudospars. Broken fragments of fossils probably reflect burrowing activity. Quartz has a mean grain size of 60 microns. Osagia and other encrusting algae are the main algal types. Microspars have a mean grain size of 12 microns.

X-ray: Calcite and quartz.

IR: 25.2%.

R_5-5, thirteen feet above the base, burrowed, partially recrystallized algae, sparse biomicrosparite; algae 12%, crinoids 2%, foraminifera 1%. Burrows are filled with granular, sparry calcite. Pseudospar composes a large proportion in the rock and has a

mosaic texture. Terrigenous constituents consist mainly of clay minerals. Quartz grains comprise only a small amount with a mean grain size of 60 microns. A few algae are slightly recrystallized into a very fine-grain calcite.

X-ray: Calcite and quartz.

IR: 25%.

R_5-7, seventeen feet above the base, burrowed, partially recrystallized, crinoid, algae biomicrosparite; algae 10%, crinoids 3%, brachiopods 2%, ostracods 1%, foraminifera 1%. The rock is homogeneous with no apparent evidence of fossil zonation. Only a few crinoid grains show syntaxial recrystallization. Burrows and algal tubes are filled with sparry calcite. Microspars have a mean grain size of 12 microns. Quartz has a mean grain size of 56 microns.

X-ray: Calcite, quartz, and a trace of dolomite.

IR: 19.7%.

TE (ppm): B 45, Ga 18, Sn 9, V 10, Cu 2, Zr 7, Ni 18, Mn 265, Cr 12, Sr 100.

R_5-8, eighteen feet above the base, algae, foraminifera, intraclast, bryozoan, crinoid biosparite; crinoids plates and spicules 30%, bryozoans 20%, foraminifera 5%, ostracods 2%, brachiopods 2%, algae 5%, intraclasts 3%. Syntaxial recrystallization and syntaxial overgrowths are found on many crinoid fragments. Intraclasts and algal grains are recrystallized into pseudospars. Quartz has a mean grain size of 80 microns. Voids in the intraclasts are filled with sparry calcite. Matrix between the grains is recrystallized to pseudospars(?).

X-ray: Calcite, quartz, and a trace of dolomite.

R_5-9, twenty feet above the base, ostracod pelsparite; pellets 65%, ostracods 5%. Pellets probably resulted from the recrystallization of the matrix. Voids were later filled with sparry calcite.

X-ray: Calcite, quartz, and a trace of dolomite.

R_5-10, twenty-one feet above the base, ostracod, intraclast pelsparite; pellets 35%, intraclasts 25%, ostracods 10%, spicules 3%. Allochemical grains are homogeneously distributed. Recrystallization of the matrix into pseudospars is common. Spicules (sponge?) are abundant.

X-ray: Calcite and quartz.

TE (ppm): B 170, Ga 9, Sn 787, V 10, Cu 23, Zr 9, Ni 20, Mn 308, Cr 3, Sr 1000.

R_5-15, twenty-two feet above the base, partially silicified intrapelsparite; intraclasts 10%, pellets 40%. A few dolomites rhombs are scattered through the matrix. Pellets and intraclasts probably originated from recrystallization of the matrix. There is no evidence of sorting and/or reworking of the grains. Sparry calcite fills the pore spaces between the allochemical grains and voids within the intraclasts.

X-ray: Calcite, quartz, and a trace of dolomite.

IR: 21%.

TE (ppm): Ga 4, Ti 1000, Sn 225, V 19, Cu 7, Zr 410, Ni 62, Cr 42, Mn 1000, Sr 650.

R_6-1, two feet above the base, sandy, poorly washed, crinoid, brachiopod biosparite; brachiopods 25%, pelecypods 8%, crinoids plates and spicules 13%, bryozoans 6%, intraclasts 2%, ostracods 3%. Intraclasts probably consist of recrystallized algae. The original matrix, in most places, has been recrystallized to pseudospars which makes it difficult to distinguish from the sparry calcite. Quartz has a mean grain size of 100 microns. Quartz is mostly straight to slightly undulose extinction and is angular.

X-ray: Calcite and quartz.

IR: 25.7%.

R_6-2, five feet above the base, sandy, coarse, intraclast, bryozoan, crinoid biosparite; bryozoans 15%, intraclasts 10%, brachiopods 5%, pelecypods 5%, crinoids 30%. The allochemical grains are moderately sorted but the terrigenous sand grains are better sorted.

Quartz grains are not rounded and quartz has a mean grain size of 100 microns. Only one brown tourmaline grain was observed. Intraclasts are probably recrystallized algae.

X-ray: Calcite and quartz.

IR: 30.7%.

R_8-1, one foot above the base, partially silicified, totally dolomitized, crinoid biosparite. Crinoid spicules and plates are the only allochemical grains that can be identified. Dolomite grains are mostly of medium size and replacement of crinoids by dolomite grains is noticeable. Silicification by chalcedonic quartz is common. A few calcareous sponge spicules are present.

X-ray: Dolomite, a trace of calcite and quartz.

IR: 12.7%.

TE (ppm): B 155, Ga 9, Sn 1, V 6, Cu 51, Zr 1, Ni 10, Mn 280, Cr 4, Sr 410.

R_8-2, two feet above the base, totally dolomitized, crinoid biosparite. Crinoid plates and spicules are the only allochems that can be recognized. Dolomite grains are coarse and are replacing crinoids. Calcedonic quartz is present in only trace amounts.

X-ray: Dolomite, a trace of calcite and quartz.

IR: 6.2%.

TE (ppm): Ga 4, Ti 2000, Sn 120, V 13, Cu 32, Zr 5, Ni 16, Mn 1000, Cr 9, Sr 150.

R_8-3, four feet above the base, totally dolomitized, crinoid biosparite. Allochemical grains are totally composed of crinoid spicules and plates. There is no apparent evidence of silicification. The dolomite grains are coarse. A good example of isolated dolomite grains replacing a crinoid fragment can be seen.

X-ray: Dolomite, calcite, and a trace of quartz.

IR: 10%.

TE (ppm): Ga 10, Ti 750, Sn 120, V 13, Cu 39, Zr 34, Ni 52, Mn 1000, Cr 10, Sr 200.

APPENDIX B

MEASURED STRATIGRAPHIC SECTIONS

The Red Eagle Limestone crops out in a north-south direction in the area. Nine sections were measured with a steel tape. The measured sections are numbered from 1 to 9, with measured section (R_1) being the northernmost outcrop and measured section (R_9) the southernmost outcrop in the area. The location of the exposures is given in figure 1. The location is described in detail at the beginning of each measured section. Thus the symbol (R_2-5) means sample five of the Red Eagle Limestone of measured section number two. The "R" refers to the Red Eagle Limestone.

The color of both the fresh and weathered surface of the samples is given according to the Rock Color Chart (1948) of the National Research Council, Washington, D.C.

The thickness of each described unit is given in feet and Ingram's Classification (1954) is used for the description of the thicknesses of the various beds.

Section R_1: Sec. 22, T. 32 S., R. 8 E., along Highway 38, about two miles west of the Cowley-Chautauqua County

line in Cowley County, Kansas. This section is measured along the north side of the road cut. The section represents an excellent exposure of the Red Eagle Limestone. The contact of the Red Eagle Limestone with the underlying Johnson Shale is gradational. The upper beds of the formation are eroded at this outcrop; thus, the upper contact with the Roca Shale cannot be investigated.

	Thickness (feet)
Limestone, yellowish gray (5Y 7/2), weathers to olive gray (5Y 3/2), thin nodular beds, irregular fractures on the upper surface, burrowed, hard, sparse, crinoids, intraclasts, algae...	1
Limestone, yellowish gray (5Y 7/2), weathers to pale yellowish brown (10YR 6/2), thin beds, very hard, slightly nodular, compact, highly fossiliferous with crinoids, algae, bryozoans, and a few brachiopods.....	1
Limestone, gray (5Y 7/2), weathers to pale yellowish brown (10YR 6/2), thin beds, very hard, compact, with fracture zone parallel to the bedding, fractures filled with sparry calcite, brownish iron stain on the surface, a few brachiopods, many crinoids and algae.....	1
Limestone, olive gray (5Y 6/1), weathers to medium gray (N5), very hard, very thin beds, conchoidal fracture, fossiliferous with crinoids and algae..	2
Limestone, gray (5GY 6/1), weathers to light olive gray (5Y 6/1), very thin beds, compact, hard, fractured, only a few scattered patches of dolomite, fossiliferous with algae and crinoids..	2

	Thickness (feet)
Limestone, yellowish gray (5GY 8/1), weathers to light olive gray (5Y 6/1), very thin beds, very hard, iron stain on the surface, crinoids and algae.....	2
Limestone, yellowish gray (5Y 8/1), weathers to light olive gray (5Y 6/1), very thin, irregular beds, hard, burrowed, sparry calcite-filled burrows, algae.....	2
Limestone, light olive gray (5Y 6/1), weathers to medium gray (N5), very thin irregular beds, hard, burrowed, iron stain, interbedded with very thin laminae of soft shale, the limestone beds are fossiliferous with brachiopods, crinoids and algae.....	3
Limestone, yellowish gray (5Y 8/1), weathers to light olive gray (5Y 6/1), thin irregular beds, hard, burrowed, scattered patches of iron stain on the surface, crinoid stems stand out in sharp relief on the weathered surface, algae, crinoids and a few brachiopods...	3
Limestone, light brownish gray (5YR 6/1), weathers to brownish gray (5YR 4/1), very thin irregular beds, hard, conchoidal fractures, algae.....	1
Limestone, light brownish gray (5YR 6/1), weathers to greenish gray, medium beds, highly fractured, burrowed, fossiliferous with crinoids, brachiopods and bryozoans.....	0.5
Limestone, greenish gray (5GY 6/1), weathers to light olive gray (5Y 6/1), very thin nodular beds, partially scattered recrystallization, burrowed, not fossiliferous.....	1
Limestone, greenish gray (5GY 6/1), weathers to brownish gray (5YR 4/1), thin irregular beds, brachiopods and crinoids.....	1

	Thickness (feet)
Limestone, greenish gray (5GY 6/1), weathers to brownish gray (5GY 6/1), very thin beds, hard, iron stain on the surface, very fossiliferous with fusulinids abundant.....	1.5
Limestone, light olive gray (5Y 6/1), weathers to light brownish gray (5YR 6/1), very thin beds, soft, fusulinids..	1
Total	23

Section R_2: Sec. 25, T. 28 N., R. 6 E., along east-west road, 2 miles southwest Foraker, Osage County, Oklahoma. This outcrop represents the middle portion of the Red Eagle Limestone.

	Thickness (feet)
Limestone, light brownish gray (5YR 6/1), weathers to brownish gray (5YR 4/1), hard, conchoidal fractures, very thin beds, finely crystalline, sparsely fossiliferous with a few crinoids.....	2
Limestone, pale yellowish brown (10YR 6/2), weathers to brownish gray (5YR 4/1), very hard, thin irregular beds, conchoidal fractures, compact, medium to coarse crystalline, sparse crinoid stems.....	2
Limestone, grayish yellow (5Y 8/4), weathers to pale yellow (10Y 6/2), hard, thin nodular beds, compact, scattered iron staining, irregular fractures, not fossiliferous.....	2
Limestone, very pale orange (10YR 8/2), weathers to dusky brown (5YR 2/2), hard, thin nodular beds,	

	Thickness (feet)
conchoidal fractures, burrowed, not fossiliferous	2
Limestone, grayish orange pink (5YR 7/2), weathers to dark yellowish brown (10YR 4/2), hard, thick beds, sparse algae	1
Limestone, pale yellowish brown (10YR 6/2), weathers to dark yellowish brown (10YR 4/2), hard, very thin, slightly nodular beds, breaks into small flat slabs, fossiliferous with algae	3
Limestone, pale yellowish brown (10YR 6/2), weathers to light olive gray (5Y 5/2), thin beds, very hard, irregular fractures, burrowed, a few scattered recrystallized patches, fossiliferous with algae, crinoids, and brachiopods	1
Total	13

Section R_3: Sec. 10, T. 26 N., R. 6 E., about 1000 ft. south of Phillips lake, measured on top of the hill, Osage County, Oklahoma. This section represents the middle portion of the Red Eagle Limestone. The lower part of the formation is covered and the upper beds are eroded away. Thus, the nature of the contacts with the overlying and underlying units cannot be investigated.

	Thickness (feet)
Limestone, yellowish gray (5Y 7/2), weathers to pale olive gray (10Y 6/2), very thin irregular beds, very hard,	

	Thickness (feet)
conchoidal fractures, iron stain on the surface, breaks to thin slabs, very finely crystalline.....	2
Limestone, pale yellowish brown (10YR 6/2), weathers to dark yellowish brown (10YR 4/2), very thin beds, very hard, breaks with an irregular surface, fossiliferous with crinoid stems standing out in sharp relief on the weathered surface.....	2
Limestone, pale yellowish brown (10YR 6/2), weathers to dusky brown (5YR 2/2), thin- to medium-beds, hard, highly fractured at right angles to the bedding, a few marl laminae, finely crystalline, fossiliferous with algae abundant.....	4.5
Limestone, light bluish gray (5B 7/1), weathers to light brownish gray (5YR 6/1), very thin beds, hard, very highly fractured, breaks into irregular fragments of various sizes, most fractures are filled with coarse, sparry calcite, burrowed, a few fossils with algae most common.....	2
Limestone, yellowish gray (5Y 8/1), weathers greenish gray (5GY 6/1), thin beds, burrowed, iron stain on the surface, finely crystalline, abundant fossils with algae, crinoids, and bryozoans.....	1.5
Limestone, yellowish gray (5Y 8/1), weathers to light bluish gray (5B 7/1), very thin beds, hard, brecciated, iron stain, a few algae.....	2
Limestone, yellowish gray (5Y 8/1), weathers to greenish gray (5GY 6/1), thin beds, burrowed, coarse to medium allochemical grains, fossiliferous with algae, bryozoans, crinoids, and brachiopods present.....	4
Total	18

Section R_4: SE 1/4 Sec. 25, T. 26 N., R. 5 E., measured in a quarry of several acres in area, about two miles east of the town of Burbank and one-fourth mile north of U.S. Highway 60 in Osage County, Oklahoma. This is an excellent exposure of the Red Eagle Limestone. The lower few feet of the formation are not exposed. The upper contact with the overlying Roca Shale is very sharp but no physical evidence of an unconformity is recognized.

	Thickness (feet)
Limestone, light bluish gray (5B 7/1), weathers to greenish gray (5GY 6/1), hard, very thin beds, clayey, with dark grayish bands parallel to the bedding, burrowed, crinoid stems.....	.5
Limestone, light bluish gray (5B 7/1), weathers to greenish gray (5GY 6/1), hard, very thin beds, interbedded with very thin shale laminae, shale disappears laterally, slightly burrowed, very finely crystalline calcite, fossiliferous with algae and crinoids common.....	2
Limestone medium gray (5N), weathers to light olive gray (5Y 6/1), thin beds, very hard, compact, interbedded with very thin, soft shale, large crinoid stems stand out in sharp relief on the weathered surface, a few algae.....	2
Limestone, light brownish gray (5YR 6/1), weathers to brownish gray (5YR 4/1), thin beds, hard, compact, clayey, fractured, burrowed, fossiliferous with algae and crinoids common.....	2
Limestone, greenish gray (5GY 6/1), weathers to pale yellowish brown (10YR	

	Thickness (feet)
6/2), very hard, highly clayey, fractured, not fossiliferous.....	3
Limestone, yellowish gray (5Y 7/2), weathers to medium light gray (N6), very hard, very thin beds, fractured, compact, very finely crystalline calcite.....	2
Limestone, light olive gray (5Y 6/1), weathers to light brownish gray (5YR 6/1), very thin beds, conchoidally fractured, interbedded with dark gray thin laminae of shale, burrowed, patches of coarse sparry calcite are noticeable in burrows, fossiliferous with crinoids and bryozoans common.....	3
Limestone, greenish gray (5G 6/1), weathers to dark greenish gray (5GY 4/1), very thin beds, hard, randomly-oriented fractures, breaks into unequal, angular slabs, burrowed.....	3
Limestone, dark greenish gray (5GY 4/1), weathers to light olive gray (5Y 6/1), thin beds, very hard, highly fossiliferous with crinoids, brachiopods, and bryozoans common.....	2
Limestone, pinkish gray (5YR 8/1), weathers to light brownish gray (5YR 6/1), hard, very thin beds, conchoidal fractures, hard, compact, slightly burrowed, not fossiliferous.....	2
Limestone, yellowish gray (5Y 8/1), weathers to medium gray (N5), thin beds, hard, iron stain on the surface, burrows filled with sparry calcite, crinoids.....	1
Limestone, yellowish gray (5Y 8/1), weathers to light brownish gray (5YR 6/1), compact, very hard, very finely crystalline.....	1

	Thickness (feet)
Limestone, yellowish gray (5Y 8/1), weathers to brownish gray (5YR 4/1), compact, hard, thin beds, burrowed.....	3
Total	26

Section R_5: SE 1/2 Sec. 25, T. 22 N., R. 5 E., about 2 miles east of Burbank and one-half mile south of U.S. Highway 60 in Osage County, Oklahoma. This section is measured in a quarry. The quarry is several acres in area and it is active at the present time. The lower few beds of the Red Eagle Limestone are not exposed. The upper contact with Roca Shale is very sharp. There is no physical evidence of an unconformity. This outcrop is an excellent Red Eagle Limestone exposure in northern Oklahoma.

	Thickness (feet)
Limestone, pinkish gray (5YR 8/1), weathers to light brownish gray (5YR 6/1), hard, medium beds, burrowed, conchoidal fractures, iron stain on the surface, not fossiliferous.....	4
Limestone, pinkish gray (5YR 8/1), weathers to greenish gray (5GY 6/1), thin beds, conchoidal fractures, compact, very hard, fracture zones filled with sparry calcite.....	3
Limestone, yellowish gray (5Y 8/1), weathers to light olive gray (5Y 6/1), very thin beds, hard, iron stain on the surface, finely crystalline calcite, crinoids.....	1

	Thickness (feet)
Limestone, light greenish gray (5GY 8/1), weathers to greenish gray (5GY 6/1), very thin beds, highly fractured, fossiliferous with crinoids and algae common.....	2
Limestone, pale yellowish brown (10YR 6/2), weathers to medium gray (5N), thin beds, very hard, compact, burrowed, voids filled with sparry calcite, very fossiliferous with crinoids and algae abundant.....	3
Limestone, light greenish gray (5GY 8/1), weathers to greenish gray (5GY 6/1), very thin beds, hard, interbedded with very thin shale laminae, fossiliferous with algae abundant.....	2
Limestone, light greenish gray (5G 8/1), weathers to greenish gray (5GY 6/1), very thin beds, hard, fossiliferous with brachiopods, crinoids, and algae common.....	3
Limestone, greenish gray (5GY 6/1), weathers to light brownish gray (5YR 6/1), hard, very thin beds, interbedded with soft, thin shale, very fossiliferous with crinoids and algae abundant.....	3
Limestone, medium gray (N5), weathers to dark gray (N3), very thin beds, hard, interbedded with soft shaly beds, a few crinoids.....	3
Limestone, greenish gray (5GY 6/1), weathers to medium dark gray (N5), hard, thin beds, conchoidal fractures, interbedded with soft, thin laminae of shale, a few fossils with algae, crinoids and brachiopods most abundant.....	3
Total	27

Section R_6: NE 1/4, Sec. 29, T. 22 N., R. 5 E. is measured on the eastern side of a road cut on State Highway 18. This outcrop is about two miles north of the town of Pawnee in Pawnee County, Oklahoma. Only the lower few feet of the Red Eagle Limestone are exposed. The contact with the underlying Johnson Shale is sharp and conformable. It is a poor exposure.

	Thickness (feet)
Limestone, pale yellowish brown (10YR 6/2), weathers to dark yellowish brown (10YR 4/2), hard, compact, iron stain, scattered dolomite patches, fossiliferous with crinoids, pelecypods, brachiopods, and bryozoans common.....	1
Limestone, yellowish gray (5Y 7/2), weathers to light brown (5YR 6/2), thin beds, hard, burrowed, iron stain, scattered sand grains, a few dolomite patches, fossiliferous with crinoids and brachiopods.....	2
Limestone, yellowish gray (5Y 7/2), weathers to light olive gray (5Y 5/6), very hard, brecciated, compact, very finely crystalline, scattered sand grains, fossiliferous with pelecypods, brachiopods, and crinoids.....	1
Limestone, yellowish gray (5Y 7/2), weathers to dusky brown (5YR 2/2), thick beds, very hard, crinoid stems stand out in sharp relief on the weathered surface, scattered sand grains, very fossiliferous with brachiopods and crinoids.....	3
Total	7

Section R_7: SE 1/4, Sec. 31, T. 22 N., R. 5 E., measured near Pawnee School, Pawnee County, Oklahoma. This is a poor Red Eagle Limestone exposure. The outcrop represents only the lower portion of the formation.

	Thickness (feet)
Limestone, grayish orange pink (10R 8/2), weathers to pale brown (5YR 5/2), hard, with irregular fractures, medium beds, nodular, finely crystalline with irregular color bands, not fossiliferous.....	2
Limestone, light brown (5YR 6/4), weathers to dark yellowish brown (10YR 4/2), hard, thin beds, iron stains, slightly burrowed, very finely crystalline, fossiliferous with crinoids and brachiopods.....	1
Limestone, pale greenish yellow (10Y 8/2), weathers to brownish gray (5YR 4/1), thin beds, hard, fractures filled with sparry calcite, fossiliferous with crinoids and brachiopods.....	3
Limestone, yellowish gray (5Y 7/2), weathers to dark greenish gray (5GY 4/1), very hard, thin beds, compact, slightly burrowed, a few crinoids.....	2
Total	8

Section R_8: NW 1/4, Sec. 28, T. 20 N., R. 5 E., Pawnee County, Oklahoma. This exposure is measured in a quarry on the south side of a dirt road, about one mile east of the intersection with Highway 18. The beds of the Red Eagle Limestone are dolomitized and

partially replaced by chalcedonic silica in a few places. The outcrop is only a few feet thick.

	Thickness (feet)
Limestone, greenish gray (5GY 6/1), weathers to light olive gray (5Y 6/1), hard, breaks with an uneven surface, finely crystalline, totally dolomitized with fine- to medium-sized dolomite grains.....	2
Limestone, dark greenish gray (5GY 4/1), weathers to light olive gray (5Y 6/1), very hard, compact, totally dolomitized with fine- to medium-sized dolomite grains.....	1
Limestone, light brownish gray (5YR 6/1), weathers to light olive gray (5Y 6/1), very thin, scattered dolomite patches, a few crinoids.....	1
Limestone, yellowish gray (5Y 7/2), weathers to dusky yellow (5Y 6/4), very thin beds, soft, clayey.....	.5
Total	4.5

Section R_9: Sec. 2, T. 17 N., R. 4 E., in Payne County, Oklahoma. This stratigraphic section is measured along the south and north sides of a road cut on State Highway 33, about two miles east of the intersection with Highway 18. This is the southernmost outcrop sampled for the petrographic study. This outcrop is characterized by the abundance of fusulinids in the lower beds. The contact with the underlying

Johnson Shale is sharp and conformable. The upper part of the Red Eagle Limestone has been eroded away.

	Thickness (feet)
Limestone, yellowish gray (5Y 7/2), weathers to pale yellowish brown (10YR 6/2), thin beds, very hard, compact, interbedded with thin laminae of shale, limestone beds are totally dolomitized, dolomite grains fine to medium in size, not fossiliferous.....	4.5
Limestone, pale yellowish brown (10YR 6/2), weathers to grayish brown (5YR 4/1), very hard, thin, irregular beds, fractured, compact, totally dolomitized, the dolomite grains are medium-sized, very fossiliferous with fusulinids, the fusulinids are soft and totally replaced by dolomite.....	3.5
Total	8.0